TECHNISCHE UNIVERSITÄT MÜNCHEN
Lehrstuhl für Bauchemie

Interaction of PCE polyelectrolytes with cement mineral surfaces: a study from the macro to the nano scale

Lucia Ferrari

Vollständiger Abdruck der von der Fakultät für Chemie der Technischen Universität München zur Erlangung des akademischen Grades eines

Doktors der Naturwissenschaften (Dr. rer. nat.)

genehmigten Dissertation.

Vorsitzender:	Univ.-Prof. Dr. Klaus Köhler
Prüfer der Dissertation:	1. Univ.-Prof. Dr. Johann P. Plank
	2. apl. Prof. Dr. Anton Lerf
	3. Univ.-Prof. Dr. Sevil Weinkauf

Die Dissertation wurde am 21 Oktober 2011 bei der Technischen Universität München eingereicht und durch die Fakultät für Chemie am 24 November 2011 angenommen.

Acknowledgement

The research project presented in this thesis was developed at Empa Dübendorf, Switzerland, with the supervision and collaboration of Professor Johann Plank, TU Munich, Germany.

Hereby, I would like to thank all the people who supported the successful achievement of this work.

First of all, I would like to express my gratitude to Professor Johann Plank for supervising my investigations with careful attention and positive enthusiasm. His wide knowledge and broad experience in the field of cement gave fruitful value to the research performed. Furthermore, the time spent at the cheerful chair in Munich was always pleasant and scientifically challenging.

Josef Kaufmann and Frank Winnefeld deserve special and precious thanks for giving me the possibility of undertaking this path trough a various combination of materials and methodologies. They leaded my PhD conceding me the opportunity to explore interesting and various experimental possibilities, trusting my ability of evaluation and my lively creativity. Their precision, experience, pragmatism and deep knowledge of cement chemistry contributed to build an ensemble of ideas which revealed to be extremely constructive.

I am definitely grateful to my co-workers at Empa, for welcoming me in Switzerland, for their assistance and friendly support in the lab, for the interesting discussions, for the delightful atmosphere present even in the coldest days, and for organizing the active festive life of our lab.

A particular thank goes to all the friends which contributed to make my time in Zurich one of the most joyful of my life.

My parents, my brothers and my sisters are greatly thanked to have always believed in my potentialities with animated appreciation.

Last but not least, I would like to thank Sebastiano to be the best accomplice in any situation.

Lucia, October 2011

Abstract

Superplasticizers are commonly used in the construction industry to increase the workability and to reduce the water demand of cement pastes, mortars and concrete mixtures. The combination of these two effects allows the production of concretes with special performances, like self compacting concrete, high strength concrete and prefabricated concrete elements.

In the presented thesis the behavior of polycarboxylate-ether based superplasticizers (PCEs) at the interface between solid (*i.e.* cement phases) and liquid (*i.e.* pore solution) was studied. Specifically, interaction forces between mineral surfaces in aqueous medium containing PCE are investigated by atomic force microscopy (AFM), in combination with rheology, adsorption and ζ-potential measurements. The main limitation for the application of AFM is the reactivity of cement with water, which requires the use of model substrates.

Four main topics are discussed:

I. suitability of model systems for the AFM technique by investigation of adsorption and ζ-potential;

II. influence of different polymer architectures, electrolyte content in solution, and cement types on PCE efficiency;

III. applicability of clinker surface as AFM substrate by verification of its surface reactions in different solutions and of superplasticizer adsorption on different cement phases;

IV. analysis of the dispersion forces occurring on ettringite crystals, tested by silicon dioxide spherical tips, in solutions holding different electrolyte and PCE contents.

Characterization of the AFM setup by adsorption and ζ-potential revealed that among the selected model substrates (calcite, quartz, mica and magnesium oxide) only MgO has a positive surface charge, which then provides high adsorption of PCEs, which are negatively charged. Furthermore, silicon nitride tips were shown to adsorb high amount of superplasticizers, thus bringing AFM results of difficult understanding. On the other side, dispersion forces were observed also between minerals that are negatively charged materials and consequently where PCE does not adsorb well, suggesting the idea that the electrostatic repulsive dispersion generated between particles with similar charge becomes considerable.

Results collected applying different polymer architectures pointed out that superplasticizers with high charge density afford low apparent yield stresses and high adsorption on particles. However, at a nano-level, PCEs with short side chains produce higher dispersion forces. Furthermore, these PCEs, with a low number of ethylene oxide groups in the side chain assemble in multi-layers on the particle surface as the polymer concentration increases. Tests on different kinds of cement confirm that formation of ettringite needles, because of their non-spherical morphology, affects cement rheology and the adsorption properties of PCEs present in the pastes. On the other side, to work with model systems allows to directly detect the influence of ions in solution. Indeed, force ranges and intensities are reduced by the presence of electrolytes, and resulting rheological properties are consequently disturbed.

Investigations on clinker surfaces allow observations of the behavior of single phases with respect to the hydration process and the adsorption of superplasticizer. The results show that in the case of clinker surface exposed to different ionic solutions hydration is mainly influenced by the type of electrolyte contained in the solution, and that the pH has a stronger influence than the ionic strength. A comparison between clinker surface hydrated in water and hydrated in aqueous superplasticizer solution revealed that the formation of portlandite on the clinker surfaces is highly reduced by the presence of PCE. Moreover, further investigations by time-of-flight ion mass spectroscopy (TOF-SIMS) revealed that the superplasticizer strongly interacts with potassium and sulfate ions contained in the solution, thus leading to arcanite formation. Additionally, AFM force measurements show how dispersion by PCE is important to avoid attraction between ettringite crystals and negatively charged phases.

Preliminary results collected on ettringite crystals probed with a silicon dioxide tips show a strong attraction between the negatively charged tip and the substrate. Nevertheless, when the pH and the ionic strength increase, the ettringite substrate becomes negatively charged, and the tip and the substrate experience repulsion forces even in absence of PCE.

This thesis shows the importance of comparing macroscopic results with the nano-scale behavior of superplasticizers directly at the minerals surface. The study highlights the potential and the limitations of AFM technique in studying PCE dispersion forces. Quantification of the surface forces can still be refined. However, the influence of different electrolyte solutions, substrate materials, polymer architectures and AFM tips was parametrically analyzed.

List of papers

This thesis includes the following papers:

Peer reviewed SCI(E) journal papers:

- **Interaction of cement model systems with superplasticizers investigated by atomic force microscopy, zeta potential, and adsorption measurements.**

  L. Ferrari, J. Kaufmann., F. Winnefeld, J. Plank. *Journal of Colloid and Interface Science* 347 (2010), 15-24.

- **Multi-method approach to study influence of superplasticizers on cement suspensions**

  L. Ferrari, J. Kaufmann., F. Winnefeld, J. Plank. *Cement and Concrete Research* 41 (2011), 1058-1066.

Manuscripts submitted to journals:

- **Study of polycarboxylate-ether based superplasticizers on cement clinker surfaces by TOF-SIMS and AFM**

  L. Ferrari, L. Bernard, F. Deschner, J. Kaufmann., F. Winnefeld, J. Plank. *Journal of American Ceramic Society,* in review.

- **Reaction of clinker surfaces investigated with atomic force microscope**

  L. Ferrari, J. Kaufmann., F. Winnefeld, J. Plank. *Construction and Building Materials,* in review.

Refereed conference papers:

- **Multi-method approach for the characterization of the behavior of superplasticizer in cement suspensions**

  L. Ferrari, J. Kaufmann., F. Winnefeld, J. Plank. Proceedings of the XIII ICCC International Congress on the Chemistry of Cement, Madrid 2011.

Table of contents

1 INTRODUCTION ..... - 1 -

2 AIMS AND LIMITATIONS ..... - 5 -

3 THEORY OF SURFACE FORCES ..... - 7 -

3.1 VAN DER WAALS FORCE ..... - 8 -
3.2 STERIC FORCE ..... - 10 -
3.3 ELECTROSTATIC FORCE ..... - 10 -
3.4 DLVO THEORY AND COLLOIDAL STABILITY ..... - 12 -

4 MATERIALS ..... - 15 -

4.1 POLYCARBOXYLATE SUPERPLASTICIZERS ..... - 15 -
4.2 SURFACE MATERIALS ..... - 16 -
4.3 POWDER MATERIALS ..... - 18 -

5 METHODS ..... - 19 -

5.1 RHEOLOGY ..... - 19 -
5.2 ADSORPTION ..... - 20 -
5.3 ζ-POTENTIAL ..... - 21 -
5.4 ATOMIC FORCE MICROSCOPY ..... - 21 -

6 RESULTS AND DISCUSSION ..... - 25 -

6.1 CHARACTERIZATION OF AFM SETUP (PAPER 1) ..... - 25 -
6.2 INFLUENCE OF DIFFERENT POLYMER ARCHITECTURES (PAPERS 2 AND 3) ..... - 26 -
6.3 BEHAVIOR OF CLINKER SURFACE (PAPERS 4 AND 5) ..... - 28 -
6.4 PRELIMINARY RESULTS OBTAINED ON ETTRINGITE SUBSTRATE ..... - 29 -

7 CONCLUSIONS AND OUTLOOK ..... - 31 -

REFERENCES ..... - 33 -

Nomenclature, units, abbreviations

Mineral name	Chemical formula	Cement notation*
Tricalcium aluminate	$3CaO{\cdot}Al_2O_3$	C_3A
Tricalcium silicate	$3CaO{\cdot}SiO_2$	C_3S
Dicalcium silicate	$2CaO{\cdot}SiO_2$	C_2S
Tetracalcium aluminate ferrite	$4CaO{\cdot}Al_2O_3{\cdot}Fe_2O_3$	C_4AF
Ettringite	$3CaO{\cdot}Al_2O_3{\cdot}3CaSO_4{\cdot}32H_2O$	$C_6A\bar{S}_3H_{32}$

*Cement compounds are expressed as sum of oxides, which are abbreviated as: C = CaO, A = Al_2O_3, S = SiO_2, F = Fe_2O_3, H = H_2O, $\bar{S}$= SO_4^{2-}.

Quantity	SI unit*	Symbol	Definition of unit
Energy	Joule	J	kg m^2 s^{-2}
Force	Newton	N	kg m s^{-2} = J m^{-1}
Electric charge	Coulomb	C	A s
Potential	Volt	V	J A^{-1} s^{-1} = J C^{-1}
Pressure	Pascal	Pa	N m^{-2}

* SI units = International System units: kilogram (kg) for mass, liter for volume (L), meter (m) for length, second (s) for time, Kelvin (K) for temperature, ampere (A) for electrical quantities, mole (mol or M) for quantity of mass.

Constant	Symbol	SI value
Boltzmann's constant	k_B	1.381 × 10^{-23} J K^{-1}
Electronic charge	$-e$	1.602 × 10^{-19} C
Permittivity of free space	ε_0	8.854 × 10^{-12} C^2 J^{-1} m^{-1}

Variables		SI unit
A_H	Hamaker constant	J
C	Concentration	mol/L
D	Distance between two objects	m
f	Force per unit area	N/m^2

Variables		SI unit
F	Force	N
R	Particle radius	m
s	Average distance between adsorption sites	m
T	Temperature	K
w	Potential energy per unit area	V/m^2
W	Potential energy	V
$\dot{\gamma}$	Shear rate	1/s
ε	Relative permittivity	C^2 / (J m)
λ_D	Debye length	m
ρ_i	Density of the species i	Unit of i $/m^3$
σ	Surface charge	C/m^3
τ	Shear stress	Pa
τ_0	Yield stress	Pa
ψ	Electric potential	V

Abbreviations	
w/c	Water-to-cement ratio
PEO	Polyethylene oxide
PCE	Polycarboxylate-ether
CD	Charge density
AFM	Atomic force microscope
SEM	Scanning electron microscope
EDX	Energy dispersive X-ray spectroscopy
TOF-SIMS	Time-of-flight secondary ion mass spectroscopy
TOC	Total organic carbon
BET	Brunauer, Emmett, and Teller (BET theory)
DLVO	Derjaguin, Landau, Verwey, Overbeek (DLVO theory)

1 Introduction

Concrete is composed of cement, water, sand and gravel and is the most widely used construction material worldwide. Cement, which works as binder, is produced by heating a mixture of limestone with clay (alumosilicates) and iron oxide-containing materials in a rotary kiln at nearly 1450°C, and grinding the obtained so-called clinker together with about 4-8% of calcium sulfates and other mineral additions, like limestone, slag or fly ash. The result of this process is a multi-phase solid consisting of round micron-sized calcium silicate particles of two different chemical compositions ($3CaO{\cdot}SiO_2$ and $2CaO{\cdot}SiO_2$), immersed in an interstitial matrix of aluminate and ferrite ($3CaO{\cdot}Al_2O_3$ and $4CaO{\cdot}Al_2O_3{\cdot}Fe_2O_3$). The reactions occurring between Ordinary Portland cement and water induce dissolutions and precipitations of cement clinker phases, forming a variety of microstructures that control the strength development and the hardening process of the fresh concrete paste [1].

Workability and rheological properties of the cement mixture is relevant for the final properties of the hardening concrete. This behavior results from a combination of different physical phenomena, the understanding of which is still ongoing [2-3]. The particle size and shape, their volume fraction, and the inter-particle forces play a significant role in influencing the rheological properties of granular system [4-5]. Specifically, the reduction of the water content in cement paste allows the production of special concretes, e.g. self-compacting concrete or high-performance concrete. This water reduction drastically influences early age strength, long-term mechanical properties, durability, permeability, strength, and many other features. Therefore, the addition of organic admixtures is paramount in the manufacture of these concretes to allow such peculiar properties.

Superplasticizers belong to the category of water reducing agents, and they are broadly classified into four groups depending on their chemistry: sulfonate melamine-formaldehyde condensate (SMF), sulfonated naphthalene-formaldehyde condensate (SNF), modified lignosulfonate (MLS), and others including sulfonic acid esters, polyacrylates and polystyrene sulfonates [6]. The last generation of superplasticizer is represented by comb-shaped polycarboxylate superplasticizers (PCE). The carboxylic groups on the main chain form an anionic charged backbone, while the hydrophilic polyethylene oxide (PEO) composes the side chain [7]. PCEs are widely used owing to their versatility. Indeed, the number of carboxylic groups, the number and length of side chains are flexible parameters that result in different polymer architectures which ensure

different effects on cement rheology and hydration [8-9]. Their effect on cement mixtures is related to induction of a dispersive inter-particle force that avoids the formation of agglomerates [10].

The amount of PCE adsorbed on particle surfaces allows to detect the effective interaction between the superplasticizer and the cement particle [11-12]. The solution depletion method in combination with the total organic carbon (TOC) analysis enables the determination of the amount of polymer left in solution after centrifugation of the water-powder mixtures. Different studies highlighted the influence of different polymer architectures and their interaction with the cementitious system, showing that short side chain superplasticizers exhibit high adsorption especially on positively charged cement phases, e.g. ettringite [8-13]. On the other side, adsorption of PCE on cement particles increases with the increase of the specific surface area available [14], and decreases with the increase of the concentration of sulfate ions [15].

The detection of the ζ–potential enables to study the influence of superplasticizers on particle charges, and to analyze the effect of electrostatic dispersion forces acting between them [16]. Titration of PCE to a particle suspension while measuring the ζ–potential gives a further confirmation of the adsorption of the polymer on particle surfaces [17]. Generally, polycarboxylate superplasticizers change particle charge into negative if they have short side chain, or into neutral if the side chains are long enough to screen the particle charge [7].

Surface forces between solid surfaces are commonly detected by using the atomic force microscope (AFM) [18-19]. Forces detected in different electrolyte solutions can vary from attractive to repulsive depending on the tip charge [20]. Considering that the AFM tip is highly sensitive to the roughness of the substrate and that cement is strongly reactive with water, different non-reactive model systems simulating cement behavior have been applied. One of the first studies was performed on a clinker surface, stating that the dispersion forces due to organic admixtures are a combination of steric and electrostatic effects [22-21]. These results were confirmed by the application of magnesium oxide spherical tips to measure the effect of superplasticizers on magnesium oxide surface in different ionic solutions [23]. Colloidal probe of aluminum oxide enabled to observe that processing variables do affect the polyelectrolyte behavior in the slurry [24]. Studies performed on calcium silicate hydrate substrates investigated the layer thickness of superplasticizers with different side chain lengths using a standard silicon nitride tip with a deposition of calcium hydroxide [25].

In this work, the characterization of the behavior of PCE in powder-suspensions and at the solid-liquid interface with the support of all the above mentioned techniques (rheology, adsorption, ζ–potential, and AFM) was done. The comparison and the correlation of the results obtained using these different methods allowed to highlight the different aspects of the same phenomena, from a macro to a nano-scale level. Rheology tests were done on cements containing different amounts of tricalcium aluminate applying different PCE polymer architectures. Adsorption and ζ-potential were detected for different model systems using different types of PCE superplasticizers as well. Application of the AFM technique requires the determination of adsorption and ζ–potential of different materials which are suitable as model systems. Thus, AFM force measurements were performed on different inert substrates, on clinker surface and on ettringite crystals using a variety of solutions and polymer architectures. The originality is to correlate a wide selection of materials and methods in order to illustrate effects of polymer architectures, the influence of ionic species in solution, the behavior of adsorbing or non-adsorbing AFM substrates, and the characterization of the dispersion forces in relation to the colloidal stability.

2 Aims and limitations

This PhD thesis aims to characterize the dispersion forces generated by PCE superplasticizers at the surface of cement mineral phases. These forces, which are in the distance-range of few nanometers and the intensity-range few nano-Newtons, are detectable by instruments which are rather sharp in individualizing local surface areas and which are relatively sensitive to the forces occurring in the proximity of the surface. For this reason, application of atomic force microscopy (AFM) is necessary to perform this kind of measurements. The questions involved while performing force measurements in a fluid containing superplasticizer are the amount of polymer effectively adsorbed on the substrate and on the tip, and the role of the electrostatic surface charge relative to the total measured force. For this reason, AFM measurements are compared with results obtained from adsorption and ζ-potential data.

The main limitations of performing AFM force measurements in liquid are the reactivity of cement with water and the limited amount of available materials for tip preparation. Indeed the sensitivity of the tip allows to use only polished and un-reactive surfaces. Such properties can not be obtained from cementitious materials. Furthermore, due to the necessity of the tips of being rather sharp, relatively few materials qualify for this application. Not every material is suitable to be deformed and modeled with preferred shapes. For instance, the sphere is the optimal shape to perform consisting AFM force measurements [26], but the production of ceramic spheres in the range of few microns is quite problematic.

For these reasons, the AFM measurements were performed on substrates representing model cementitious materials with different kinds of tips that do not have the same chemical composition of the substrate. The model substrates were selected according to their suitability as building material, favoring the ones which present a crystalline structure. The following research steps were achieved to develop a methodology to study the effect of polycarboxylates at the solid-liquid interface:

- suitability of silicon nitride tips and of model systems for the AFM technique by investigation of adsorption and ζ-potential;
- influence of different polymer architectures and concentrations, electrolyte solution, and cement type on PCE efficiency and on AFM force measurements;

- applicability of clinker surface as AFM substrate by verification of surface reactions in different solutions and of adsorption of PCE superplasticizer on different cement phases;
- analysis of the dispersion forces occurring on ettringite in presence of PCE and in different electrolyte solutions measured with spherical tips.

These experiments allow to understand which parameters influence the AFM force measurements. The wide selection of tested materials and employed methods offers an overview of the potential and limitations of the AFM technique. Furthermore, the correlation of all the applied techniques provides a comprehensive understanding of the effect of PCE on cement and mineral surfaces.

3 Theory of surface forces

A wide range of natural phenomena occurring at the solid-liquid interface revolve around the effect of surface forces. In colloid science, the stability of the particles in suspension and the rheology of the mixture are affected by forces among colloidal particles [18]. For this reason, a detailed analysis of forces occurring at the solid-liquid interface in presence or absence of superplasticizer is fundamental to understand the behavior and the role of these admixtures.

The forces occurring between particles in colloidal suspensions are attractive or repulsive, and they depend on the particle distance. If the attractive forces are stronger than the repulsive forces, then the two particles will collide one on the other. On the other side, if the repulsive forces are stronger than the attractive forces, the particles will remain separated. As consequence of this effect, from a macroscopic point of view, attraction leads to particle agglomeration, while dispersion leads to stability of particle suspensions. The medium in which particles are present is also a factor, owed to effects from pH and ionic strength [27].

The dominating forces at the solid-liquid interface are:

- Van der Waals
- Steric
- Electrostatic

There is also a group of other forces, like hydration or adhesion forces, which will not be discussed in this work, due to their minor role in the particle suspensions considered in this study. Van der Waals forces are usually attractive at short range, resulting in a rapid flocculation of the particles from the liquid. Steric forces are generally repulsive, producing a hindrance between particles that prevents collision and cohesion. Electrostatic forces depend on particle charge, on pH and on ionic strength, and they can be attractive or repulsive. The combination of all these effects provides a description of the stability of colloidal suspensions. The DLVO theory includes the effect of the Van der Waals attraction and the double-layer repulsion as function of the distance between the particles.

In this chapter the mathematical description, the physical meaning and the contribution of the above mentioned forces to colloidal stability are described, mainly referring to the previous work published by Butt [18], Birdi [27] and Israelachvili [28].

3.1 Van der Waals force

The *Van der Waals* force is originated between molecules by the complex dipole-dipole interaction. The rapid fluctuation of the dipole moment of a neutral molecule leads to polarization of a neighbor molecule, which then forms an induced dipole. The potential energy W related to the dipole-oscillations decrease with $1/D^6$, where D is the distance between the two dipoles, and it is quantified by three main components. *Keesom* energy, between two dipoles randomly oriented, represents the tendency of two next dipoles to orient with their opposite charges facing each other. *Debye* energy, between a static dipole and an induced dipole, represents the induction of a dipole moment on a polarizable molecule. *London* energy, between two oscillating dipoles, represents the mutual induction of a dipole moment between two oscillating dipoles.

The sum of these components results in the potential energy of interaction between a molecule A and a molecule B:

$$W_{AB} = -\frac{C_{AB}}{D^6} \qquad (1)$$

where C_{AB} embodies all the dipole-dipole interactions mentioned above.

The calculation of the Van der Waals energy between two macroscopic solids extends the interaction volume by integrating equation (1) on the densities of the two solids, ρ_A and ρ_B. This produces the Van der Waals energy per unit area

$$w_{AB} = -\frac{A_H}{12\pi D^2} \qquad (2)$$

where

$$A_H = \pi^2 C_{AB} \rho_A \rho_B \qquad (3)$$

is the definition of the so-called *Hamaker* constant. Furthermore the corresponding force per unit area is calculated by deriving equation (2):

$$f_{AB} = \frac{dw_{AB}}{dD} = -\frac{A_H}{6\pi D^3} \qquad (4)$$

The Hamaker constant is then determined by the dielectric permittivities and the optical properties of the interacting media, *i.e.* refractive index and main absorption frequency in the ultraviolet (UV). Since the water molecules have a strong dipole moment, A_H plays an important role for forces in water, and it is nearly $10^{-20}\,J \approx 2.5 k_B T$ at $T = 300K$, where k_B =1.381 × 10^{-23} J K^{-1} is the *Boltzmann* constant. In general, $k_B T$ represents the thermal energy to which the molecules are subjected, and it indicates the strength of an interaction. For instance, if an interaction exceeds the thermal energy $k_B T$, then the molecule will be able to win the disorganizing effect of thermal motion. C_{AB} can be positive or negative, thus influencing the sign of A_H and consequently the sign of f_{AB}. An attractive Van der Waals force corresponds to a positive sign of the Hamaker constant, while repulsion corresponds to a negative Hamaker constant. In typical ceramic or metallic materials immersed in water, A_H is positive, thus producing an attractive force at short range between two approaching bodies. From a physical point of view, when two bodies arrive close enough to feel the Van der Waals attraction, they approach each other and they get in contact, since the force is increasing exponentially with the decrease of the distance.

Starting from equation (4) it is possible to calculate the Van der Waals force between solids having different geometry. Considering the case of two spheres of radius R_1 and R_2, in the approximation of $D << R_1, R_2$, the resulting force is

$$F = -\frac{A_H}{6D^2}\frac{R_1 R_2}{R_1 + R_2} \qquad (5)$$

For the following cases it results as:

- $R_1 = R_2 = R$ equal spheres $\Rightarrow F = -\frac{A_H}{6D^2}\frac{R}{2}$
- $R = R_1 << R_2$ sphere – planar surface $\Rightarrow F = -\frac{A_H R}{6D^2}$

Thus, the Van der Waals force between particles of comparable size is half than the force between particles of widely different sizes. Therefore, in a polydisperse particle system like cement the small sized hydration products have most likely the tendency to precipitate on the large

clinker grains, instead of agglomerating with each other. This effect was experimentally confirmed in [10].

3.2 Steric force

Steric interaction is relevant to stabilise colloidal dispersions. A suspension in which only the Van der Waals force is active has the tendency to flocculate and to collapse. For this reason, dispersing polymers are often used in many industrial applications to provide steric stabilization. When added to a colloidal suspension, the polymers adosorb on the particle surface and provide a repulsive force, contrasting the previously presented attraction.

To understand steric interaction it is important to consider two main factors. They mainly concern the adsorption process, or more specifically *how* and *how much* polymer is bound to the surface. Another important aspect is the adsorbed polymer layer thickness, since it is responsible for the range of the steric force.

Generally, models simplify the presence of polymer for example by reducing it to a chain of spheres or to a compact brush with a layer thickness L, and these assumptions result in forces with an exponential trend that decrease with the increase of the distance D. For instance, *Israelachvili* reports a theory that considers a surface with high coverage of polymer, *i.e.* $s < R_g$ where s is the average distance between adsorption sites and R_g is the radius of gyration of the polymer. The repulsive pressure between two layers in the case of $0.2 < D/2L < 0.9$ results as

$$P(D) \approx \frac{100 k_B T}{s^3} e^{-\pi D/L} \qquad (6)$$

However, at this time, there is no simple and comprehensive theory of the steric forces. One of the reasons for this lack may be related to the flexible structure of polymer chains in solution. Since these chains follow the Brownian motion in water, it is sort of impossible to predict the position of the single atoms with respect to the surface.

3.3 Electrostatic force

Electrostatic forces are relevant since most of the surfaces are charged in water. Due to its high dielectric constant, water works as solvent for ions. Indeed, charging at the surface can occur in

two ways: by ionization or dissociation of surface groups, or by adsorption of ions from solution onto the surface. The final surface charge is balanced between oppositely charged regions. The first ion layer adsorbed on the surface form the so-called *Stern layer*, while the cloud of ions in rapid thermal motion close to the surface form the *diffuse layer*. The Stern layer and the diffuse layer form the *electrostatic double layer*. Two equally charged surfaces repel each other, thus that in a homogeneous colloidal suspension the electrostatic forces stabilize the dispersion. On the other side, oppositely charged surfaces attract each other, and this is the reason why in heterogeneous suspensions like cement formation of agglomerates from particle flocculation may be observed.

The calculation of the electrostatic double layer force is extracted by the formulation of the electric potential ψ as a function of the distance D from a planar surface. The local charge density ρ_e in the proximity of the electrical double layer is the difference between anion concentration c^- and cation concentration c^+, which are related to the local potential ψ by the Boltzmann distribution. The local charge density is then

$$\rho_e = c^+ - c^- = c_0 e \cdot \left(e^{-\frac{e\psi(D)}{k_B T}} - e^{\frac{e\psi(D)}{k_B T}} \right) \qquad (7)$$

where c_0 is the bulk concentration of the salt, and e is the electric charge.

In general, charge density and electric potential are related to the *permittivity in free space* ε_0 and *relative permittivity* of the medium ε by the Poisson equation:

$$\frac{d^2\psi}{dD^2} = \frac{\rho_e}{\varepsilon_0 \varepsilon} \qquad (8)$$

This equation can be resolved analytically assuming that $e|\psi| << k_B T$, *i.e.* for $T = 300K \Rightarrow \psi \leq 25mV$, and giving boundary conditions for which the potential is ψ_0 at the surface and 0 at infinite distance:

$$\begin{cases} \psi(D=0) = \psi_0 \\ \psi(D \to \infty) = 0 \end{cases} \qquad (9)$$

The resulting electrical double layer potential then is:

$$\psi(D) = \psi_0 e^{-D/\lambda_D} \qquad (10)$$

where

$$\lambda_D = \sqrt{\frac{\varepsilon_0 \varepsilon k_B T}{c_0 e^2}} \qquad (11)$$

is called Debye length. This parameter is related to the ion cloud around any ion. For instance, each negative ion is surrounded by an oppositely charged ion at a certain distance. The Debye length represents this distance, which decreases with the increase of the concentration of the added electrolyte.

Starting from equations (9) and (10) it is possible to calculate the electrical double layer force between solids having different geometries. For example, for two spheres of radius R it becomes

$$F \approx \frac{2\pi R \varepsilon_0 \varepsilon \psi_0^2}{\lambda_D} e^{-D/\lambda_D} = \frac{2\pi R \sigma^2 \lambda_D}{\varepsilon_0 \varepsilon} e^{-D/\lambda_D} \qquad (12)$$

relating the surface potential ψ_0 with the surface charge density $\sigma = \frac{\varepsilon_0 \varepsilon \psi_0}{\lambda_D}$.

To summarize, the electrostatic double layer force depends on surface charge and on the concentration of electrolytes in solution. Furthermore it increases with the decrease of the distance between the two approaching bodies. However, at a certain distance it overlaps with the effects of the Van der Waals force. The combination of these two effects is described by the DLVO theory.

3.4 DLVO theory and colloidal stability

The DLVO theory is named after *Derjaguin* and *Landau*, *Verwey* and *Overbeek*, and it describes the behavior of charged particles interacting in a liquid medium. The total interaction energy $W(D)$ depends on the distance D between particles and is defined as the sum of the electrostatic repulsion and the Van der Waals attraction:

$$W(D) = W_{el}(D) + W_{vdw}(D) \qquad (12)$$

Figure 1 shows the interaction between two particle surfaces under the combined effect of these forces.

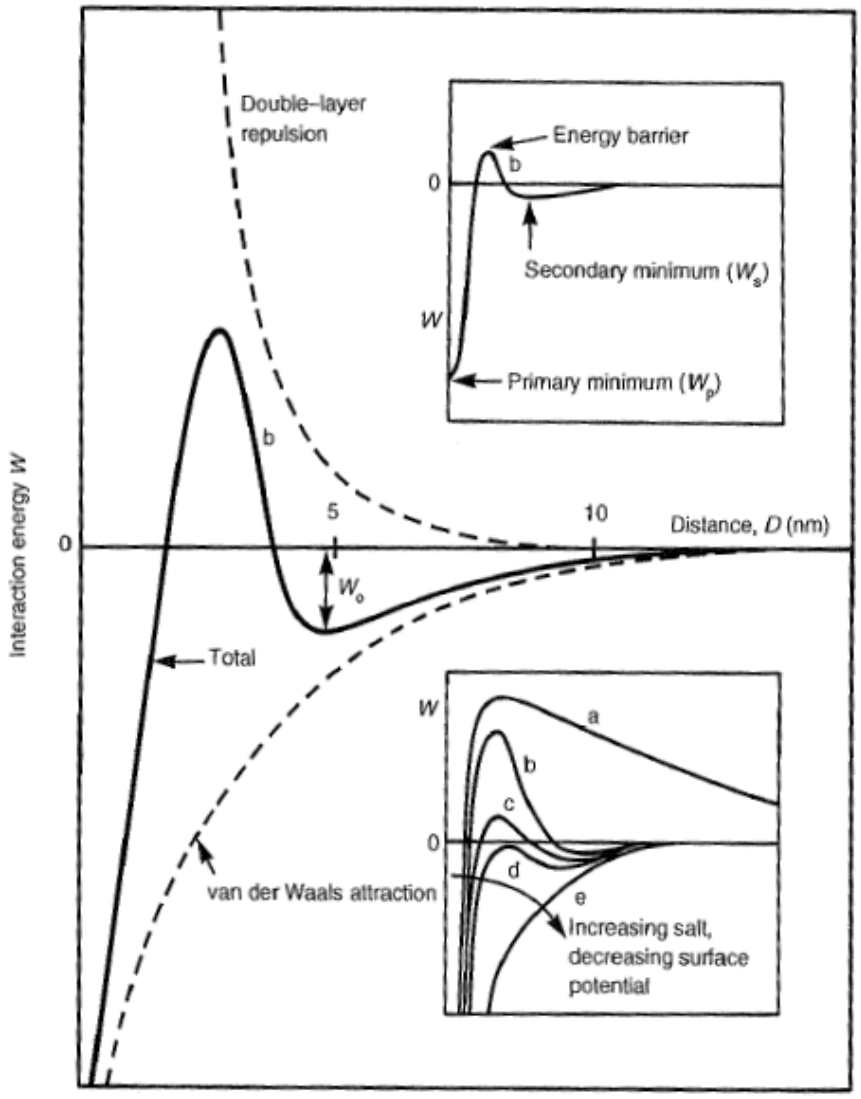

Figure 1: DLVO potential energy of two particles as function of the particle distance [28].

In dependency on the electrolyte concentration and surface charge density one of the following situations may occur:

I. For highly charged surfaces in a diluted electrolyte system, there is a strong long-range repulsion that produces an energy barrier which avoids contact between particles (Fig. 1 – curve a). The suspension is then *stable*.

II. For highly charged surfaces in more concentrated electrolyte solutions there is a significant secondary minimum before the energy barrier (Fig. 1 – curve b). The particles will

either stay in the weak secondary minimum or they will be dispersed in the suspension. The suspension is then *kinetically stable*.

III. For low charged surfaces in a diluted electrolyte system, the energy barrier is lower (Fig. 1 – curve c). This leads to slow aggregation or flocculation. The suspension is then *unstable*.

IV. For low charged surfaces in a concentration of electrolyte above a certain threshold concentration, known as *critical coagulation concentration*, the energy barrier disappears (Fig. 1 – curve d). The suspension is then *unstable* and the particles coagulate rapidly.

V. For a surface charge around zero, the potential of interaction approaches the pure Van der Waals curve, and the particles attract each other strongly (Fig. 1 – curve e). The suspension is then *unstable* and collapses.

The main difference among the analyzed curves is the presence or absence of the energy barrier. This barrier avoids particle attraction, and the consequent flocculation. Steric repulsion owed to presence of a polymer in solution is not included in this theory. It is not described in the literature; however it is reasonable to assume that the repulsive force provoked by the adsorbed polymer layer around the particles increases the height of this maximum of the potential curve, providing a strong hindrance to particles agglomeration. No experimental evidence for this effect exists, as the present models fail to quantify structural effects observed for large molecules [29].

In the following chapters, the experimental investigations of these forces playing a role at the solid-liquid interface are presented. Solutions containing different concentrations of electrolytes and polyelectrolytes are studied to allow a comprehensive understanding of the behavior of polycarboxylate superplasticizers in cement mixtures.

4 Materials

The complete set of the applied materials is presented in this chapter. A general overview about their usage and the motivations of these choices are reported here. Additional details and related results can be found in the publications which are part of this thesis.

4.1 Polycarboxylate superplasticizers

Different polycarboxylate ether-based superplasticizers were tested in this study. Their chemical composition (Figure 2) is presented by a main chain of carboxylic groups (n) organized in a comb structure with ethylene oxide (EO) units in the side chain (m).

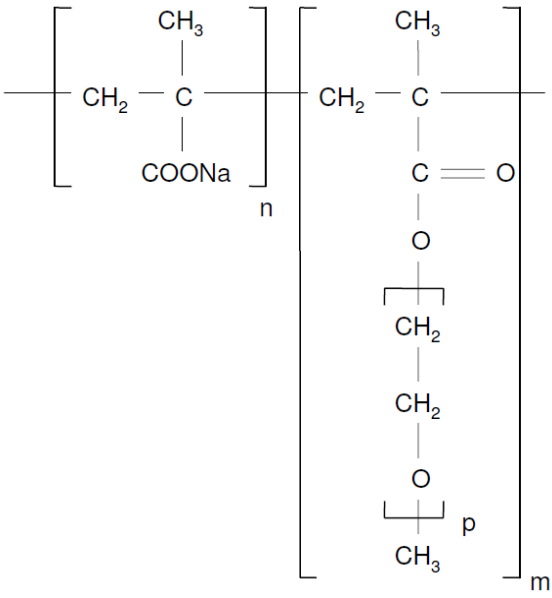

Figure 2: Chemical structure of polycarboxylate ether (PCE) superplasticizer.

Varying the number of carboxylic groups and the number of EO units (p), different polymer architectures are obtained. The superplasticizers tested in this work differentiate between n:m = 1.5, 3, 6, 12, and p = 8.5, 23, 45, 111. The average molecular weights varied from 18,900 g/mol up to 520,400 g/mol. The corresponding charge densities (CD), calculated as the ratio between the moles of anionic charge and the molar mass of each PCE unit, ranged from 0.3 to 4.2 anion mol/ total mol A complete table with details about the PCEs tested is reported in paper 2.

4.2 Surface materials

As already mentioned, the AFM method requires well-defined, smooth and non-reactive substrates. For this reason, different model systems were applied to perform the force measurements. The selection of materials to be tested as suitable AFM substrates was carried out according to their actual or potential use as building materials, their purity, their low reactivity, and their relatively smooth external surface, or their importance in early cement hydration.

In a first analysis, quartz, mica, calcite and magnesium oxide substrates (see Figure 3) were considered.

Mica Quartz Calcite Magnesium oxide Cement clinker

Figure 3: Model mineral substrates for the AFM force measurements.

Crystals provide an atomically flat surface which is ideal for AFM force measurements in liquids. Mica can be easily cleaved, while amorphous MgO required a polishing treatment. However, among this set of materials, only magnesium oxide shows a high affinity to PCE (see paper 1). For this reason, the other three substrates, which display a poor superplasticizer adsorption, were dropped from the force AFM measurements.

In order to work with a substrate that is closer to cement, the surface of a polished clinker was analyzed. The main questions related to this substrate are its reactivity with water and the coexistence of different phases, which were shown to behave quite differently with respect to PCE [17-30]. The clinker reactivity was assessed by AFM images scanned in different positions, at various time intervals of hydration performed in deionized water and in solutions containing different kinds of electrolytes (see Table 1) [31]. These results are reported in paper 4.

Table 1: Ionic composition of the solutions tested with AFM technique (mmol/L)

	SO_4^{2-}	Na^+	K^+	Ca^{2+}	OH^-	pH
0.1 M KOH	0	0	100	0	100	13.0
0.1 M K_2SO_4	100	0	200	0	0	8.1
Synthetic cement pore solution	200	40	444	10	104	12.8

To observe PCE adsorption on different phases, Time-of-Flight Secondary Ion Mass Spectrometry (ToF-SIMS) measurements were performed on clinker surface previously wetted with a solution containing superplasticizer, and then washed and dried (see paper 5).

Since the highest affinity between PCE and different cement phases was shown by ettringite [17], this pure substrate was also applied in the AFM force measurements. Unfortunately, ettringite crystals show a relatively small size (few µm) that creates difficulties to handle them for the substrate preparation (see Figure 4).

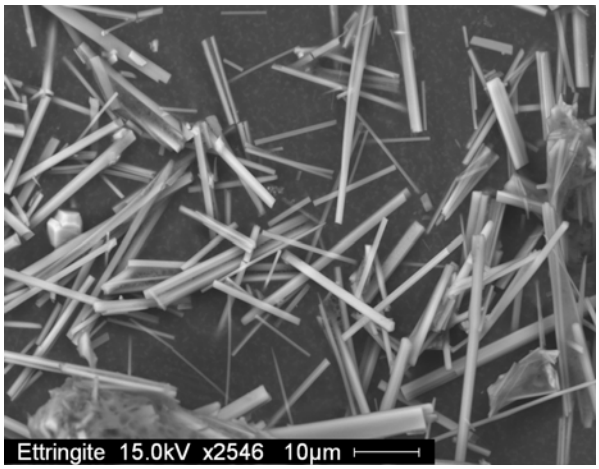

Figure 4: SEM image of synthesized ettringite crystals.

Dispersion forces due to polycarboxylate-ether-based superplasticizer (PCE) in different electrolyte solutions at the surface of ettringite crystals were studied by atomic force microscope (AFM) applying a spherical glass probe. The goal was to reproduce in the AFM setup the attraction, usually occurring in cement mixtures, between positively charged ettringite particles and negatively charged cement grains. More details can be found in the section *Supplementary results*.

4.3 Powder materials

In order to detect the adsorption and the ζ-potential of the substrates applied with the AFM technique, measurements on inert and model powders were also performed. The investigated inert powders were the same materials as used for the AFM force measurements: quartz, mica, calcite and magnesium oxide. Details about these materials are reported in paper 1. However, as already explained, all of them, with the exception of MgO, showed a low affinity towards PCE. Additionally, silicon nitride powder was also tested to detect superplasticizer adsorption on standard AFM tips (see paper 1). Due to the different specific surface areas, the water-to-solid ratios used to mix them varied from experiment to experiment, form material to material. More details are reported in papers 1, paper 2 and paper 3.

To test the effect of PCE on the workability of cement pastes, two cements possessing different amounts of tricalcium aluminate were considered. They were mixed with deionized water at a water-to-cement ratio (w/c) of 0.36. This low w/c allowed a clear detection of the effect of PCE on cement rheology. Moreover, to compare workability properties with the AFM measurements, magnesium oxide and calcite pastes were also tested using a rheometer. Details about rheology tests are reported in paper 2 and paper 3.

5 Methods

In this chapter, an overview of the main methods applied in this thesis is presented. The scope and the working principles of the techniques used are described. The sample preparation and further details about the measurements performed can be found in the papers.

5.1 Rheology

Rheological measurements were performed to test the workability of different pastes and to quantify the effect of superplasticizers. In cement pastes, as well as in blends characterized by a high solid fraction, the particles which are in contact with each other create a sort of weak solid structure, which needs to be broken to allow the flow of the paste. From a mathematical point of view, this effect is described as *Bingham* model [32]. Below a certain applied yield stress τ_0, the paste behaves as a rigid body and it does not move. Above this limit, the paste starts flowing and the particles move with the liquid under viscous forces, with a shear rate which is linear to shear stress.

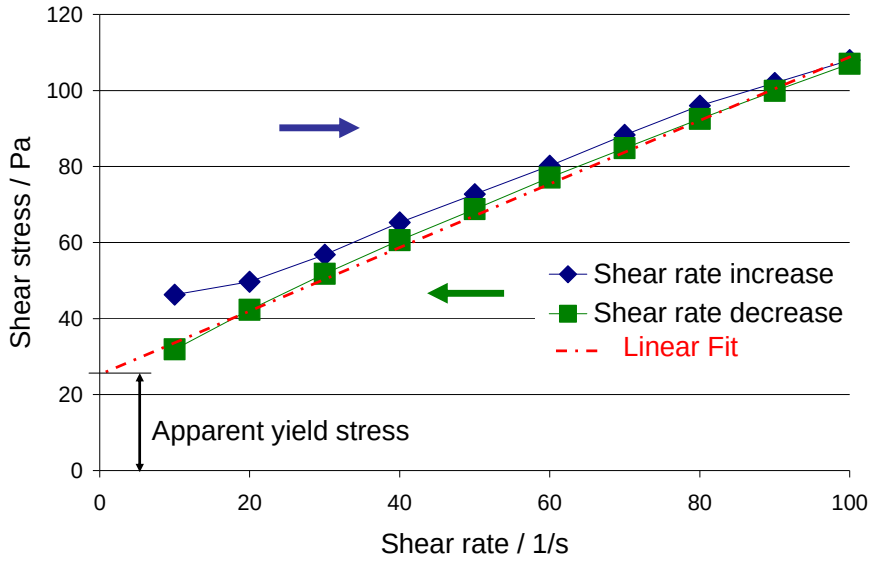

$$\begin{cases} \tau < \tau_0 \rightarrow rigid-body \Rightarrow \dot{\gamma} = 0 \\ \tau \geq \tau_0 \rightarrow viscous-\ fluid \Rightarrow \dot{\gamma} - \tau : linear \end{cases}$$

Figure 5: Bingham model representing the flow behavior of a typical cement paste.

The effect of PCE is to reduce the apparent yield stress, provoking good flowability to the cement paste. During rheology measurements performed by a Paar Physica MCR 300 rheometer with concentric cylindrical geometry, the shear stress applied was increased from 10 to 100 s^{-1} and then decreased from 100 to 10 s^{-1}, and the corresponding shear rates were measured. The apparent yield stress was extracted as the intercept of the linear regression curve calculated from the data collected. A detailed explanation of the data analysis starting from a flow curve to the calculation of the yield stresses is reported in paper 2. Water-to-powder ratios ranging from 0.32 to 1 were tested, due to the large difference in specific surface areas of the sample materials.

5.2 Adsorption

Adsorption isotherms were collected to determine the amount of PCE adsorbed on the materials tested. The solution depletion method was used to prepare the samples. After the mix of the powder with the superplasticizer and the solution, the suspension was centrifuged and the polymer left in the liquid phase was detected by total organic carbon (TOC) analysis (see Figure 6).

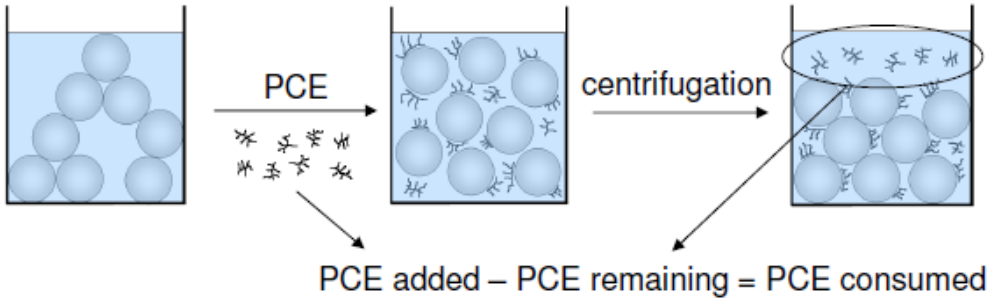

Figure 6: Illustration of the solution depletion method utilized to asses PCE adsorption.

To detect the carbon content, the UV/persulfate oxidation method was employed by a Sievers 5310 Laboratory TOC-Analyzer. This method uses UV light to oxidize the carbon within the sample producing CO_2. Detection and quantification of the carbon dioxide, by membrane conductometric method, provides then the amount of carbon contained in the analyzed solution.

Different particle concentrations and different PCE dosages were used. For instance, to compare the results with those gained from the AFM method, a diluted regime with a particle solid fraction of 5 % or 10 % was used (see paper 1 and paper 2). On the other side, to compare results

with the rheology tests, the samples were prepared with the same water-to-powder ratios as applied in the rheometer (see paper 2).

5.3 ζ-potential

ζ-potential is the potential of the electric double layer measured a certain distance from the particle surface (see Figure 7). In many cases, the surfaces in liquid bind layers of molecules or ions or polyelectrolytes, and as result the slipping plane is often not directly at the solid-liquid interface. At a distance away from the surface where the molecules start to move, the ζ-potential is occurring.

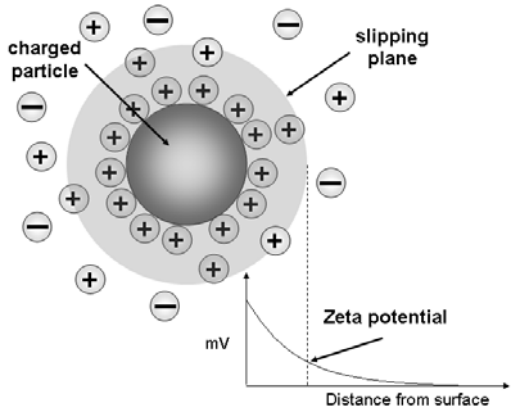

Figure 7: Schematic illustration of the electric double layer and ζ-potential

Quantification of the ζ-potential of particles in suspension was performed by the electroacoustic method applying a ZetaProbe instrument from Colloidal Dynamics Inc. The motion of particles in suspension driven by an electrical field is recorded as dynamic electrokinetic mobility, from which the ζ–potential is then calculated. All the ζ-potential tests were performed in diluted suspensions, in order to compare the results with the AFM force measurements (see paper 1, paper 2, and paper 3).

5.4 Atomic force microscopy

Atomic force microscopy (AFM) enabled the detection of nano-forces occurring in the liquid system as a result of superplasticizer interaction. The AFM apparatus consists of a cantilever with a sharp tip (probe) at its end that is used to scan the specimen substrate (see Figure 8). When the tip is brought into proximity of a sample surface, the interaction between the tip and the sub-

strate allows to perform topography images and force-distance curves. In this work, besides force measurements in liquid (see paper 1, paper 2, paper 3, paper 4, paper 5, and supplementary results), AFM was also applied to quantify surface reactions (see paper 1 and paper 4), and to observe PCE displacement on the surface in dry conditions (see paper 3).

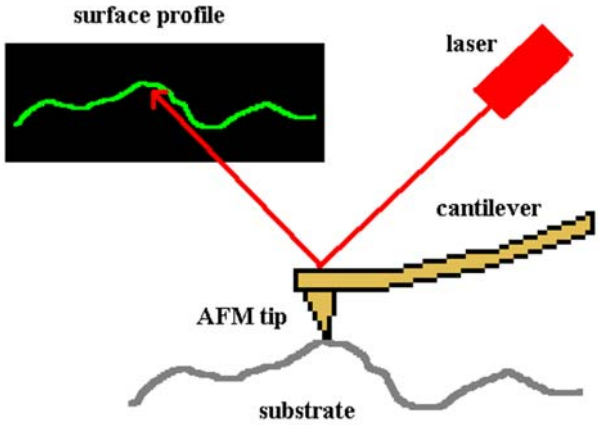

Figure 8: Basic principles of AFM measuring technique

Figure 9 shows step by step how the force measurements in liquid were performed. From left to right, a picture of the fluid cell, its schematic representation, the tip-substrate approach and the force-distance curve are shown.

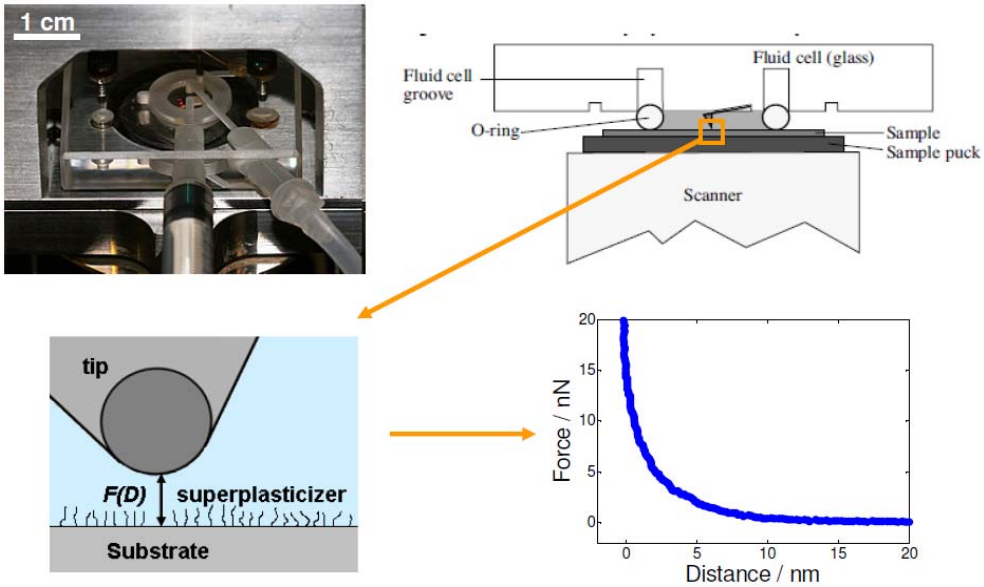

Figure 9: AFM measuring technique. From top-left to down-right: photo of fluid cell, schematic illustration of fluid cell, tip-substrate approach, and measured force-distance curve.

The Nanoscope IV instrument from Veeco enables the installation of the wet-cell facility which provides contact mode AFM in fluid environments. A silicon O-ring enclosed a fluid with the ability to exchange liquids. Notice that the whole tip-substrate system is immersed in the solution, and while the tip is approaching the surface, the cantilever deflects in response to the surface forces. The deflection is collected as function of the distance and converted into a force by the cantilever spring constant, measured by the resonant frequency method [33]. Details about the conversion of the raw data into a force-distance curve are reported in Table 2 and in paper 1.

Table 2: Steps involved in the conversion of raw AFM data into a force-distance curve.

Steps to convert Force - Z-position curve to Force - Distance curve:	
1. plot the raw data of Deflection - Z-positon curve, take either approach curve or withdraw curve; 2. define the zero line, take the average value of data points far apart from the surface (as far as no tip-surface interaction); 3. shift the curve so that the deflection at zero line is 0 nm; 4. fit the linear part of the F-Z curve, plot the fit line, obtain the sensitivity (S) (slope of the linear part); 5. calculate the distance D, using: D= (Z-Z_0) + (F-F_0)/S + 0.2nm (solid contact distance = 0.2 nm), where S is sensitivity, Z is raw data of position, F is raw data of deflection, Z_0 is the defined surface, F_0 is the deflection at the Z_0; 6. calculate the force, Force = deflection data * spring constant; 7. Plot the F - D curve.	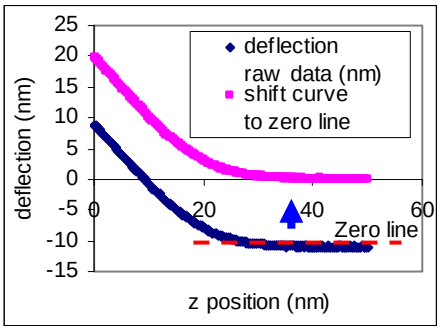 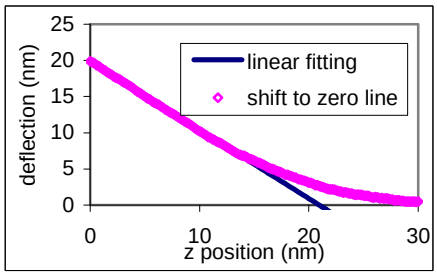 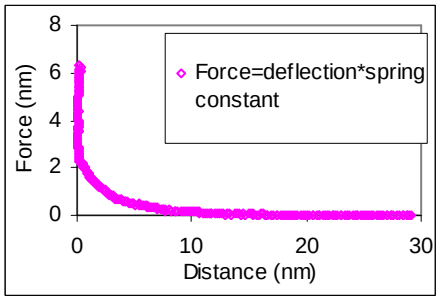

In this work, different AFM tips were applied according to the necessity (see Figure 10). Standard silicon nitride tips were applied due to their easy availability on the market. However, since

they adsorb PCE and their radius is unpredictable, silicon plateau tips coated with platinum were used [34]. Working on heterogeneous substrate, such as clinker surface, a silicon sharp tip is desirable to distinguish between forces caused by one phase or the other. A proper quantification of dispersion force was then performed by spherical tips.

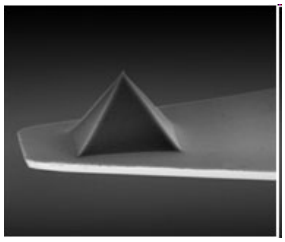

Silicon nitride

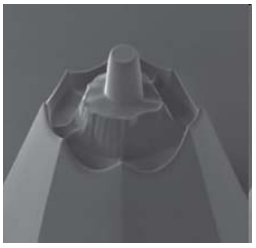

Plateau platinum

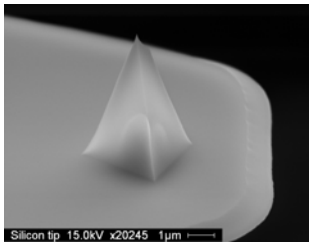

Sharp silicon dioxide

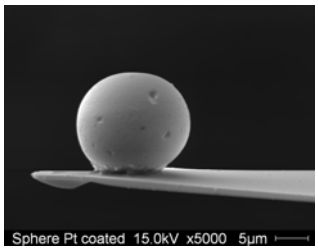

Spherical silicon dioxide

Figure 10: Images of the AFM tips tested.

Utilizing this apparatus, different solutions (see Table 1 in chapter 4) containing concentrations of PCE ranging from 0.2 g/L to 4 g/L were flushed on different substrates (see section 4.2). For each of the paper included in this thesis, different combinations of tips, substrates, solutions and PCEs were used.

6 Results and discussion

The main results emerging from the whole set of publications are collected and correlated in this chapter. They are distinguished according to the topics.

6.1 Characterization of AFM setup (paper 1)

Possible model substrates and characterization of the AFM setup were carried out by comparing AFM dispersion forces with adsorption and ζ–potential measurements. The results are presented in paper 1.

The results show that PCE-type superplasticizers have a tendency to adsorb preferentially on positively charged materials, due to their negative backbones. Consequently, magnesium oxide represents a good model system owing to its affinity towards superplasticizer. On the other side, it was shown that also silicon nitride tips adsorb PCE, providing misleading results caused by the unpredictability of the tip radius.

Furthermore, when adsorbed, PCEs change the particles' zeta potential from positive to negative or zero. The results obtained show that repulsive forces can also occur between low adsorbing materials, *i.e.* negatively charged particles. These dispersion forces are reasonably generated by electrostatic contribution (see Figure 11).

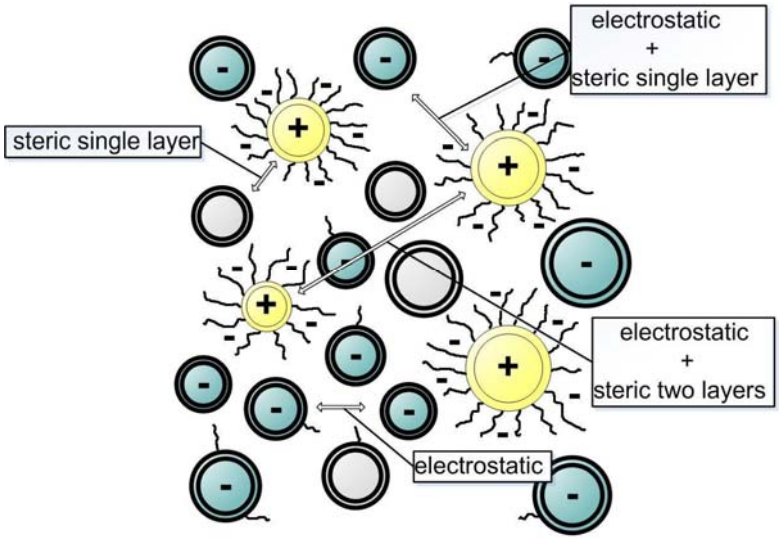

Figure 11: Schematic illustration of a multi-phase particle suspension

It was concluded that in a multi-phase suspension PCEs are mainly adsorbed by positively charged particles, and when adsorbed they change the particle charge from positive to negative. Thus, the particles in a mixture become homogeneously charged, and consequently well dispersed. Additionally, the steric force helps the stabilization of the particle suspension.

6.2 Influence of different polymer architectures (papers 2 and 3)

The influence on PCE performance with respet to its dispersion ability in respect to different polymer architectures, ion contents in solution, and the amount of ettringite formed in cement is presented in paper 2 and 3.

The results elucidate that a high anionic polymer charge affords high adsorption of superplasticizers and good rheological properties of the mixed pastes. However, the electrostatic and steric dispersion forces are influenced by the length of side chains, which provide different effects. Indeed, PCEs holding short side chains provoke strongly negative values of the ζ–potential, and higher ranges and intensities in the AFM force measurements, in contrast to superplasticizers holding long side chains. Figure 12 a diagram in which this concept is schematically summarized.

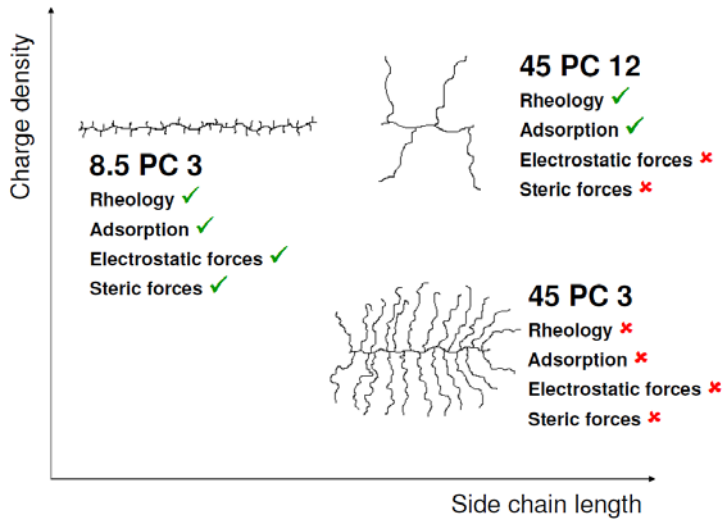

Figure 12: Diagram of superplasticizer performances with respect to different polymer architectures.

Moreover, tests on inert powders clarify that the presence of different electrolytes in solution affects PCE adsorption, and consequently the apparent yield stress values. The comparison be-

tween force measurements obtained in milli-Q water and in synthetic cement pore solution reveals that dispersion forces are also affected by ionic species in solution.

The AFM measurements also show that PCE architectures with relatively short side chains lead to dispersion forces which vary with the concentration of superplasticizer in solution, possibly because of the formation of multi-layers at the surface. Images of PCE displacement on flat surfaces confirmed that PCEs with short side chains accumulate on the surface overlapping different polymer films, while PCEs possessing long side chains remain mainly separated, thus forming domains on the surface (see Figure 13).

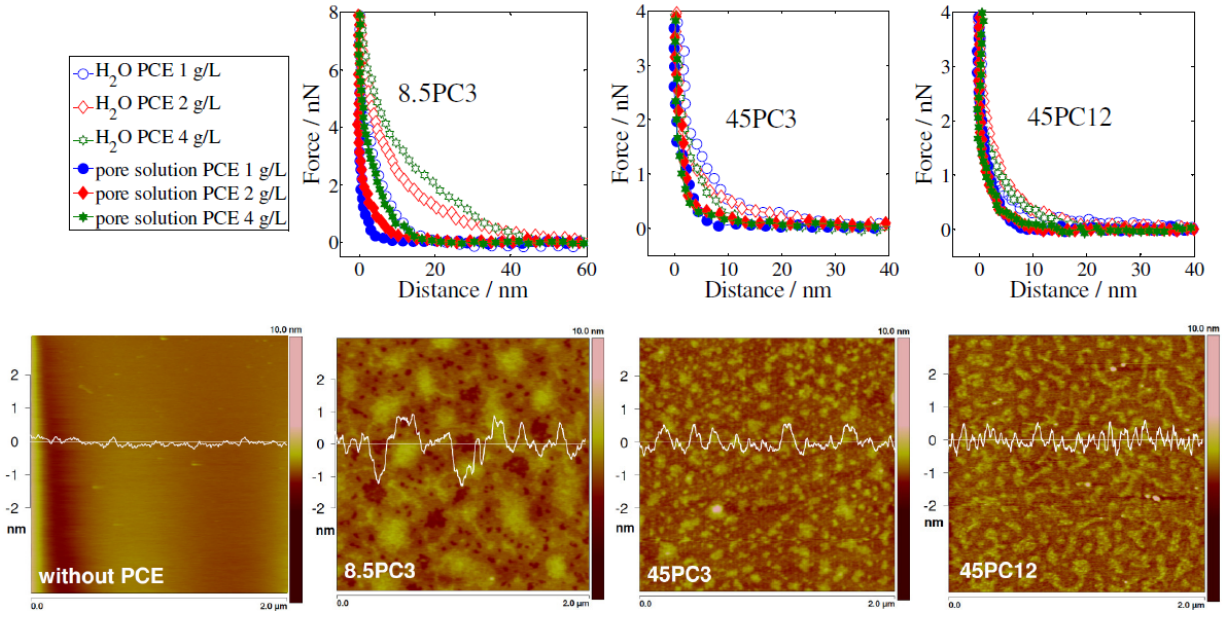

Figure 13: Above: AFM force measurements in water and synthetic cement pore solution containing different PCE concentrations. Below: AFM images of the appearance of adsorbed PCE on mica surfaces.

Another aspect emerging from this multi-method analysis concerns the idea that rheological properties are not only depending on PCE adsorption and PCE dispersion forces. This observation could potentially be explained by the existence of a third effect which avoids direct contact between particles and lubricate particle surfaces, in order to reduce the friction between adjacent grains. Furthermore, it is expected that the properties of the liquid also are affected by the presence of PCE: if the water-solid interface is energetically favorable, then it increases the wettability of the particle surface and the water will have the tendency to distribute around the particles. More research in this direction is hence needed.

6.3 Behavior of clinker surface (papers 4 and 5)

Studies about reactions at the clinker surface in different electrolyte solutions and PCE adsorption on clinker substrates are reported in paper 4 and paper 5.

The surface reactions of most of the studied systems occur very fast, depending on the ion species in solution and on the pH, which both accelerate the reactions. The formation of hydration products varies according to the ions present in solution. Precipitation of gypsum increases when the clinker is immersed in a potassium sulfate solution, while when immersed in cement pore solution, a variety of mixed phases is detected on the clinker surface. Furthermore, the direct comparison between clinker hydrated in deionized water and clinker hydrated in deionized water containing PCE shows that the presence of superplasticizer retards effect in the formation of portlandite and other hydrated phases (see Figure 14).

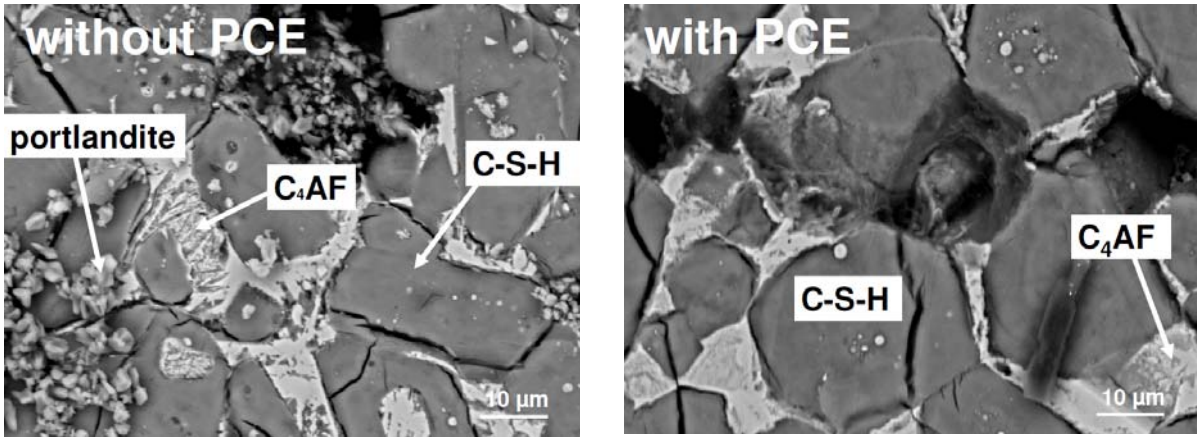

Figure 14: Optical microscopy of the clinker surface after 18 hours of hydration in water without PCE (left) or in water with PCE (right). Note that the amount of hydration products formed is reduced when the clinker is exposed to PCE solution.

Due to the high reactivity of the clinker surface, force measurements were performed only in deionized water. On the other side, the heterogeneity of the surface does not allow a good interpretation and characterization of the AFM results, because not all the cement phases show the same affinity towards superplasticizer. For this reason, adsorption of PCE on clinker phases was studied by time-of-flight secondary ion mass spectrometry (TOF-SIMS).

The results obtained with TOF-SIMS in combination with SEM/EDX analysis reveal the morphology and the chemical distribution of elements on the substrate. The comparison between spectra obtained on samples with and without superplasticizer gives the opportunity to directly detect

PCE fragments, and to directly observe their position on the clinker surfaces. It is shown that PCE induces precipitations of K_2SO_4, thus reducing the amount of sulfate ions available in the pore solution, and probably reducing the amount of ettringite formed during cement hydration (see Figure 15).

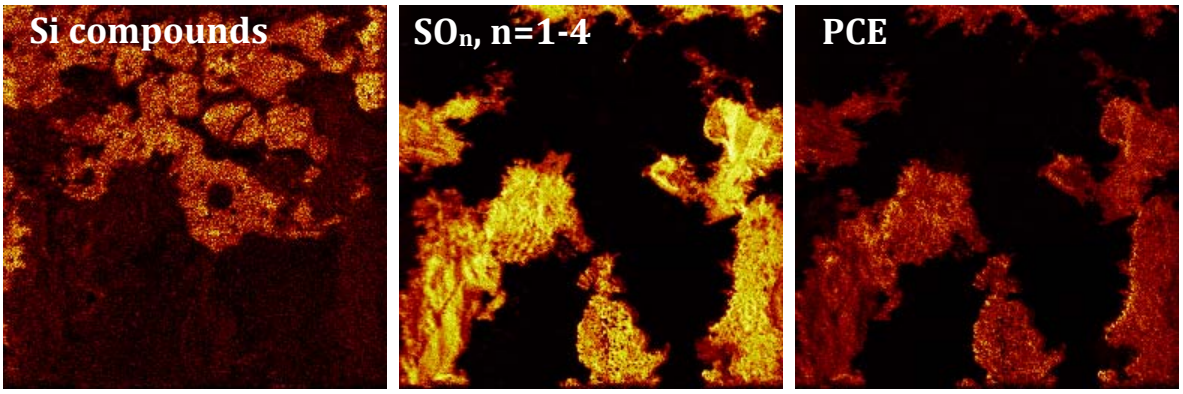

Figure 15: TOF-SIMS representative maps of the most significant compounds, *i.e.* Si, SO_n, and PCE, on the clinker surface after adsorption of PCE from solution. Size 200x200 µm². Note that the pattern of sulphur compounds is the same as that of PCE.

Force measurements by AFM reveal the different charges of cement phases, which is negative in most cases. Curves detected on needle-shaped ettringite crystals, which are rather narrow in width, were possible owing to the application of a sharp tip. The collected plots support the idea that in a multiphase suspension superplasticizers lead to a homogeneity in charge and interaction between phases. In the future work, better characterization of the ettringite phase is required to allow further information about the role of this phase in cement workability.

6.4 Preliminary results obtained on ettringite substrate

Investigations of ettringite surfaces probed with a spherical AFM tip made of silicon dioxide aim to properly investigate the forces occurring between these two materials which form agglomerates in cement suspensions. Preliminary results show that forces collected in water without PCE present a strong attraction between the silicon dioxide tip and the ettringite crystal. However, when the pH and the ionic strength increase, the ettringite substrate becomes negatively charged, and the tip and the substrate experience repulsion forces even in absence of PCE (see Figure 16).

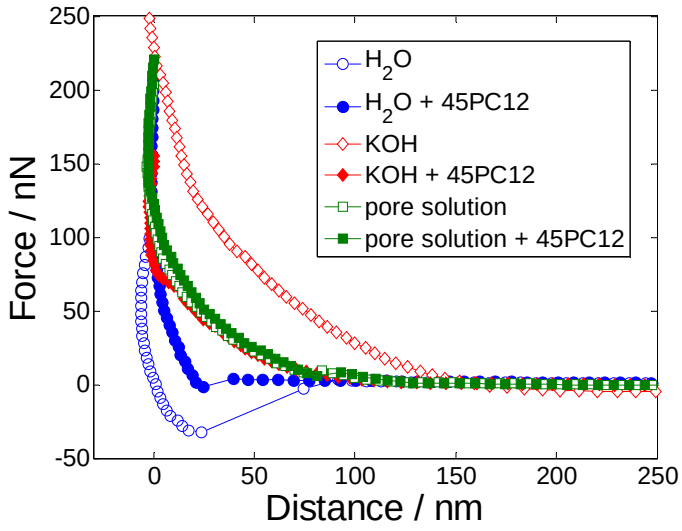

Figure 16: Force-distance measurements collected on ettringite crystal surface by the application of silicon dioxide spherical tips.

7 Conclusions and outlook

In this thesis, different aspects of AFM force measurements in solutions containing PCE superplasticizer are highlighted.

A list of suitable materials to be applied as substrate is presented underlining positive and negative aspects of each of them. Quartz, calcite and mica are smooth and unreactive substrates, but they do not adsorb high amounts of PCE due to their negative surface charge. Magnesium oxide adsorbs superplasticizers well, but it reacts relatively quickly in high pH solutions. Clinker polished surface is also suitable for AFM force measurements, but the results can be collected exclusively in deionized water, due to the high reactivity of cement clinker in electrolyte solutions. Furthermore, the heterogeneity of the clinker surface requires as sophisticated technique for direct detection of PCE adsorption on the different phases. Ettringite shows a relatively optimal surface for AFM force measurements, trough the preparation of large ettringite crystals is not trivial.

Relevant effects influencing the effects of PCEs are adsorption and concentration of superplasticizer, the electrolyte solution, the polymer architecture, and the cement phase on which the forces were tested. Indeed, PCEs with short side chains form multi-layers when the concentration of polymer increases. Moreover, the presence of ions in solution reduces the Debye length at the surface, thus reducing force-ranges and force-intensities. On the other side, surface charge causes attraction or repulsion forces between the tip and the substrate in absence of superplasticizer.

Some issues remained unresolved regarding different aspects of AFM force measurements and the effect of PCE on cement suspensions. These open questions can be highlighted as:

- How to quantify force measurements? The way to reproduce a perfect and ideal environment representative of the solid-liquid interface generally occurring in cement is still not optimized, due to the variety of possibilities existing in concrete mixtures.
- Is total organic carbon a suitable technique to verify the adsorption of superplasticizer at the solid-liquid interface? The solution depletion method explained does not allow to detect if the polymer really adsorbs on particle surface or if the polymer remains simply trapped between particles. It is possible that the techniques used to extract the liquid phase from the suspensions, *i.e.* filtration or centrifugation, are relatively too strong,

causing partial desorption of PCE. Indeed, working with AFM in liquid containing PCE, attraction between the tip and the substrates was never observed, revealing the presence of a polymer layer also on materials where, according to TOC measurements, the polymer was not adsrobed.

- Is magnesium oxide a proper and satisfying cement model system? MgO shows high affinity towards PCE, but its chemical composition is rather distant from the typical composition of cement phases, bringing the question that it might be not really representative.

- Dispersion forces due to PCE have intensities of few nano-Newtons at distances of around 10 nanometers from the surface. Is this enough to disperse particles in cement pastes, which have an average radius of around 10 μm? Do these forces simply represent a lubricating effect of the superplasticizers? Does PCE play an entropic role at the solid-liquid interface, increasing the wettability of the particle surface?

- How to directly link dispersion forces and final rheological properties of particle pastes? The DLVO theory is well applicable to colloidal systems, which range in a particle size distribution between 1 nm and 1 μm. Cement pastes are still far from behaving as a colloidal suspension, due to the different size of its particles, which has the tendency to sink due to their high weight.

Research with additional techniques is needed to understand the effects which are not explainable with the presented methods. Measurements by fixed angle laser reflectometry in fluid can provide information about PCE coverage of a surface, with a relatively less intrusive method in comparison to the depletion method. Contact angle and surface tension data can confirm or contradict the hypothetical entropic role of superplasticizers in increasing the wettability of particle surfaces. Moreover, further results may contribute to the construction of a new rheological model that considers particle-particle interactions as a starting point to calculate an effective potential which includes the steric effect, in order to predict the stability and the rheological properties of cement pastes.

References

[1] H.F.W. Taylor, Cement Chemistry, second ed., *Thomas Telford Publishing*, London, 1997.

[2] C. Hu and F. De Larrard. The rheology of fresh high performance concrete. *Cem. Concr. Res.* 26 (2) 1996, 283-294.

[3] K. Kovler, N. Roussel. Properties of fresh and hardened concrete. *Cem. Concr. Res.* 41 (2011) 775-792.

[4] T. G. Mezger. The rheology handbook. Hannover, *Vincentz Network* (2006), 2nd Edition Coatings Compendia.

[5] O. H. Wallevik and E.J. Wallevik. Rheology as a tool in concrete science: The use of rheographs and workability boxes. *Cem. Concr. Res.* (2011).

[6] V.S. Ramachandran. Concrete Admixtures Handbook: properties, science and technology. *Noyes Publication* (1995) 2nd Edition, Printed in USA.

[7] J. Plank, K. Pöllmann, N. Zouaoui, P. R. Andres, and C. Schaefer. Synthesis and performance of methacrylic ester based polycarboxylate superplasticizers possessing hydroxy terminated poly(ethylene glycol) side chains. *Cem. Concr. Res.* 38 (2008), 1210-1216.

[8] F. Winnefeld, S. Becker, J. Pakusch, T. Götz. Effects of the molecular architecture of comb-shaped superplasticizers on their performance in cementitious systems. *Cem. Concr. Compos.* 29 (2007) 251-262.

[9] G. H. Kirby and J. A. Lewis. Comb Polymer Architecture Effects on the Rheological Property Evolution of Concentrated Cement Suspensions. *J. Am. Ceram. Soc.* 87 [9] (2004) 1643-1652.

[10] A. Zingg, L. Holzer, A. Kaech, F. Winnefeld, J. Pakusch, S. Becker, L. Gauckler, The microstructure of dispersed and non-dispersed fresh cement pastes - New in-sight by cryo-microscopy. *Cem. Concr. Res.* 38 (2008) 522-529.

[11] S. Hanehara, K. Yamada. Interaction between cement and chemical admixture from the point of cement hydration, adsorption behaviour of admixture, and paste rheology. *Cem. Concr. Res.* 1999; 29(8) 1159-65.

[12] A. Zingg, F. Winnefeld, L. Holzer, J. Pakusch, S. Becker, R. Figi, L. Gauckler. Interaction of polycarboxylate-based superplasticizers with cements containing different C_3A amounts. *Cem. Concr. Comp.* 31 (2009) 153-162.

[13] J. Plank, Ch. Winter. Competitive adsorption between superplasticizer and retarder molecules on mineral binder surface, *Cem. Concr. Res.* 38 (2008) 599-605.

[14] K. Yamada, A Summary of Important Characteristics of Cement and Superplasticizers, Proceedings of the *9th International Conference on Superplasticizers and Other Chemical Admixtures in Concrete* (2009) ACI SP-262, pp.85-95.

[15] K. Yamada, S. Ogawa, and S. Hanehara. Controlling of the adsorption and dispersing force of polycarboxylate-type superplasticizer by sulfate ion concentration in aqueous phase. *Cem. Concr. Res.* 31, (3) (2001) 375-383.

[16] J. Plank, C. Hirsch. Impact of zeta potential of early cement hydration phases on superplasticizer adsorption. *Cem. Concr. Res.* 37 (2007) 537-542.

[17] A. Zingg, F. Winnefeld, L. Holzer, J. Pakusch, S. Becker, L. Gauckler. Adsorption of polyelectrolytes and its influence on rheology, zeta potential, and microstructure of various cement and hydrate phases. *J. Coll. Int. Sci.* 323 (2008) 301-312.

[18] H.-J. Butt, K. Graf, M. Kappl. Physics and Chemistry of Interfaces. 2003 *Wiley-VCH Verlag GmgH & Co. KGaA*, Weinheim.

[19] H.-J. Butt, M. Jaschke, W.A. Ducker, Measuring surface forces in aqueous electrolyte solution with the atomic force microscope. *Bioelectrochemistry and Bioenergetics* 38 (1995) 191-201.

[20] H.-J. Butt, Measuring electrostatic, van der Waals, and hydration forces in electrolyte solutions with an atomic force microscope. *Biophys. J.*, 60 (1991) 1438-1444.

[21] H. Uchikawa, S. Hanehara, D. Sawaki. The role of steric repulsive force in the dispersion of cement particles in fresh paste prepared with organic admixtures. *Cem. Concr. Res.* 27 (1997) 37-50.

[22] S. Yamamoto, M. Ejaz, Y. Tsujii, M. Matsumoto, and T. Fukuda, Surface interaction forces of well-defined, high-density polymer brushes studied by atomic force microscopy. Effect of chain length. *Macromolecules*, 33 (2000) 5602-5607.

[23] A. Kauppi, K.M. Andersson, L. Bergström. Probing the effect of superplasticizer adsorption on the surface forces using the colloidal probe AFM technique. *Cem. Concr. Res.* 35 (2005) 133-140.

[24] H. Yilmaz, T. Isobe, Y. Hotta, K. Sato, and K. Watari. Polyelectrolyte mediated interaction of alumina in wet jet milled slurry/ball milled slurry supernatants. *Journal of the Ceramic Society of Japan* 114 [11] 2006, 1100-1102.

[25] R.J. Flatt, I. Schober, E. Raphael, C. Plassard, and E. Lesniewska. Conformation of adsorbed comb copolymer dispersants. *Langmuir* 25 (2009) 845-855.

[26] W.A. Ducker, T.J. Senden, and R.M. Pashley. Direct measurement of colloidal forces using an atomic force microscope. *Nature* 353 (1991) 239-241.

[27] K. S. Birdi. Surface and Colloid Chemistry: principles and applications. CRC press, 2010, *Taylor & Francis Group*.

[28] J. Israelachvili. Intermolecular & Surface Forces. 2nd edition, Academic press, 1991, *Elsevier Ltd*.

[29] U. Aschauer, O. Burgos-Montes, R. Moreno, and P. Bowen. Hamaker 2: A Toolkit for the Calculation of Particle Interactions and Suspension Stability and its Application to Mullite Synthesis by Colloidal Methods. *J. Disper. Sci. Technol.*, 32:4 (2011) 470-479.

[30] F. Kreppelt, M. Weibel, D. Zampini, M. Romer, Influence of solution chemistry on the hydr tion of polished clinker surfaces – a study of different types of polycarboxylic acid-based admixtures, *Cem. Concr. Res.* 32 (2002) 187-198.

[31] B. Lothenbach, F. Winnefeld. Thermodynamic modeling of the hydration of Portland cement, *Cem. Concr. Res.* 36 (2) (2006) 209-226.

[32] G. H. Tattersall, and P. F. G. Banfill. The Rheology of Fresh Concrete, *Pitman Advanced Publishing*, Boston (1983).

[33] J. E. Sader, I. Larson, P. Mulvaney, L. R. White, Method for the calibration of atomic force microscope cantilevers. *Rev. Sci. Instrum.* 66 (1995) 3789-2799.

[34] B. Beyribey, B. Corbacioglu, Z. Altin. Synthesis of platinum particles from H_2PtCl_6 with hydrazine as reducing agent. *G.U. Journal of Science* 22 (4): 351-357 (2009).

Paper 1

Interaction of cement model systems with superplasticizers investigated by atomic force microscopy, zeta potential, and adsorption measurements

L. Ferrari, J. Kaufmann, F. Winnefeld, J. Plank

Journal of Colloid and Interface Science 347 (2010) 15-24

Journal of Colloid and Interface Science 347 (2010) 15–24

Contents lists available at ScienceDirect

Journal of Colloid and Interface Science

www.elsevier.com/locate/jcis

Interaction of cement model systems with superplasticizers investigated by atomic force microscopy, zeta potential, and adsorption measurements

Lucia Ferrari [a,b,*], Josef Kaufmann [a,**], Frank Winnefeld [a], Johann Plank [b]

[a] Empa, Swiss Federal Laboratories for Materials Testing and Research, Laboratory for Concrete/Construction Chemistry, Ueberlandstr. 129, 8600 Duebendorf, Switzerland
[b] Technische Universität München, Department of Chemistry, Lichtenbergstr. 4, 85747 Garching, Germany

ARTICLE INFO

Article history:
Received 11 January 2010
Accepted 4 March 2010
Available online 7 March 2010

Keywords:
Atomic force microscopy
Zeta potential
Adsorption
Superplasticizer
Cement model system

ABSTRACT

Polyelectrolyte-based dispersants are commonly used in a wide range of industrial applications to provide specific workability to colloidal suspensions. Their working mechanism is based on adsorption onto the surfaces of the suspended particles. The adsorbed polymer layer can exercise an electrostatic and/or a steric effect which is responsible for achieving dispersion. This study is focused on the dispersion forces induced by polycarboxylate ether-based superplasticizers (PCEs) commonly used in concrete. They are investigated by atomic force microscopy (AFM) applying standard silicon nitride tips exposed to solutions with different ionic compositions in a wet cell. Adsorption isotherms and zeta potential analysis were performed to characterize polymer displacement in the AFM system on nonreactive model substrates (quartz, mica, calcite, and magnesium oxide) in order to avoid the complexity of cement hydration products. The results show that PCE is strongly adsorbed by positively charged materials. This fact reveals that, being silicon nitride naturally positively charged, in most cases the superplasticizer adsorbs preferably on the silicon nitride tip than on the AFM substrate. However, the force–distance curves displayed repulsive interactions between tip and substrates even when polymer was poorly adsorbed on both. These observations allow us to conclude that the dispersion due to PCE strongly depends on the particle charge. It differs between colloids adsorbing and not adsorbing PCE, and leads to different forces acting between the particles.

1. Introduction

Polyelectrolytes are commonly used as chemical additives in industry sections where well-dispersed colloidal suspensions are required. These polymers are utilized as effective dispersants in order to avoid particle aggregation and to improve the rheological properties of different kinds of suspensions. Their key function is simply to disperse the colloids in fresh particle–water mixtures, bringing a repulsive force among them. This effect widely improves many properties of fresh and hardened materials, allowing new developments in technology and practices.

For instance in the field of cement, where these dispersing polyelectrolytes are commonly known as superplasticizers or water-reducing admixtures, their addition to a fresh concrete achieves a reduction of the water to cement ratio of the hardened paste. This reduction allows special flow properties, which are very important for, e.g., high-performance concrete and self-compacting concrete. This water reduction drastically influences early age strength, long-term mechanical properties, durability, permeability, strength, and many other features.

This work is focused on comb-shaped polycarboxylate ether-type superplasticizers (PCE) that are characterized by an adsorbing backbone unit and a hydrophilic polyethylene oxide side chain [1]. PCEs are widely used owing to their versatility: the number and the length of side chains and their grafting density are flexible parameters. When PCE is adsorbed at the solid–liquid interface in a particle suspension, it induces a repulsive interparticle force that avoids the formation of agglomerates [2]. Despite numerous studies investigating the mode of action of superplasticizers, their fundamental interaction mechanisms still remained without complete understanding.

The interaction of colloidal particles with superplasticizers is generally examined applying different methods: adsorption analysis is necessary to quantify the amount of molecules effectively adhering to the colloidal particles; on the other side zeta potential measurements of cement–water suspensions detect the electrostatic impact of the adsorbed polymer layer. Another method utilized to quantify the dispersing force induced by PCE is atomic force microscopy (AFM). AFM, which is generally used to scan

* Corresponding author at: Empa, Swiss Federal Laboratories for Materials Testing and Research, Laboratory for Concrete/Construction Chemistry, Ueberlandstr. 129, 8600 Duebendorf, Switzerland. Fax: +41 (0)44 823 4035.
** Corresponding author.
E-mail addresses: lucia.ferrari@empa.ch (L. Ferrari), josef.kaufmann@empa.ch (J. Kaufmann).

0021-9797/$ - see front matter © 2010 Elsevier Inc. All rights reserved.
doi:10.1016/j.jcis.2010.03.005

image topography of surfaces with high resolution, allows direct quantitative measures of the force as a function of the distance from the surface in aqueous solution [3]. However, when the AFM tip is immersed in a pure electrolyte solution above a substrate reporting a charged surface, it experiences forces of many different origins, and they may change from attractive to repulsive, depending on the tip charge [4]. This complicates the interpretation of the force–distance curves.

If the electrolyte solution contains superplasticizers, the main three forces felt by the tip are van der Waals attraction, steric repulsion, and electrostatic interaction. The attractive van der Waals force decreases depending on the dimension of the object approaching the substrate and on the inverse of the distance. Since the radius of the commercially available standard V-shaped tip is estimated in the range of less than 20 nm, the van der Waals contribution is so low that it can be neglected. In this way, the measured force is accepted to be the sum of steric and electrostatic components [2]. The electrostatic force arises because particle surfaces are charged at the liquid–solid interfaces; however, the steric interaction is given by the brush formed by the side chains of adsorbed PCE [5]. When the tip and the substrate have the same charge sign, the resulting electrostatic interaction is repulsive. The mathematical description of the repulsive electrostatic force follows an exponential trend, and also the steric repulsion shows an exponential behavior [6]. Since these two effects follow the same mathematical law, a multimethod approach is required to determine the origin of the repulsion forces observed. Our multimethod approach consists of investigating superplasticizer adsorption and zeta potential of analyzed substrates in order to characterize the polymer displacement and the charge of the tip and the substrates.

Considering that the AFM tip is highly sensitive to the roughness of the substrate and that cement is strongly reactive with water, different nonreactive materials simulating cement behavior have been studied here. They were treated with synthetic solutions containing the main ion species present in actual cement pore solutions, in order to achieve results that relate to effective conditions in concrete. Such procedures have been applied to magnesium oxide powder, due to its similar charge to that of cement and because of its good affinity to superplasticizers [7]. On the other side, spherical probes attached to the AFM cantilever are useful for mimicking real colloidal behavior of a suspension particle [8]. For these two reasons, Kauppi et al. used magnesium oxide spherical tips to measure the effect of superplasticizers on a magnesium oxide surface in different ionic solutions [9]. However, the porosity of the MgO spherical probe must be smaller than the interaction range of the superplasticizers; otherwise the sphere roughness does not allow direct force measurements on superplasticizer layers. Recent studies performed on a main cement phase (C–S–H, i.e., calcium silicate hydrate) as substrate investigated the layer thickness of superplasticizers with different side chain lengths using a standard silicon nitride tip with a deposition of calcium hydroxide [10]. There, the author assumed that superplasticizers were adsorbed by the C–S–H and by the tip. They did, however, not confirm the adsorption of PCE on the substrate and the tip, and the origin of the forces then remained unclear.

This paper intends to investigate by AFM the repulsion force that superplasticizers exert between the tip and the different substrates. Additional data from the electrostatic potential of the particles in suspension (zeta potential) and from adsorption measurements allow a good derivation of the origin of the repulsion forces caused by superplasticizers in these model systems. The ideal AFM probe simulating a colloidal particle is a sphere, but unfortunately spherical tips are difficult to handle. They need to be well shaped, their diameter must be around 5–50 μm which is a difficult size for ceramic sphere production, and they must be extremely smooth because surface roughness can lead to misinterpretation of the data. This study investigates whether standard silicon nitride pyramidal tips may be utilized, despite their nonideal geometry, as an alternative to spheres to measure the repulsive forces caused by superplasticizers.

2. Materials

2.1. Superplasticizers

The intention of this study is to focus on a particular kind of comb-shaped polycarboxylate ether-type superplasticizers (PCE) that are composed of methoxy polyethylene glycol side chains attached on a poly methacrylic acid backbone. Fig. 1 illustrates its general chemical structure [11].

The polymers were synthesized as described in [11] by esterification of (meth)acrylic acid with alkoxy-polyethylene glycol followed by radical copolymerization with additional (meth)acrylic acid. During the polymerization step the molar concentrations of all monomers were kept constant to ensure the same reaction kinetics in all cases. The architecture of the polymer used here, identified with PCE 23-6, shows side chains with a length of 23 PEO units and a side chain grafting density of 6:1. Its number-average molecular weight (M_n) was found at 7600 g/mol, the mass-average molecular weight (M_w) was 18900 g/mol, and the polydispersity index (M_w/M_n) was 2.5. This composition with a relatively low density of side chains affords a highly charged backbone that enables high adsorption on Portland cement [12].

2.2. AFM substrates

The AFM method requires well-defined, flat, and nonreactive substrates. These characteristics cannot be guaranteed by cementitious materials that interact with water to form hydration products becoming drastically rough after several minutes in a wet environment. However, to understand adsorption and zeta potential results, the concentration and the type of chemical species in solutions must be monitored; otherwise, the influence of ions would lead to ambiguous data. For these reasons, the materials selected as substrates for the experimental procedures were characterized by a well-known chemical composition, a low reactivity with water and relatively smooth external surface. Calcite and quartz were investigated as substrates because they represent mineral constituents of common building materials; mica-muscovite was selected for its clay nature that affords an easy cleavage; magnesium oxide was chosen for its high affinity with superplasticizers. All materials were treated with synthetic solutions of 0.1 M K_2SO_4 (pH 6.3) and 0.1 M KOH (pH 13.0) chosen on the basis of ionic species present in cement pore solutions. It was established that after 1 h of hydration, the pore solution of cement is dominated by K^+, SO_4^{2-}, and OH^- ions, while other cations and anions exist in lower concentrations [13].

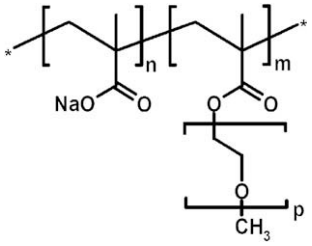

Fig. 1. General chemical structure of a methacrylate ether-based PCE superplasticizer (copolymer of methoxy polyethylene glycol methacrylate and methacrylic acid, sodium salt).

The AFM substrates were prepared from birefringent calcite and quartz crystals purchased commercially, muscovite sheets (Ted Pella Inc.) and magnesium oxide periclase (MagChem-p98, Martin Marietta Magnesia). To obtain flat substrates each material required a different preparation. Mica sheets and calcite crystals were cleaved respectively on [0 0 1] and $[1\,0\bar{1}\,1]$ planes. The quartz crystal, a six-sided prism terminating with six-sided pyramids at each end, did not require any polishing on its external lateral surface. Magnesium oxide was polished with oil base diamond suspensions on a flat side for 10 min with the 6-μm suspension, then continuing for 30 min with the 1-μm suspension, and concluding for 60 min with the ¼-μm suspension.

2.3. Adsorption and zeta potential powders

The same chemicals used as AFM substrates but with different purity were used to perform adsorption and zeta potential measurements. These materials are quartz (Quarzmehl K8, Carlo Bernasconi AG), magnesium oxide (Magnesia 298, Magnesia GmbH), calcite (Nekafill 15, Netsthal), and muscovite powder (Micamineral Jürgen Pfeiffer, Brunnen) reduced in size and sieved with a 63-μm sieve. In addition to these materials, silicon nitride powder (StarCeram N 3000, Starck) was used to characterize the behavior of the AFM tip related to PCE. Table 1 shows details of these powders.

Particle size distributions were obtained by laser diffraction measurements (Mastersizer X, Malvern, UK). Surface areas were derived from BET theory measuring nitrogen sorption (SA 3100, Beckman Coulter, Fullerton, CA).

3. Methods

3.1. Zeta potential

Measurements of the zeta potential of the colloidal particles in suspension at different PCE concentrations in various electrolyte solutions were performed using the ZetaProbe instrument (Colloidal Dynamics Inc., North Attleboro, MA). This instrument, working on the basis of the electroacoustic method, utilizes an alternating electrical field that induces oscillation of the charged particles. The motion of the particles gives a sound wave response that corresponds to the dynamic mobility of the colloidal particles. A special sensor detects the pressure changes produced by the wave motion and the software calculates the zeta potential from these pressure changes.

Before measuring the samples, pH-meter (4, 7, and 10) and zeta dip probe (KSiW-standard, provided by Colloidal Dynamics Inc.) were calibrated. All samples were measured in a polypropylene blade-stirred beaker and mixed (300 rpm) in order to keep the suspension homogeneous, avoiding segregation. The syringe unit for titration is flushed three times with deionized water and two times with superplasticizer solution to ensure the purity of the titrated solution.

For each kind of powder (quartz, magnesium oxide, calcite, mica, and silicon nitride), three suspensions (deionized water, 0.1 M K_2SO_4, and 0.1 M KOH) were prepared at volumes of 270 mL, with a solid volume fraction of 5%. The usual water to cement ratio in concrete is between 0.35 and 0.5. However, a more diluted suspension was used here in order to simulate conditions similar to the AFM system, where the amount of solid is much lower than the amount of liquid. These suspensions were checked by single point data series, and all the sample powders were found to yield a stable zeta potential after no more than 10 min. A suspension containing 17 g/L of PCE is added during the titration in steps of 0.07 mL volume, ranging from 0 to 12 mg PCE/g solid. The increase of volume is taken into account by the ZetaProbe instrument.

Raw data of zeta potential measurements are highly affected by the ionic species and charged polymers. By using synthetic solutions, this effect is controlled and limited, affording repeatable results. However, background corrections were performed for each titration measurement. Each suspension was purified from large-size particles by paper filters (5–8 μm), and the remaining solution was placed in a Teflon small volume static beaker. The conductivity was adjusted to the same value observed during the titration by adding deionized water drops to the solution, and the background measurement was started. The zeta potential of each suspension was recalculated by the ZetaProbe software including the corresponding background correction measurement.

During the experiments, no flocculation was observed and each measurement was conducted at 23 °C.

Table 1
Properties of the powders used for adsorption and zeta potential measurements.

Material	Purity (wt.%)	Surface area BET (m^2/g)	Density (g/cm^3)	% Volume diameters (μm)		
				d_{10}	d_{50}	d_{90}
Quartz	97.0	0.84	2.65	2.4	22.5	78.9
Magnesium oxide	99.5	5.77	3.51	1.8	7.4	65.3
Calcite	90.9	1.33	2.71	1.5	12.4	103.0
Mica	–	3.57	2.76	10.2	42.1	95.5
Silicon nitride	99.0	11.70	3.23	0.6	0.9	2.1

3.2. Adsorption isotherms

Adsorption isotherms were measured by total organic carbon (TOC) analysis. For these experiments, the same materials as for the zeta potential analysis were used. Each suspension is mixed at 5% of solid content with PCE (0, 2, 4, and 7 mg PCE/g solid) on a total volume of 50 mL. Higher concentrations of superplasticizers (up to 18 mg PCE/g solid) were reserved for silicon nitride powder. Since no differences in adsorption after 5, 10, and 20 min were observed, 5 min after mixing the suspensions were centrifuged for 10 min (40×100 rpm) with a commercial instrument (Rotofix 32, Hettich Zentrifuge), and the remaining solutions were filtrated with nylon filters 0.45 μm and diluted (1:10) in Milli-Q water.

The total organic carbon of the samples was detected by using a commercial TOC analyzer (Sievers 53010 C, GE Water & Process Technologies). The instrument was set to reject the first two measured values and to make an average of the remaining three values. Reference solutions with the same concentration and same ionic composition of the suspensions (without superplasticizers) revealed the amount of organic carbon given by the powder itself, while the TOC values of the suspension of PCE alone (without powder) revealed the amount of added superplasticizers. Both these values were used to calculate the amount of superplasticizers consumed by the adsorption.

3.3. Atomic force microscopy

All AFM measurements were performed by a commercial instrument (Nanoscope IV by Veeco Digital Instruments, Santa Barbara, CA), using V-shaped tips made of silicon nitride.

The AFM system consists of a cantilever with a sharp tip (probe) at its end, which is used to scan the specimen substrate (see Fig. 2). When the tip is brought into proximity of a sample surface, forces between the tip and the sample lead to a deflection of the cantilever. Typically, the cantilever deflection is measured using a laser spot reflected from the top surface of the cantilever into an array of photodiodes. This deflection of the cantilever gives information about substrate topography and allows direct measurements of the

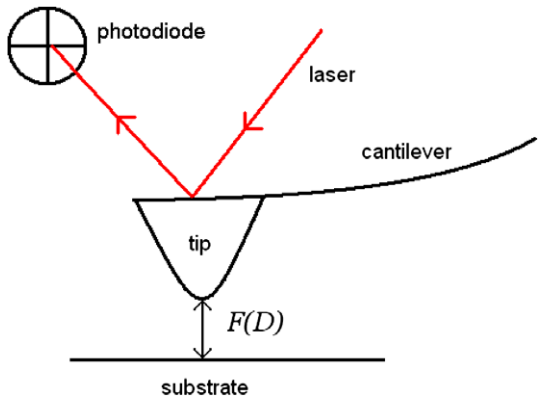

Fig. 2. General AFM setup.

force between the tip and the substrate as a function of the distance separating them.

3.3.1. Substrate roughness

Four different areas of $5 \times 5\ \mu m^2$ were scanned for each sample under dry conditions in contact mode. To control surface reactions, roughness values were also checked after different times of immersion in 0.1 M KOH solution. Measurements with 0.1 M K_2SO_4 and deionized water were also set, but they gave lower roughness values. In order to find each time the same region after the removal of the sample from the AFM scanner, pictures of the cantilever on the substrate were captured with particular software (VideoStudio, Ulead Inc.) connected to the optical microscope positioned on top of the AFM. With this method, the forces detected within the same area showed the same ranges, allowing a comparison between the roughness values.

The AFM software offers a section analysis module that can calculate the standard deviation (*RMS*) of the vertical movement of the tip (Z) on a mean plane (Z_{ave}) while scanning a selected area. Therefore, roughness is defined as

$$RMS = \sqrt{\frac{\sum_{i=1}^{N}(Z_i - Z_{ave})^2}{N}}, \quad (1)$$

where Z_i is the value of Z at the point i, and N is the number of points (pixels: 512×512) within the given area.

3.3.2. Force–distance measurements

The AFM software is able to capture plots of the cantilever deflection as a function of substrate position along the vertical Z axis. At large distances the tip does not feel any force, thus the cantilever is not deflected. Whenever the tip starts to experience some forces approaching the surface, the cantilever starts deflecting and/or oscillating until the tip is in contact with the surface. When this happens, the cantilever deflection becomes linear; the sample surface called Z_0 is defined in this Z position in which the deflection starts being linear. These observations allow calculating the distance D between the tip and the sample by

$$D = (Z - Z_0) + (d_c - \bar{d}_c), \quad (2)$$

where Z is the raw data of vertical position, d_c is the cantilever deflection, and $\bar{d}_c$ is the cantilever deflection at the defined surface Z_0. A minimal separation distance of 0.2 nm, the typical distance of two bodies in contact [3], is taken into account in this calculation. The cantilever deflection d_c is converted into force F by the simple relationship known as Hooke's Law:

$$F = -kd_c. \quad (3)$$

Here k is the cantilever spring constant. The cantilever spring constants were measured by the resonant frequency method [14], and they were in the range of 0.13–0.19 N/m for long cantilevers (triangle shape, 200 μm long, 28 μm wide, 0.6 μm thick) and around 0.5 N/m for the short ones (triangle shape, 100 μm long, 13.5 μm wide, 0.6 μm thick).

Nanoscope IV enables the installation of a wet-cell facility which provides contact mode AFM in fluid environments. Fluid cells consist of a glass cantilever holder and silicon O-ring to form an enclosed fluid environment with the ability to exchange liquids. Utilizing this apparatus, Milli-Q water, 0.1 M K_2SO_4, and 0.1 M KOH solutions were flushed one by one on the different substrates, at first without PCE as reference, followed by a PCE solution at a concentration of 0.2 g/L (concentration of PCE in the liquid solution required to have saturation of magnesium oxide). The areas of interest were scanned before the flushing to detect the roughness of the substrate in those regions. Ten minutes after the flushing, the force was measured. Each substrate is investigated with 7–10 curves for each solution. Between one measurement and the other, the force–distance curve in pure water is observed to check that the entire amount of polymer has been removed from the wet-cell volume.

4. Results

4.1. Interaction powder—superplasticizers

The zeta potentials of calcite, quartz, and mica are negative in each suspension within a range from −5 to −26 mV (Fig. 3). The addition of superplasticizer solutions does not significantly change their zeta potential; they remain negative with nonwide oscillations.

The only powder material showing a positive zeta potential is magnesium oxide. The addition of PCE completely changes its positive zeta potential, bringing it to negative values (from +8 to −10 mV in H_2O, from +6 to −4 mV in 0.1 M KOH), except for 0.1 M K_2SO_4 where the electrostatic potential is stable around the isoelectric point.

The corresponding conductivity values measured during the PCE titration are reported in Table 2.

Adsorption isotherms are shown in Fig. 4. These plots highlight that the superplasticizers are weakly adsorbed on quartz, calcite, and mica (saturation concentration less than 1 mg PCE/g solid), independent of the liquid environment. Contrary to this, magnesium oxide reaches a saturation concentration of 4 mg PCE/g solid, the same concentration used for the AFM force measurements. Consequently, one can conclude that the different ionic species in solution do not affect the adsorbed amount of PCE on MgO powder.

The silicon nitride behavior with PCE is displayed in Fig. 5.

The two plots show how silicon nitride is widely sensitive to the ionic background. When no PCE is added, its zeta potential changes completely depending on the ionic species in solution, from very positive (+53 mV in H_2O) to zero (in 0.1 M K_2SO_4) and to stoutly negative (−54 mV in 0.1 M KOH). Adding the PCE superplasticizer, the zeta potential of the aqueous suspension is strongly influenced (from +53 to −33 mV), whereas it remains almost stable in the other electrolyte solutions (from 0 to −5 mV in K_2SO_4, constant at −54 mV in KOH).

Also, the adsorption isotherm is strongly influenced by the ionic species in solution. When immersed in 0.1 M KOH, the powder manifests a low adsorption of superplasticizer (saturation concentration around 1 mg PCE/g solid), while for the other two solutions the saturation level is at a much higher concentration, higher than all the other materials (saturation concentration around 7 mg PCE/g solid in H_2O and in 0.1 M K_2SO_4). This could be due to the smaller

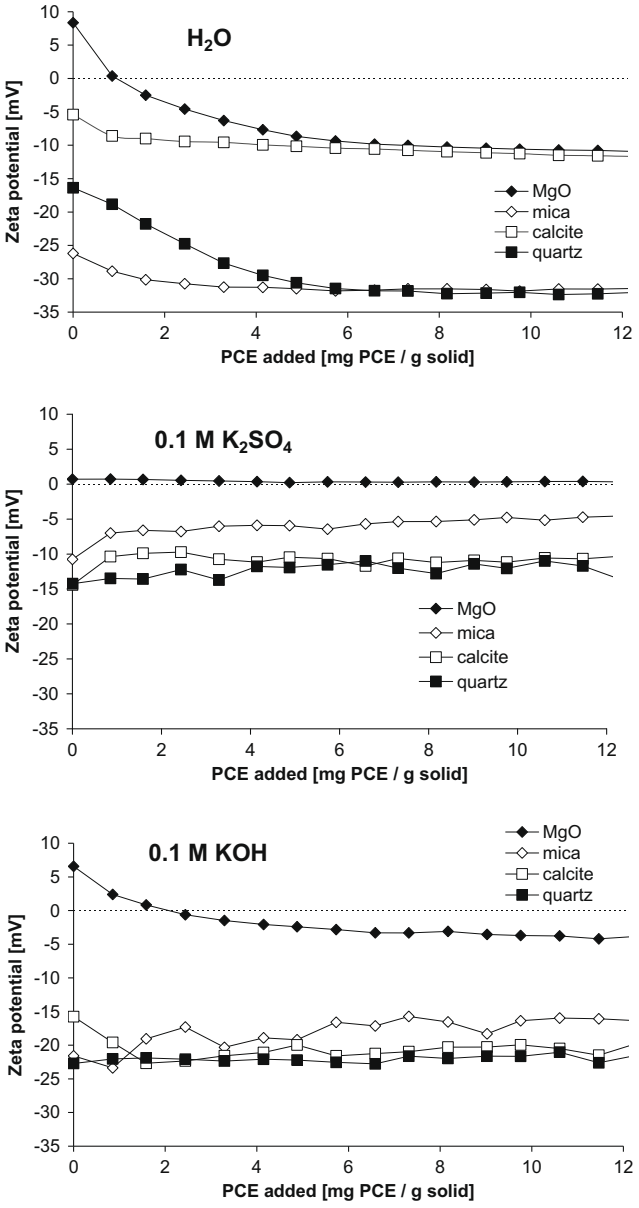

Fig. 3. Zeta potential as a function of PCE titrated to powder suspensions in different solutions.

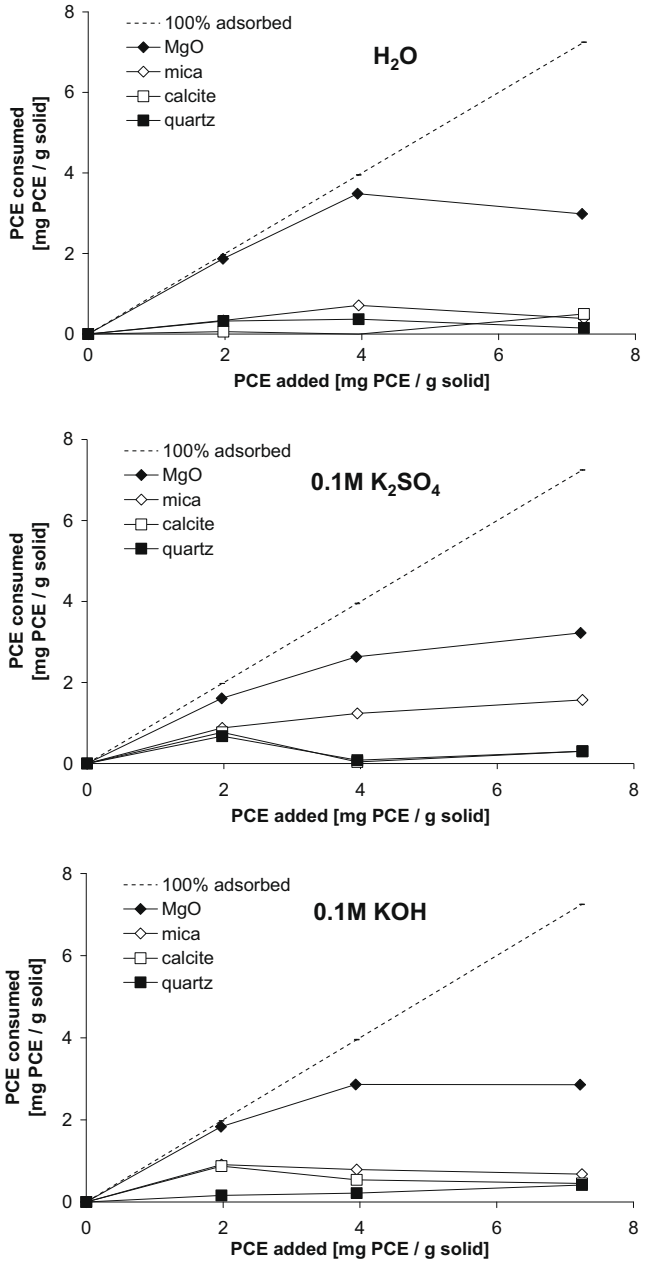

Fig. 4. Adsorption isotherms for PCE adsorbed on different substrates after 5 min of exposure to different solutions.

Table 2
Conductivity measured during the PCE titration.

Conductivity (mS/cm)	Mica	Quartz	Calcite	MgO	Silicon nitride
H_2O	0.15	0.13	0.15	0.50	0.3
K_2SO_2	16.5	17.5	17.2	16.6	18
KOH	19.8	20.8	19.9	20.2	20.3

size of the silicon nitride powder, compared to the other powders, which results in a higher specific surface area for the same weight. However, the fine powder well represents the size of the AFM tip, affording a good comparison with the real situation occurring in the wet cell.

4.2. Surface characterization and force measurements

The characterization of the substrates is reconnected to the roughness analysis. All the *RMS* data are reported in Table 3.

The most reactive material is magnesium oxide: after 3 h of hydration in synthetic 0.1 M KOH it displays a *RMS* value of 17.0 ± 1.2 nm. This is probably due to the high porosity of that material in comparison to the nearly atomically flat surface of the other substrates. In order to ensure the quality of the force–distance curves, roughness values must be lower than the side chain length of the PCE. The maximum side chain length was estimated in the order of 6 nm according to [15]. For its reactivity, magnesium oxide is not an optimum model system for the AFM. However, if it is exposed for less than 3 h to water, then the change in roughness is acceptable for AFM measurements. Nevertheless, our samples only need to be smooth and homogeneous on a small scale, since the interacting areas while capturing force plots are relatively small (typically 10–100 nm^2) [3]. Thus, an area of 25 μm^2 is much larger compared to the area involved in measuring the force–distance curve and the *RMS* values reported here represent a relatively

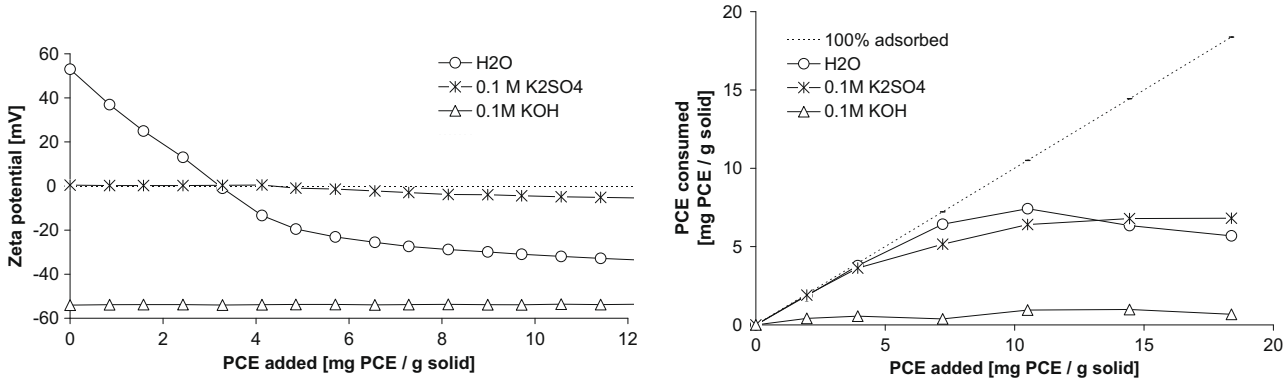

Fig. 5. Left: zeta potential of silicon nitride suspension titrated with PCE. Right: adsorption isotherm for PCE adsorption on silicon nitride. Both analyses were obtained in different solutions.

Table 3
RMS values (nm) calculated for each sample on four surfaces of 5×5 μm^2 after different immersion times into a solution of 0.1 M KOH.

Material	Without treatment	10 min	3 h	17.5 h
Quartz	5.4 ± 1.9	5.8 ± 1.1	7.4 ± 0.3	7.0 ± 2.3
Calcite	3.3 ± 0.7	4.6 ± 0.3	4. 6 ± 0.8	4. 5 ± 0.3
Mica	0.7 ± 0.1	3.8 ± 0.4	7.1 ± 2.3	7.1 ± 1.8
Magnesium oxide	4.4 ± 0.2	9.2 ± 0.4	17.0 ± 1.2	36.6 ± 5.4

low roughness. In any case, during force measurements, the samples were kept in contact with the solution for no more than 3 h, except for magnesium oxide.

The force–distance curves obtained in solutions without superplasticizer (Fig. 6) reveal a general attraction between the silicon nitride tip and the substrates. The only nonattractive material is magnesium oxide. Its Z_0 distance is not even well defined, probably due to hydration occurring on the substrate. Also, the 0.1 M KOH solution in some cases generates repulsive interaction between the tip and the sample (see quartz and calcite).

The addition of PCE (Fig. 7) completely eliminates this attraction, revealing a clear repulsion within the region of interaction between the tip and the surface. It is observed that water (lines with circles) displays a longer range interaction force, even if the plots are cut at a distance of 15 nm for more ideal comparison of the data. For magnesium oxide, owing to the stronger interaction, a different force range (vertical axis from −2 to +15 nN) had to be applied.

5. Discussion

5.1. Impact of ions on zeta potential and adsorption

Zeta potential titration curves reveal that the only positively charged sample powders are magnesium oxide and silicon nitride. Consequently, these two materials show the strongest adsorption of anionic superplasticizers. This happens, as already known from the literature [16,17], because a positive zeta potential is required to achieve a strong PCE adsorption due to electrostatic interaction between negatively charged backbones of superplasticizers and particle surfaces. According to Plank [16] and Zingg (2008) [17,18] when colloidal particles are first negatively charged, they may become positive later by adsorbing cations from the environment. This layer of ions around the particles generates a positive zeta potential that allows the adsorption of the superplasticizers' backbone containing COO^- groups, and also of the SO_4^{2-} ions present in solution. However, if a particle has an intrinsic positive charge, it affords a direct adsorption of the negative backbone of PCE on its surface, leading to a stronger adhesion.

5.1.1. Negatively charged powders

The effective charge of mica, quartz, and calcite is negative. When immersed in ionic solution, they adsorb differently positive and/or negative ions, but these slight changes do not cause an inversion of the zeta potential. Titration of superplasticizers does not influence it, thus confirming poor adsorption of PCE.

5.1.2. Positively charged powders

Magnesium oxide colloidal particles show a positive zeta potential in deionized water and in 0.1 M KOH solution, while in 0.1 M K_2SO_4 it is around 0 mV. When superplasticizers are added to the suspensions, a significant change in zeta potential is observed, revealing a strong interaction between powder and polymer. This change does not occur when magnesium oxide is suspended in 0.1 M K_2SO_4 (zeta potential constantly 0 mV). However, the adsorption isotherms show a high saturation adsorption concentration in all the liquid environments, including K_2SO_4 solution. From these observations it is reasonable to conclude that colloidal particles adsorb SO_4^{2-} ions, but the anions influence poorly PCE adsorption. A possible explanation may be that the sulfate ions are adsorbed by the colloidal particles, but they did not fully cover their surface, leaving some free space for the superplasticizer adsorption. Indeed the zeta potential of the positive particles does not become negative, but it reaches its isoelectric point revealing that the MgO particles are not completely coated by sulfate anions. This fact allows us to assume that for MgO an average neutral zeta potential results from regions of surface left unoccupied that are positively charged, and regions of surface covered by sulfate ions that are negatively charged. Since SO_4^{2-} ions partially occupy the surface of the particles, PCE has less available space. Thus the adsorption process is not interrupted, it is simply slowed.

A behavior similar to MgO is shown by silicon nitride. Without superplasticizer, its zeta potential is highly sensitive to ion species in solution that are responsible for changes from positive (H_2O) to zero (K_2SO_4) and to negative (KOH). Titrating superplasticizer to the suspension in deionized water, the COO^- groups are strongly adsorbed, bringing a negative zeta potential to the colloidal particles. In 0.1 M K_2SO_4, the presence of PCE does not have much impact (from 0 to −5 mV), revealing some interaction between the powder and the superplasticizer and confirming a significant adsorption. In 0.1 M KOH, the negative zeta potential of silicon nitride is responsible for very poor interaction between this powder and the PCE, and consequently very poor adsorption. Probably the OH^- anions of the solution adhere strongly to the colloidal

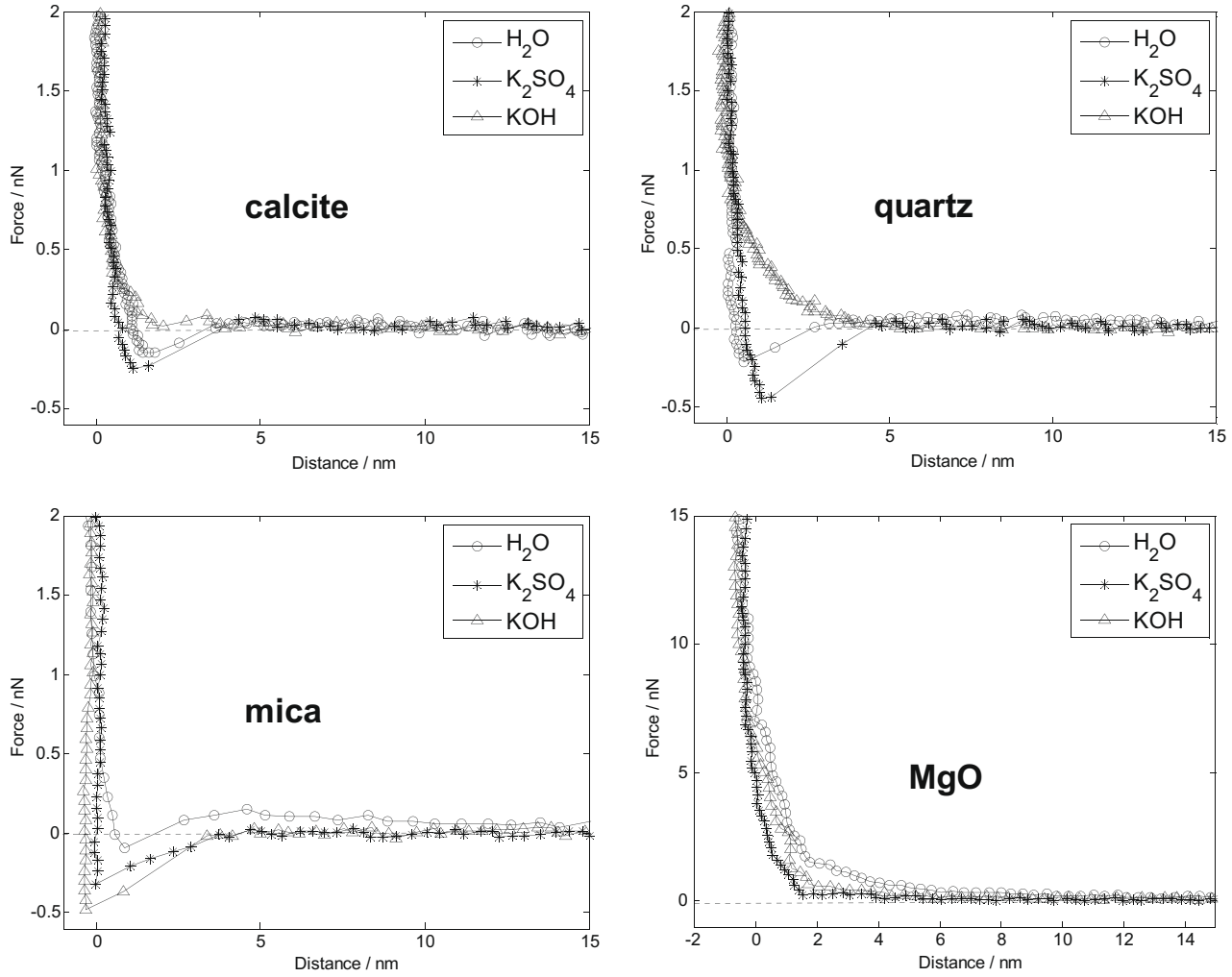

Fig. 6. AFM force measurements between the AFM tip and the different substrates, measured in the absence of PCE, approaching curves. Note that a different force scale was used for magnesium oxide.

particles, screening their positive charge and not allowing any adsorption of the COO^- backbone groups.

Summarizing, from these results it becomes evident that the zeta potential is highly responsible for the adsorption of PCE on colloidal particles. In general, stronger adsorption occurs on positively charged powders, due to the direct adhesion of the backbone to the particle surfaces. Additionally, SO_4^{2-} ions compete with the negative COO^- groups of PCE, thus slowing down the adsorption process, but not preventing it.

5.2. AFM force measurements

In solutions not containing superplasticizers (Fig. 6) the electrostatic and the adhesion forces play a fundamental role. If the tip and the substrate have opposite charge sign, they attract each other adding an electrostatic contribution to the adhesion force (calcite, mica, and quartz curves collected in H_2O and 0.1 M K_2SO_4). On the other hand, if they have the same charge sign, the electrostatic repulsion could even compensate the adhesion attraction (0.1 M KOH curves on quartz and calcite, and all the curves on magnesium oxide).

When the AFM tip is submersed in a solution with superplasticizer (Fig. 7), the presence of PCE eliminates the adhesion effect and the tip experiences mainly steric and/or electrostatic forces. The strong interaction between the silicon nitride and the superplasticizer reveals that PCE molecules are mainly positioned on the tip and, according to the TOC analysis, they are typically not adsorbed on the substrate, except for MgO. Since the pyramidal tip does not allow a precise detection of the geometry of the contact area, the corresponding disposition of the side chains of the adsorbed superplasticizers is not predictable. From this point of view, the AFM force plots here represent a qualitative idea of the interactions involved in these systems, and cannot be utilized as quantitative results. However, since repulsion force was observed in each single case, even when there was low adsorption of PCE on both the tip and the substrate, one can assume that in these situations the electrostatic repulsion is dominant. It could be hypothesized that the repulsion in this case is due to superplasticizers floating in the solution interposing between the tip and the substrate, but since they were not adsorbed by the surface they would be easily removed by the tip oscillations while collecting the force plot. Thus, the force–distance curves reported here show different situations depending on the system environment. In certain cases it is possible to distinguish between steric repulsion due to a single layer of adsorbed PCE and repulsion due to two separate layers; in other cases, the interaction is just electrostatic.

5.2.1. Negatively charged substrates

Calcite, mica, and quartz show negative charges and poor adsorption of PCE, so the differences in force measurements on

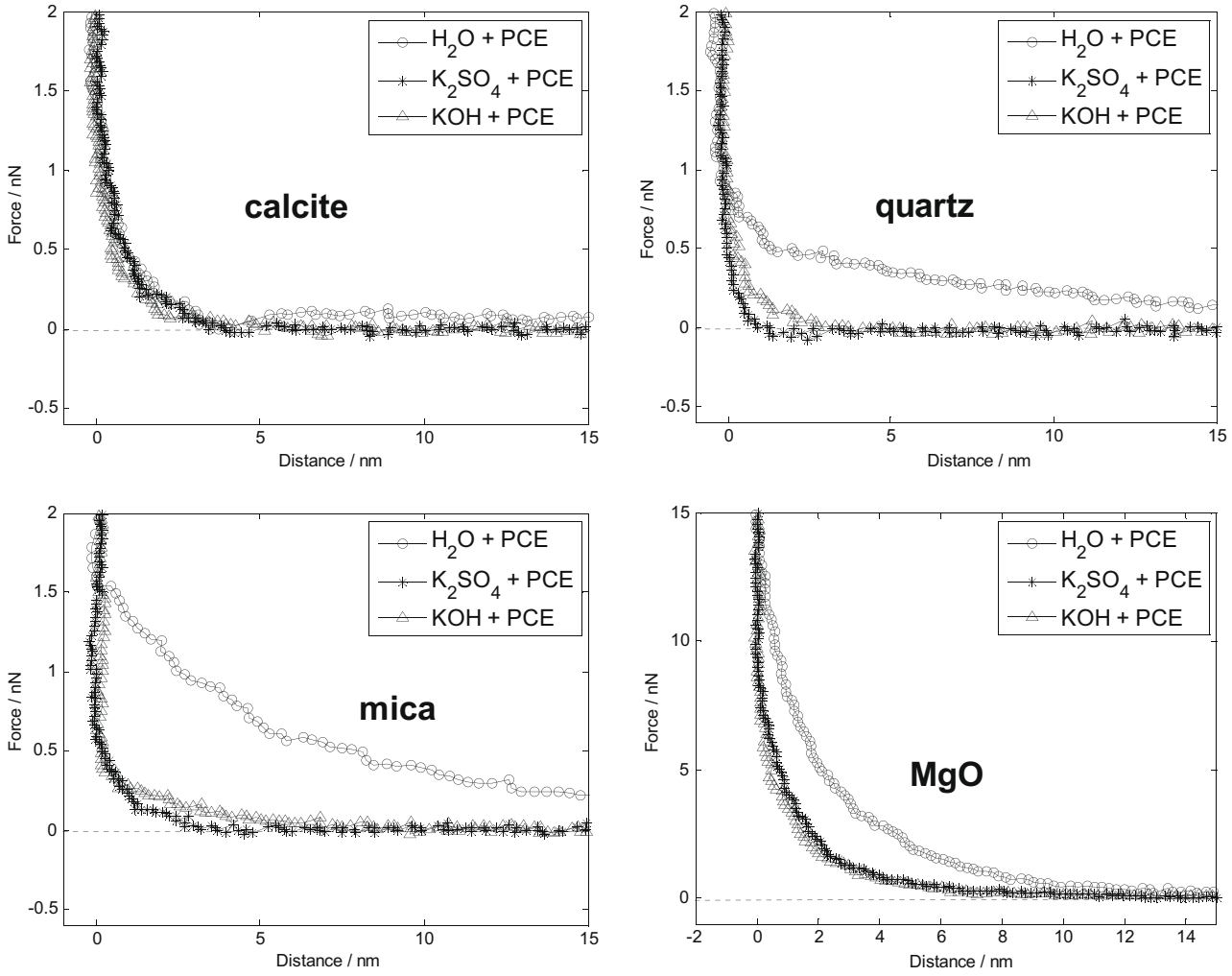

Fig. 7. AFM force measurements between the AFM tip and the different substrates, measured in the presence of 0.2 g/L PCE, approaching curves. Note that a different force scale was used for magnesium oxide.

these substrates are mainly due to tip behavior. The results are summarized in Table 4, where values of the zeta potential between −4 and +4 mV are considered to represent essentially an overall zero surface charge, as a result of positive charges matching the negative ones.

The understanding of the origins of the repulsion comes from the adsorption analysis and zeta potential measurements. These results are confirmed by the AFM force plots, where the curves taken in deionized water (circles line), compared to the ionic solutions (stars and triangles curves), show a longer range and a stronger repulsion force due to the sum of the steric and electrostatic components. However, on these negatively charged substrates it was not possible to measure the interaction force due to two separate layers on these substrates, because of their low adsorption. In KOH solution, neither the silicon nitride tip nor the substrate adsorb the superplasticizers, so the entire repulsion is attributed to the electrostatic force.

The right column illustrates the surface charge and polymer layers displacement, of the tip and the substrate, respectively, occurring in different solutions.

5.2.2. Positively charged substrates

Zeta potential graphs and TOC analysis reveal a high affinity between PCE and magnesium oxide. These results allow us to assume that superplasticizers formed a well-defined layer on this substrate, leading to a significant change in the force-curve range in comparison with the other materials. The results are summarized in Table 5.

Only in the presence of potassium hydroxide, the steric component of the force is due to a single layer of PCE adsorbed on MgO; while in the other cases the steric repulsion is due to two separate layers: one on the substrate and one on the tip. From this point of view, the curves captured in 0.1 M KOH solution (steric single layer) should have been comparable with the curves observed for mica, quartz, and calcite in 0.1 M K_2SO_4 (steric single layer, too). Despite this, the single layer of PCE adsorbed on the flat magnesium oxide substrate has a better defined geometry; thus, the side chains were likely arranged in a compact brush giving a stronger steric effect. Similar assumptions about the ordered organization of the side chains could not be made about the silicon nitride tip, because the tip vertex does not have such a well-defined geometry. This difference generates a stronger force on magnesium oxide substrate, even if the nature of the force is the same for mica, quartz, and calcite in 0.1 M K_2SO_4.

The right column illustrates the surface charge and polymer layers displacement, of the tip and the substrate respectively, occurring in different solutions. Data for the silicon nitride tip are provided in Table 3.

In all the examined cases, there is no attraction between the tip and the substrate in the presence of superplasticizers, even if there

Table 4
Tabulation of zeta potential, % of adsorbed PCE, and AFM force measurements obtained for mica, quartz, and calcite in H_2O, 0.1 M K_2SO_4, and 0.1 M KOH at 0.2 g/L PCE concentration.

Fluid system and substrate	Zeta potential (mV)	Adsorption ratio (%)	0.5 nm	Force 1 nm	(nN)2 nm	5 nm	System illustration
H_2O	Repulsion: electrostatic + steric from a single layer of PCE adsorbed on the tip						
Mica	−32	18	1.54	1.34	1.20	0.51	
Quartz	−31	9	0.70	0.62	0.48	0.35	
Calcite	−19	0	0.78	0.44	0.19	0.09	
Silicon nitride	−13	97	–	–	–	–	
K_2SO_4	Repulsion: steric from a single layer of PCE adsorbed on the tip						
Mica	−5	28	0.33	0.23	0.12	0.02	
Quartz	−12	2	0.09	0.00	0.01	0.01	
Calcite	−11	1	0.80	0.48	0.21	0.02	
Silicon nitride	−3	91	–	–	–	–	
KOH	Repulsion: electrostatic between tip and substrate						
Mica	−16	18	0.34	0.28	0.21	0.07	
Quartz	−22	6	0.35	0.21	0.10	0.00	
Calcite	−21	14	0.49	0.31	0.09	0.03	
Silicon nitride	−53	14	–	–	–	–	

Table 5
Tabulation of zeta potential, % of adsorbed PCE, and AFM force measurements obtained for magnesium oxide in H_2O, 0.1 M K_2SO_4, and 0.1 M KOH at 0.2 g/L PCE concentration.

Fluid system and substrate	Zeta potential (mV)	Adsorption ratio (%)	0.5 nm	Force 1 nm	(nN) 2 nm	5 nm	System illustration
H_2O	Repulsion: electrostatic + steric from two separate layers of PCE adsorbed on tip and MgO						
Magnesium oxide	−10	87	10.61	7.85	5.27	2.05	
K_2SO_4	Repulsion: steric from two separate layers of PCE adsorbed on tip and MgO						
Magnesium oxide	0	66	5.91	4.12	2.30	0.68	
KOH	Repulsion: steric from single layer of PCE adsorbed on MgO						
Magnesium oxide	−3	72	4.54	3.47	1.73	0.53	

are cases in which steric repulsion is not possible because of the low adsorption of superplasticizers. This allows an interpretation in which the electrostatic effect plays an important role. On the other hand, in an actual cement suspension the electrostatic interaction is weaker due to the high ionic strength. Unfortunately, this electrostatic interaction is usually neglected when discussing particles repulsion, while it still is an important parameter for particle aggregation.

Flatt et al. obtained force–distance curves similar to ours approaching calcium silicate hydrate (C–S–H), a main cement hydration product, with a V-shaped tip coated with C–S–H [10]. They utilized them to measure the layer thickness of adsorbed polycarboxylate, interpreting the PCE as chains of hemispheres forming two layers, one on the tip and one on the substrate. However it has been shown that the adsorption of PCE on C–S–H is relatively poor and hence the zeta potential is not highly influenced when superplasticizer is titrated on C–S–H [17]. Comparing the curves they found for polymer PC 23–3 (same number of monomers along the side chains as our PCE 23–6), the plots display a similar range and shape to those we found working with a standard commercial AFM tip on a low adsorbing substrate. According to our interpretation, their results represent a situation in which the superplasticizers form a single layer on the tip and no layer on the substrate, so this setup is not optimum for measuring the approach between two layers. Furthermore, the undefined geometry of the tip does not ensure such detailed conclusions because the tip radius in this case is not predictable. From a modeling point of view, however, this radius is a parameter which influences the contact area and thus the force values.

In conclusion, in a colloidal suspension PCEs are preferably adsorbed on positively charged particles and with their side chains they avoid positive–negative particle aggregation. In this study we showed that, when particles do not adsorb superplasticizers, the electrostatic interaction becomes dominant, while in other cases it is supplemented by steric repulsion. However in an actual cement suspension the presence of a high concentration of different ions in solution reduces this electrostatic repulsion. These observations allow us to imagine a suspension as a bulk composed by dispersed particles, some of which are coated by superplasticizers and others are not. This leads to a system in which the origin of the repulsive forces is different from case to case, depending on the particles charge (see Fig. 8). This interpretation is in good agreement with results obtained with cryo-FIB and cryo-SEM techniques on fresh cement paste with superplasticizers [18]. It explains how in the presence of PCE the hydrates—mainly ettringite—are well dispersed in the interstitial pore space as a population of fine particles, while in a nondispersed suspension ettringite tends to agglomerate and to precipitate on the clinker surfaces.

Since superplasticizers do not need to cover each single particle of the suspension, but only the positive charged particles, a

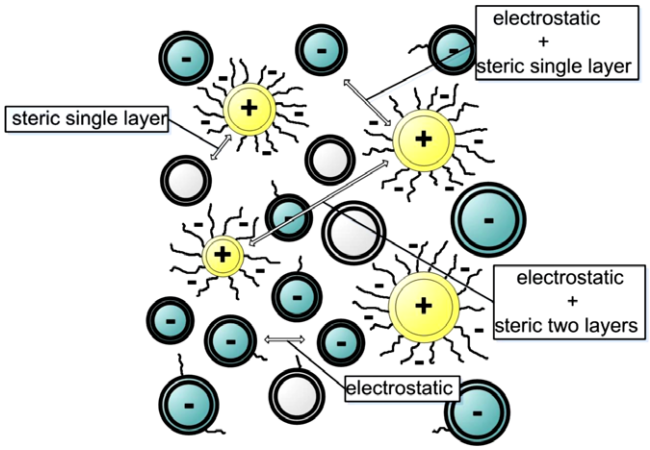

Fig. 8. Schematic representation of a multiphase suspension dispersed through different mechanisms exercised by superplasticizers.

relatively low concentration of superplasticizers may be enough to give a well-dispersed suspension.

6. Conclusions

The aim of the addition of superplasticizers to a suspension is to avoid particle agglomeration and to increase the flowability. One of the main reasons for agglomeration is the attraction between oppositely charged particles that form aggregates in the colloidal suspensions. In order to prevent this attachment, dispersants adhere to the particle surface, exerting repulsion forces between them.

PCE-type superplasticizers have a tendency to be adsorbed on positively charged materials, due to their negative backbones. When adsorbed, they change the particles' zeta potential from positive to negative or zero. The results obtained here with the AFM show how repulsive forces also occur among low adsorbing materials, i.e., negatively charged particles, reasonably generated by electrostatic contribution.

Generally a suspension can be viewed as a bulk of differently charged colloidal particles. When PCEs are added, they are adsorbed by the positively charged particles; thus there is a difference between particles which adsorb and those which do not adsorb polymers. Between particles not coated by superplasticizers, the nature of the repulsion force is strictly electrostatic.

This view of the system may explain why a relatively low concentration of superplasticizers is usually necessary to obtain dispersed systems; it is not necessary to cover each single particle of the suspension, but only those with a positive charge.

Acknowledgments

Luigi Brunetti, Boris Ingold, Hansjürgen Schindler (Empa), and Hermann Mönch (eawag) are gratefully thanked for their assistance during the laboratory experiments.

References

[1] J. Plank, K. Pölllmann, N. Zouaoui, P.R. Andres, C. Schaefer, Cem. Concr. Res. 38 (2008) 1210.
[2] H. Uchikawa, S. Hanehara, D. Sawaki, Cem. Concr. Res. 27 (1997) 37.
[3] H.-J. Butt, M. Jaschke, W.A. Ducker, Bioelectrochem. Bioenerget. 38 (1995) 191.
[4] H.-J. Butt, Biophys. J. 60 (1991) 1438.
[5] S. Yamamoto, M. Ejaz, Y. Tsujii, M. Matsumoto, T. Fukuda, Macromolecules 33 (2000) 5602.
[6] W.F. Heinz, J.H. Hoh, Trends Biotechnol. 17 (1999) 143.
[7] R.J. Flatt, Y.F. Houst, P. Bowen, H. Hofmann, J. Widmer, U. Sulser, U. Maeder, T.A. Bürge, In: 5th CANMET/ACI International Conference on Superplasticizers and Other Chemical Admixtures in Concrete, ACI, Farmington Hill, MI, USA, 1997, p. 743.
[8] W.A. Ducker, T.J. Senden, R.M. Pashley, Nature 353 (1991) 239.
[9] A. Kauppi, K.M. Andersson, L. Bergström, Cem. Concr. Res. 35 (2005) 133.
[10] R.J. Flatt, I. Schober, E. Raphael, C. Plassard, E. Lesniewska, Langmuir 25 (2009) 845.
[11] F. Winnefeld, S. Becker, J. Pakusch, T. Götz, Cem. Concr. Compos. 29 (2007) 251.
[12] A. Zingg, F. Winnefeld, L. Holzer, J. Pakusch, S. Becker, R. Figi, L. Gauckler, Cem. Concr. Compos. 31 (2009) 153.
[13] B. Lothenbach, F. Winnefeld, Cem. Concr. Res. 36 (2006) 209.
[14] J.E. Sader, I. Larson, P. Mulvaney, L.R. White, Rev. Sci. Instrum. 66 (1995) 3789.
[15] A. Ohta, T. Sugiyama, and Y. Tanaka, 5th CANMET/ACI International Conference on Superplasticizers and Other Chemical Admixtures in Concrete, ACI, Farmington Hills, MI, USA, 1997, p. 359.
[16] J. Plank, C. Hirsch, Cem. Concr. Res. 37 (2007) 537.
[17] A. Zingg, F. Winnefeld, L. Holzer, J. Pakusch, S. Becker, L. Gauckler, J. Colloid Interface Sci. 323 (2008) 301.
[18] A. Zingg, L. Holzer, A. Kaech, F. Winnefeld, J. Pakusch, S. Becker, L. Gauckler, Cem. Concr. Res. 38 (2008) 522.

Paper 2

Multi-method approach to study influence of superplasticizers on cement suspensions

L. Ferrari, J. Kaufmann, F. Winnefeld, J. Plank

Cement and Concrete Research 41 (2011), 1058-1066

Cement and Concrete Research 41 (2011) 1058–1066

Contents lists available at ScienceDirect

Cement and Concrete Research

journal homepage: http://ees.elsevier.com/CEMCON/default.asp

Multi-method approach to study influence of superplasticizers on cement suspensions

L. Ferrari [a,b,*], J. Kaufmann [a], F. Winnefeld [a], J. Plank [b]

[a] Empa, Swiss Federal Laboratories for Materials Testing and Research, Laboratory for Concrete/Construction Chemistry, Ueberlandstr. 129, 8600 Duebendorf, Switzerland
[b] Technische Universität München, Department of Chemistry, Lichtenbergstr. 4, 85747 Garching, Germany

ARTICLE INFO

Article history:
Received 15 December 2010
Accepted 23 June 2011

Keywords:
Admixture
Adsorption
Atomic force microscope (AFM)
Cement
Rheology

ABSTRACT

Superplasticizers are widely used in concrete processing to increase the rheological properties of hardening pastes. In this study, different techniques (rheology, adsorption, atomic force microscopy—AFM, and ζ-potential) are used to characterize the impact of polycarboxylate-ether based superplasticizer (PCE) on particle suspensions. Results obtained with two cements and two inert powders (MgO and calcite) show that superplasticizer efficiency is strongly influenced by polymer architecture and by the ionic species present in solution. Additionally, experiments performed with AFM and ζ-potential contributed to characterize dispersion forces exerted by superplasticizers at the solid–liquid interface. The application of plateau AFM-tips coated with platinum reveals that dispersion forces depends on the presence of ions in solution, and that multilayer formation occurs with certain superplasticizer types. A further conclusion includes the idea that the PCE has a lubricating effect between adjacent particles and PCE increases surface wettability.

1. Introduction

Polycarboxylate-ether based superplasticizers (PCEs) are widely used in different industrial fields to improve the rheological properties of particle suspensions. Especially in cement application, their addition allows a reduction of the water-to-cement (w/c) ratio, thus strongly increasing the workability of the fresh mixtures and the performances of the hardened pastes, mortars or concretes. Despite their widespread utilization, these polymers are currently still the subject of many studies, because details about their working principles lack of a full understanding. Indeed, sometimes unpredictable incompatibility with certain cements was observed [1–3].

A multi-method approach is required to understand different aspects of superplasticizer behavior in fresh cementitious suspensions. The workability of a particulate mixture is usually characterized by detecting its rheological properties [4,5]. Apparent yield stress and viscosity, which describe the fluid's internal resistance to flow, are the two main macroscopic parameters which are used to quantify the effects of PCE addition to the suspensions. A further key factor, to quantify the efficiency of a superplasticizer, is to investigate how much polymer is really interacting and remaining on the particle surfaces. The adsorption behavior on colloid surface may be determined by means of total organic carbon (TOC) measurements [6,7]. Moreover, the detection of the ζ-potential enables to study the influence of superplasticizers on particle charges and to analyze the effect of electrostatic dispersion forces acting between them [8].

Houst et al. [9] recently collected results, obtained with many techniques, to asses the adsorption behavior and the rheological properties of different systems, and to model superplasticizer action at the solid–liquid interface. Studies from Plank et al. [10–12] highlighted the influence of different polymer architectures and their interaction with cementitious systems. They showed that short side chains, resulting in a high polymer charge, perform strong adsorption especially on positively charged particles. Other studies by Zingg et al. on pure cement phases confirmed that ettringite is the cement phase which most adsorbs superplasticizers [13].

Additionally to this variety of techniques, atomic force microscopy (AFM) was applied in the past to measure in liquid the dispersion forces due to PCE [14]. In order to obtain reliable results with this technique, substrates that are smooth, flat and non-reacting are a prerequisite. Since these characteristics can not be provided by cement, the use of inert model systems is necessary to enable these kinds of force measurements. Spherical probes of magnesium oxide approaching MgO substrates were used to simulate a cement-like colloidal particle [15]. It was proposed that, for a more complete understanding of the measured force–distance curves, additional studies on the polymer adsorption and the ζ-potential are required [16]. This investigation revealed that the standard AFM tips, composed of silicon nitride, are positively charged, and so they adsorb PCE.

In the present study, a multi-method approach involving all these experimental techniques (rheology, adsorption, ζ-potential, and AFM) is reported, in order to contribute to a more general

* Corresponding author at: Empa, Swiss Federal Laboratories for Materials Testing and Research, Laboratory for Concrete/Construction Chemistry, Ueberlandstr. 129, 8600 Duebendorf, Switzerland. Tel.: +41 58 765 43 60; fax: +41 58 765 40 35.
E-mail address: lucia.ferrari@empa.ch (L. Ferrari).

0008-8846/$ – see front matter © 2011 Elsevier Ltd. All rights reserved.
doi:10.1016/j.cemconres.2011.06.010

understanding of the influence of superplasticizers on cement suspensions. The aim of this work is to separately analyze different behaviors of PCEs, from a macroscopic to a nanoscopic point of view. In a first moment, a series of superplasticizer architectures was tested on two cements with different chemical compositions, and on two model powders (magnesium oxide and calcite), in water or in synthetic cement pore solution. Experiments about rheological properties and PCE adsorption were performed on these systems. In a second moment, the focus was shifted toward the characterization of the electrostatic and steric dispersion forces, detected respectively by ζ-potential and AFM. The use of an AFM device restricted the set of the used materials to magnesium oxide only. Steric forces were detected by means of an AFM technique applying plateau tips coated with platinum. This new tool reasonably permits to probe the liquid–solid interfaces with a non-adsorbing, neutral tip, which prevents the adsorption of PCE on the AFM tip, due to its negative zeta potential [17].

2. Materials

2.1. Superplasticizers

Different polycarboxylate superplasticizers composed of methoxy-polyethylene-glycol side chains attached on a poly-methacrylic-acid backbone were tested in this study (see Fig. 1). One of the aims is to understand the influence of anionic charge density, side chain length and side chain density on the interaction between PCE and particles at the liquid–solid interface, in order to capture the efficiency of different polymer architectures. Table 1 reports superplasticizer properties, while Fig. 2 illustrates their architectures. The first number in the name of superplasticizer, here called *p*, refers to the number of polyethylene oxide (PEO) units and it represents the side chain length, while the second one, *n*, refers to the number of anionic functional groups. M_n is the number-average molecular weight, M_w is the mass-average molecular weight, and their ratio M_w/M_n represents the polydispersity index. Superplasticizers with high side chain density ($n=1.5$ and $n=3$) were synthesized as described in [10], 45PC12 was synthesized according to [12], and 23PC6 was synthesized following the process explained in [18]. Main chain length (MCL) and side chain length (SCL) were estimated according to [19]. Charge density (CD) is calculated as the ratio between the moles of anionic charge and the molar mass of each PCE unit.

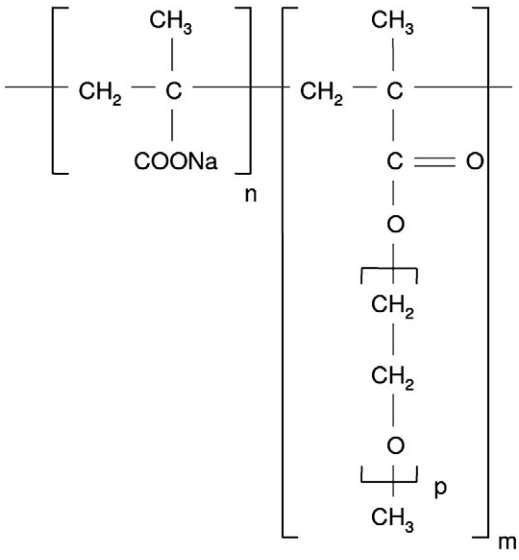

Fig. 1. Chemical structure of the studied PCE.

Table 1
Characteristic properties of PCE.

*p*PC*n*[a]	M_n[b] (g/mol)	M_w[c] (g/mol)	*PDI*[d]	MCL (nm)	SCL (nm)	CD[e] (mmol/g)
8.5PC1.5	121,700	520,400	4.3	130.4	2.4	2.6
8.5PC3	25,800	106,000	4.1	36.3	2.4	4.2
23PC6	7600	18,900	2.5	8.3	6.4	3.7
45PC1.5	35,000	161,300	4.6	10.0	12.5	0.8
45PC3	50,100	156,700	3.1	21.7	12.5	1.4
45PC12	11,800	342,500	2.9	12.5	12.5	3.9
111PC1.5	57,100	98,000	1.7	7.0	30.9	0.3
111PC3	53,000	149,100	2.8	10.2	30.9	0.6

[a] p = number of PEO groups, n = number of carboxylic groups.
[b] M_n = number-average molecular weight.
[c] M_w = mass-average molecular weight.
[d] $PDI = M_n/M_w$ = polydispersity index.
[e] CD = charge density.

2.2. Cements and model powders

To study the influence of different superplasticizer architectures on particle suspensions, two kinds of cements and two almost inert model-powders (magnesium oxide and calcite) were used (see Table 2). Magnesium oxide was used in the past to model cement suspensions, due to their similar isoelectric points [20], while calcite is ordinarily used as a mineral constituent of common building materials. The BET value of MgO is significantly higher than the other three powders. Furthermore specific surface area of cement changes during the first minutes of hydration, generally increasing. Considering all these aspects, at least for the inert powders, adjustment of the water-to-powder ratio was empirically considered to compensate the increase of water demand with the increase of BET values.

Particle size distributions were obtained by laser diffraction measurements (Mastersizer X, Malvern, UK), and surface areas were derived from BET theory measuring nitrogen sorption (SA 3100, Beckman Coulter, Fullerton, CA).

Table 3 reports the chemical compositions of the cements (by polarized X-Ray fluorescence), while the main clinker phases were estimated by the Bogue calculation (Cement N (wt.%): $C_3S=58$, $C_2S=14$, $C_3A=6$, $C_4AF=11$; Cement HS (wt.%): $C_3S=47$, $C_2S=15$, $C_3A=1$, $C_4AF=18$). Since many studies showed the affinity between ettringite and superplasticizers [1,7,8,21], the two cements were selected with different C_3A contents in order to test the influence of ettringite formation on the effect of PCE performance. The amount of ettringite formed was measured by thermogravimetric analysis. 10 min after preparing the paste the hydration was stopped by solvent exchange with isopropanol and washing with ether. The quantity of ettringite was then calculated by the water loss between 50 °C and 125 °C determined by means of thermogravimetric analyses. The ettringite contents after 10 min were 2.7% for cement N and 1.1% for cement HS, which is related to the respective content of C_3A in the cement.

The decision of testing inert powder allows to control the influence of ionic species on the behavior of the different superplasticizers, and permitted the comparison with the AFM measurements on model substances. On the other side, the cements were mixed with deionized water and the two model powders were treated with deionized water or a synthetic solution simulating a typical ionic composition of the cement pore solution after 1 h of hydration for a w/c ratio of 0.5 [22]. Table 4 reports the chemical composition of the synthetic pore solution, of the two cements and of the inert powders after 10 min of hydration analyzed by ion chromatography system (ICS-3000, Dionex Corporation, Sunnyvale CA, USA). The synthetic pore solution represents well the ionic composition of the standard cement N, while for cement HS with low C_3A content the concentration of sulfate and potassium ions is reduced.

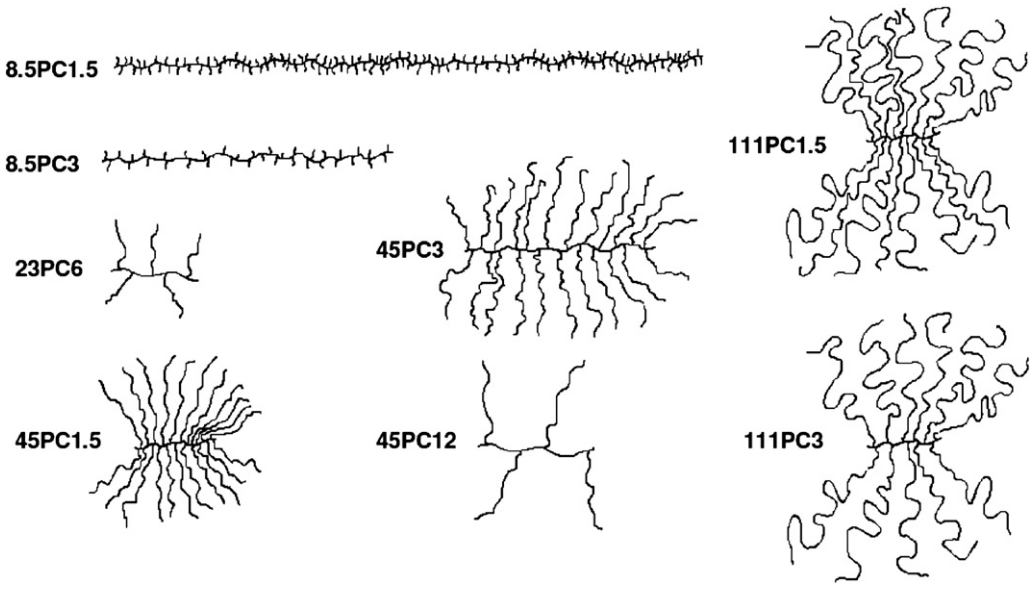

Fig. 2. Schematic representation of PCE architecture.

3. Methods

3.1. Rheology

Rheological measurements were performed using a Paar Physica MCR 300 rheometer with concentric cylindrical geometry. A rotating bob was lowered to the measuring position, and shear stress was detected recording a flow curve with shear rates increasing from 10 up to 100 s^{-1} and decreasing from 100 down to 10 s^{-1}. Apparent yield stress was estimated interpolating the data of the return curve following the Birmingham model (see Fig. 3).

For each powder, different volume fractions were tested. For the two cements the w/c ratio was kept constant at 0.36, while for the model powders the w/p ratio was adjusted in order to find the right paste consistence displaying apparent yield stresses around 27 ± 5 Pa in absence of superplasticizer. These water-to-powder ratios were highly different, 1 for MgO and 0.32 for calcite. Consequently, PCE was added at a constant dosage of 1 mg/g of solid and the new apparent yield stress was recorded. All the suspensions were mixed by a commercial electronic mixer for 1 min, then the addition of PCE was done and the paste was mixed for an additional minute prior to the measurement. The temperature was kept constant at 20 °C using a water bath during the tests, and no segregation of particles was observed. Some additional experiments applying higher dosages (2 and 4 mg/g) of 8.5PC3 and 45PC3 to MgO suspensions were performed in order to test the effect concentrations higher than 1 mg/g of solid.

Table 2
Characteristic properties of powders used for PCE tests.

Material	Name	Blaine (cm^2/g)	BET (m^2/g)	Density (g/cm^3)	% volume diameters (μm)		
					d_{10}	d_{50}	d_{90}
Cement N	CEM I 42.5 N	3150	0.94	3.11	2.8	17.1	52.74
Cement HS	CEM I 42.5 N HS	4050	1.21	3.11	2.9	14.2	45.3
Magnesium oxide	Magnesia 298 (MgO 99.5%)	–	5.77	3.51	1.8	7.4	65.3
Calcite	Nekafill 15 ($CaCO_3$ 90.9%)	–	1.33	2.71	1.5	12.4	103.0

3.2. Adsorption

Adsorption measurements were performed to detect the quantity of superplasticizer adsorbed on the solid particles. This value is usually determined by the solution depletion method. After mixing the powder with the solution containing the polymer, the amount of superplasticizer remaining in the solution can be measured by separating the liquid phase from the suspension. The consumed polymer is estimated to be the difference in concentration before and after contact with the powder.

Volume fractions and superplasticizer dosages were the same as used for the rheological experiments. Ten minutes after mixing, the samples were centrifuged and the liquid part was removed and filtrated through a 0.45 μm nylon filter. Then a Sievers 5310 Laboratory TOC-Analyzer was used to determine the total organic carbon (TOC) of the remaining liquid phase, which gives direct information about the amount of remained polymer. TOC content of the pore solution without superplasticizer was considered as background to calculate the consumed PCE. The solution depletion method explained does not allow to detect whether the polymer really adsorbs on the particle surface or if the polymer remains simply trapped between the particles after the centrifugation. The term 'consumed' instead of 'adsorbed' is hence preferred to avoid false statements.

3.3. ζ-potential

The electrokinetic potential of colloidal systems is called ζ-potential. It represents the potential difference between the dispersion medium and the stationary layer of water molecules and ions attached to the dispersed particle. In other words, it may be interpreted as particle charge measured on a slip plane usually composed by the species adsorbed in proximity of the surface.

Table 3
Chemical composition (wt.%) of cements.

	CaO	SiO_2	Al_2O_3	Fe_2O_3	MgO	Na_2O	K_2O	SO_3	CO_2	Total amount
Cement N	62.6	19.0	4.5	3.1	2.2	0.21	0.82	3.3	2.1	97.8
Cement HS	59.8	17.9	4.3	5.9	2.4	0.59	0.82	3.1	2.7	97.5

Table 4
Chemical composition of the solutions extracted from the mixtures after 10 min of hydration (mmol/L).

	SO_4^{2-}	Na^+	K^+	Mg^{2+}	Ca^{2+}	OH^-	pH
Synthetic pore solution	200	40	444	<0.1	10	104	12.8
Cement N	237	37	449	<0.1	14	121	13.0
Cement HS	124	58	216	<0.1	11	99	12.9
Magnesium oxide	6	4	0.4	15	0.2	0.4	10.7
Calcite	0.5	0.4	0.3	0.2	0.4	0.1	9.4

Actually, it does not represent the charge directly detected on the particle surface; hence it is highly influenced by the presence of ions or charged polymers in solution.

All the ζ-potential data were collected with a ZetaProbe instrument (Colloidal Dynamics Inc., North Attleboro, MA), which works on the basis of the electroacoustic method. The motion of particles in suspension driven by an electrical field is recorded as dynamic mobility, from which the software calculates the ζ-potential.

The aim of measuring ζ-potential is to detect changes in particle charges according to superplasticizer concentration. The adsorption of the negatively charged backbone on the solid particles forms an additional slipping layer which influences particle charge. A change in particle charge is the first indication that the adsorption process is occurring, and it gives information about electrostatic dispersion forces eventually taking place at the particle surfaces. To detect these effects of powder–polymer interaction, 8.5PC3 and 45PC3 were titrated up to a concentration of 5 mg/g of solid to a relatively diluted suspension (wt = 5%) of magnesium oxide using deionized water or synthetic pore solution, respectively.

3.4. Atomic force microscopy

AFM force measurements in liquid solution containing superplasticizers were performed by a commercial instrument (Nanoscope IV, Veeco Digital Instruments, Santa Barbara, CA). This atomic force microscope consists of a cantilever with a sharp tip (probe) at its end, which is used to scan the specimen substrate. When the tip approaches the sample substrate, forces between the tip and the sample lead to a cantilever deflection, which is measured using a laser spot reflected from the top surface of the cantilever into a photodiode. This deformation gives information about substrate topography and the force interacting between the tip and the substrate. A schematic representation of AFM general setup and the translation of a deflection signal into a force–distance curve, using the cantilever spring constant, are presented elsewhere [16]. The distance = 0 is determined as the point of the raw deflection–distance curve in which the deflection of the cantilever becomes linear. The linearity of the cantilever deformation versus the distance indicates the position in which the tip is in a static position in contact with the substrate, thus the movement of the scanner is fully converted in the cantilever deformation.

Since it was previously measured that the silicon nitride showed a high affinity with superplasticizers [16], a commercially available plateau tip (NanoAndMore GmbH, Wetzlar, D) coated with a platinum layer of 20 nm of thickness was used here to probe the dispersion forces (see Fig. 4 from NanoAndMore GmbH).

In this way it was possible to approach the substrate covered with superplasticizer with a neutral and flat surface. The idea is to prevent superplasticizer adsorption on the probe. The coating process influenced the elasticity of the cantilever, and this effect was taken into account by measuring the spring constant after the sputtering process.

Water or artificial cement pore solutions containing different amounts (1, 2 and 4 g/L) of superplasticizers (8.5PC3 and 45PC3), which correspond to the concentrations used for the rheology and adsorption experiments, were flushed into a fluid cell and the forces were then detected.

4. Results and discussion

Results and discussion are divided into two parts. In Section 4.1, the influence of eight different superplasticizer architectures on the rheology and on the adsorption behavior of two kinds of cements and inert model suspensions is analyzed. In Section 4.2, a more detailed study on two representative PCEs is provided, focusing on the origin of the dispersion forces directly interacting among the particles. This second analysis is based on experimental results obtained with MgO powder and MgO substrates for AFM experiments. This restriction is dictated by the use of AFM in liquid environment.

4.1. Influence of superplasticizer architecture on suspensions

With this first set of results, a wide range of polymer architectures is discussed to test their influence on rheological properties and adsorption, relating them to the presence of ions in solution.

4.1.1. Rheology

The apparent yield stresses of suspensions holding the same dosage (1 mg of PCE per g of solid) of different superplasticizers are reported in Figs. 5 and 6.

Differences in superplasticizer side chain length and in side chain density affect the collected data significantly, on cements and on

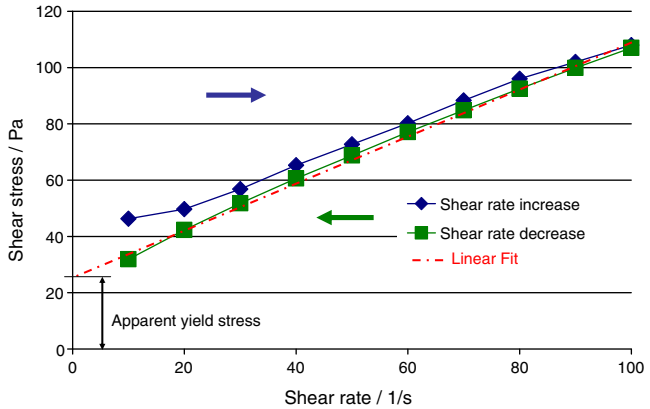

Fig. 3. Typical example of flow curve.

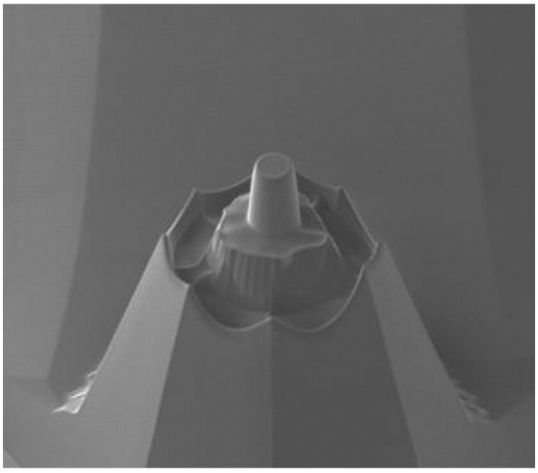

Fig. 4. Image of the AFM-tip. Plateau diameter = 1.8 μm.

model powders. Generally, low charge density confers low apparent yield stresses to the cement suspensions. For instance, 8.5PC3 and 45PC3 have the same density of grafted side chains, but 8.5PC3, because of higher charge density, enables more effective rheological properties. On the other side, comparing 45PC3 with 45PC12, i.e. superplasticizers with same side chain length but different charge densities, the higher charge of 45PC12 brings a significant contribution to improve the rheology of the mixture, leading to a lower apparent yield stress in all the considered suspensions.

The two kinds of cement show generally different behaviors, although the same w/c ratio was used for the mix. Cement N, despite its lower Blaine value and lower BET surface area in dry conditions, provides higher apparent yield stresses in comparison to the cement HS. Accordingly, the cement HS presents different fineness and smaller particle size distribution. In principle, these features of cement HS would lead to a loss of workability, due to the larger area in contact with water; though it allows a more compact packing of particles within the mixture which usually provides good fluidity. On the other side, the reactions occurring at the first minutes of hydration change the total surface area of the cement particles [23], thus misleading the discussion of the influence of specific surface area on cement rheology. Indeed, due to its high content of C_3A, cement N produces more ettringite. The needle-shaped crystals of ettringite [24] at the early age of hydration contribute to increase the total surface area of the cement particles in the paste, influencing the rheological properties of the mixture. As consequence of these facts, the hydration process plays an important role in influencing the flowability of the cement paste.

Looking at results obtained with inert powders (Fig. 6), they show a significant difference between suspensions prepared with pore solution and suspensions prepared with water. Especially in the calcite system, the measurements performed with water show a drastic decrease of the apparent yield stress after the superplasticizer addition, even for those PCEs which do not have strong influence in the other systems (111PC1.5 and 111PC3). This comparison between the different inert mixtures reveals that the presence of ions in the solution disturbs the PCE efficiency.

4.1.2. Adsorption

The adsorption ratios of suspensions with the same dosage of superplasticizers (1 mg of PCE per g of solid) are shown in Table 5. Three different normalizations are provided: adsorption per unit weight of powder (mg/g), adsorption per surface BET unit area of dry powder (mg/m^2) and adsorption ratio between PCE added and PCE consumed (%). Each of this normalization is in principle correct, and they take into account different aspects of the adsorption process. These data provide more information to the reader and allow a more complete understanding of the adsorption phenomenon. The normalizations emphasize the difficulties of a direct comparison of the

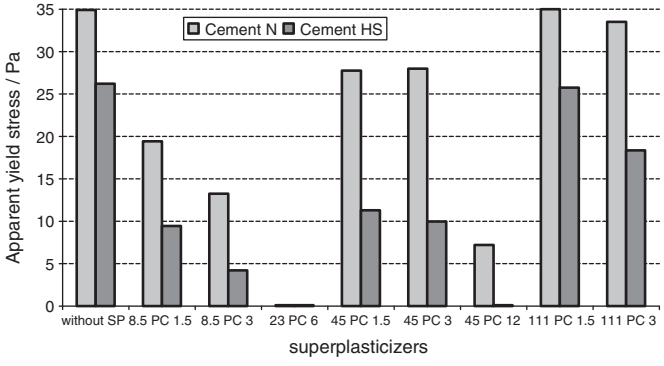

Fig. 5. Apparent yield stress of cement suspensions mixed with water and different superplasticizers (1 mg of PCE per g of solid).

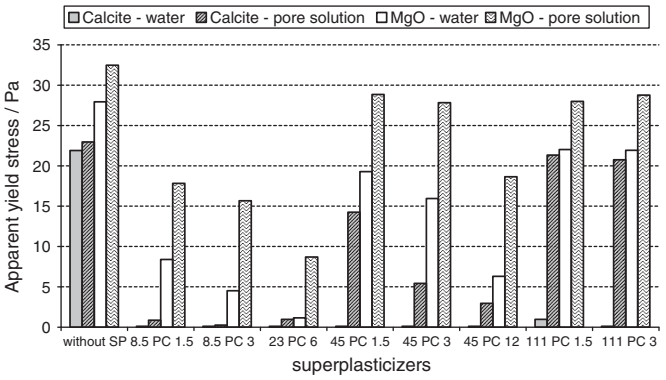

Fig. 6. Apparent yield stress of inert powder suspensions mixed with water or synthetic cement pore solution containing superplasticizers (1 mg of PCE per g of powder).

adsorption data due to the differences in specific surface area. However some trends can be observed and the discussion is led according to the different types of PCE architecture, to the two kinds of cement and to the influence of ions.

In each liquid–solid system, higher charge density of PCE enables stronger adsorption in particle suspensions. Indeed, 111PC1.5 and 111PC3 afford rather poor adsorption compared to 8.5PC1.5 or 23PC6. This is also due to the high molar mass of the side chains, which results in a lower molar charge density. The concept to supply high charge density and long side chains at the same time is to reduce the

Table 5
Adsorption of superplasticizer on tested powders.

	Cement N			Cement HS		
	Per weight (mg/g)	Per surface area (mg/m^2)	Adsorption ratio (%)	Per weight (mg/g)	Per surface area (mg/m^2)	Adsorption ratio (%)
8.5PC1.5	0.66	0.70	67	0.61	0.51	63
8.5PC3	0.63	0.67	61	0.55	0.45	54
23PC6	0.65	0.69	66	0.62	0.52	64
45PC1.5	0.30	0.32	31	0.15	0.12	15
45PC3	0.40	0.43	39	0.34	0.28	33
45PC12	0.49	0.52	49	0.45	0.37	45
111PC1.5	0.01	0.01	1	0.01	0.01	1
111PC3	0.02	0.02	2	0.06	0.05	1

	Calcite–water			Calcite–pore solution		
	Per weight (mg/g)	Per surface area (mg/m^2)	Adsorption ratio (%)	Per weight (mg/g)	Per surface area (mg/m^2)	Adsorption ratio (%)
8.5PC1.5	0.67	0.50	66	0.32	0.24	32
8.5PC3	0.46	0.34	47	0.18	0.13	18
23PC6	0.40	0.30	50	0.41	0.31	51
45PC1.5	0.54	0.40	52	0.27	0.20	26
45PC3	0.61	0.46	62	0.25	0.19	26
45PC12	0.38	0.28	37	0.29	0.22	29
111PC1.5	0.27	0.20	27	0.09	0.06	9
111PC3	0.32	0.24	31	0.18	0.13	17

	MgO–water			MgO–pore solution		
	Per weight (mg/g)	Per surface area (mg/m^2)	Adsorption ratio (%)	Per weight (mg/g)	Per surface area (mg/m^2)	Adsorption ratio (%)
8.5PC1.5	0.84	0.15	80	0.74	0.13	71
8.5PC3	0.86	0.15	79	0.61	0.11	56
23PC6	0.64	0.11	81	0.52	0.09	66
45PC1.5	0.50	0.09	52	0.21	0.04	21
45PC3	0.45	0.08	47	0.24	0.04	25
45PC12	0.69	0.12	65	0.47	0.08	45
111PC1.5	0.01	0.01	1	0.01	0.01	1
111PC3	0.23	0.04	21	0.01	0.01	1

grafting density. Indeed, 45PC12 in comparison to 45PC3 generally performs stronger adsorption on the tested suspensions.

Regarding cement mixtures, cement N adsorbs slightly larger amounts of PCE in comparison to cement HS, despite the double amount of sulfate presence in the extracted pore solution. In the first 10 min of hydration, the ettringite formed from C_3A phase allows adsorption properties to the cement suspensions. More ettringite is formed, more PCEs are required to obtain a high workability. Furthermore, ettringite formation increases the specific surface area if cement, providing more available surface for PCE adsorption.

On the other side, regarding the inert powders, the adsorption is strongly influenced by the presence of ions in the suspensions. In general, the ions present in the pore solution have the tendency to interfere with the adsorption process, reducing the amount of consumed polymer in both systems treated with pore solution. It was shown that sulfate ions, with their high negative charge, compete with PCE to occupy the surface of positively charged particles [25], affecting the adsorption of the polymer on grain surface. Thus, among all the ionic species present in solution, sulfates are the most likely candidates to interfere with the adsorption process.

4.1.3. Discussion about superplasticizer efficiency

To obtain a similar initial apparent yield stress in suspension without superplasticizer, very different solid fractions had to be used. This significant difference is probably due to different particle size distributions, which may create disparity in the water demand. Indeed, MgO has a d_{50} value that is much smaller than the one of the other three powders, and also its specific surface area (BET) is nearly five times larger than the other ones. This means that, at the same weight, the area at the solid–liquid interface is five times more, hence increasing the water demand. This fact is the main reason why a higher water-to-powder ratio was required for MgO in order to obtain similar apparent yield stresses.

Different superplasticizer architectures achieve differences in adsorption and in rheological properties. Generally, high charge density is responsible for high adsorption, which then leads to low apparent yield stresses. Long side chains reduce the molar charge density of the polymer, and this effect creates some difficulties in the adsorption process, since it is mainly driven by electrostatic attraction between the negatively charged polymer and the positively charged particles. By theory, longer side chains should exert higher steric repulsion between two particle surfaces, thus affording more effective rheological properties, and higher performance in cement pastes. However, the superplasticizer with the longest side chain does not produce the best performance in fresh mixtures, probably owing to their poor adsorption.

Regarding the two cements used here, cement N contains a larger amount of C_3A, which forms ettringite during the early hydration. The ettringite is directly related to PCE adsorption, due to the increase of the available positively charged surface area. However, rheological properties clearly show the tendency of having low apparent yield stress in suspension prepared with cement HS. Indeed, whenever there is a substantial quantity of ettringite formed, more PCEs are required to provide fluidity to the suspension, because the large surface area of ettringite adsorbs much polymer. Thus, on one side this hydration product negatively impacts the rheological properties, but on the other side it provides a strong adsorption. This effect suggests the idea that large amount of adsorbed PCE does not necessarily imply low apparent yield stresses.

The use of inert powders to test rheology and adsorption clearly shows a strong influence of ions on superplasticizer behavior, reducing the PCE action when the liquid–powder mix is prepared with pore solution. Actually, it is reasonable to imagine that many ionic species in the suspension and the pH may influence the ζ-potential of the particles, consequently negatively affecting the adsorption ratio, resulting in worse rheological properties.

A comparison between all these data suggests the idea that another aspect of PCE efficiency has to be considered. Calcite treated with water and PCE shows a drastic decrease of the apparent yield stresses, which does not match with similarly strong adsorption of superplasticizer. In a previous publication [16], the adsorption of PCE has been detected on the same calcite–water system used here, but the suspensions were prepared with a much lower solid content. There, the results displayed that superplasticizer interaction with calcite powder is very poor. The increase of adsorbed polymer according to the increase of particles in suspension suggests the idea that in certain cases superplasticizers are not really sticking on particles, but they remain trapped and framed between two adjacent particle surfaces. This effect may give less friction and less pressure among particles, thus affording a more compact packing of the solid grains. This allows effective rheological properties even without specific attachment of the polymer on the particles.

4.2. Detailed analysis of dispersion forces

In this second part a detailed analysis of the dispersion forces owed to superplasticizer is presented. Since some experiments were performed using the AFM, it was necessary to limit the set of previously used materials to inert materials. However, calcite was not considered because of its poor ability to adsorb superplasticizer in diluted systems, which is the case of the AFM set-up, thus reporting low force ranges [16]. Thus all the measurements were performed on magnesium oxide. The variety of superplasticizer structures tested also was reduced to only two kinds, 8.5PC3 and 45PC3, in order to focus on the effect of different side chain lengths, different charge densities, and different PCE concentrations.

4.2.1. AFM

Force–distance curves measured with AFM are displayed in Fig. 7, which reports plots for the curves collected with 8.5PC3 and 45PC3 in concentrations of 1, 2 and 4 g/L in water or synthetic cement pore solution. Without superplasticizer, an attraction between the tip and the substrate was observed.

One of the most evident differences between these two plots is the change in dispersion forces occurring at different concentrations when superplasticizer 8.5PC3 is used. Opposite to this, measurements performed with 45PC3 show no apparent impact on repulsion between the tip and the substrate as a result of higher polymer concentration in solution. Accordingly, all the curves collected in water (empty markers) and in pore solution (filled markers) overlap. For interpretation of the force curves, some assumptions were made. For instance, one possible explanation for this effect is the probable formation of multi-layers of 8.5PC3, which accumulate on the MgO substrate. For a PCE possessing low charge density and long side chain, i.e. 45PC3, the interaction with particles may be weak, so after the formation of a first layer of PCE on the particle surface, the other side superplasticizer remains in the solution not producing the accumulation of many layer of PCE. These differences in dispersion forces by varying the concentration of PCE was already directly observed with highly charged superplasticizers, and similar conclusions about multilayer formation were made [27]. AFM images scanned in air on substrates with depositions of PCE provide a further confirmation of this accumulation of superplasticizer on the substrate [28].

A second observation is related to experiments done in pore solution, which display a significant reduction of dispersion force values, compared to results obtained in water. It shows once again the strong influence of ions on the effect of superplasticizer. The reduction of the force ranges in presence of ions was already observed in the literature. Sindel et al. (1999) speculated that the presence of electrolytes disrupts hydrogen bonds required to form an extended polymer conformation [26], and Kirby and Lewis (2004) attributed the shrinkage of polyelectrolytes in high ionic strength solution to

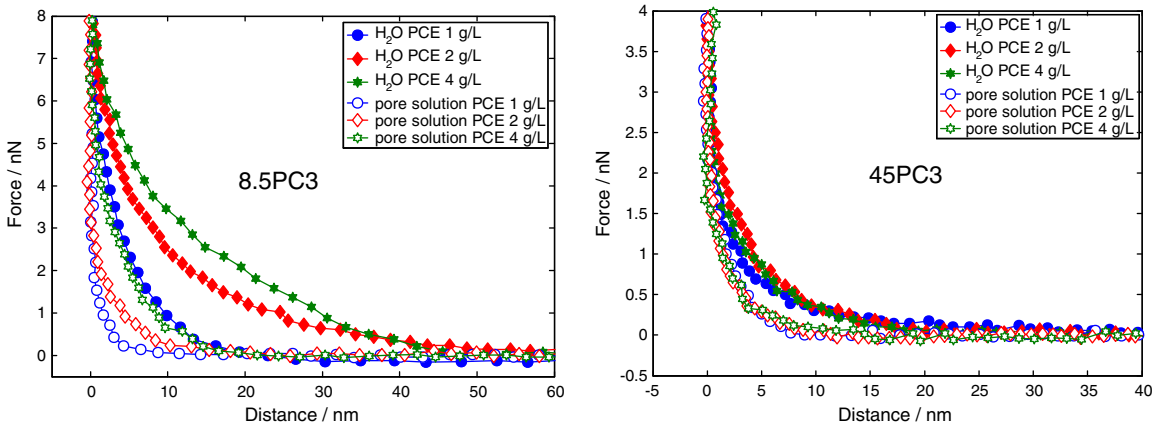

Fig. 7. AFM force measurements.

reduced intersegment repulsion between screened COO^- groups [5]. Both interpretations can in principle be true and can explain the decrease of the force ranges.

4.2.2. Adsorption

Adsorption isotherms obtained on magnesium oxide at increasing concentrations of superplasticizer are reported in Fig. 8.

As expected from previous discussions, short side chains afford high charge density, hence strong adsorption on solid particles. Indeed, the isotherm curve of 8.5PC3 displays a higher adsorption, compared to the one obtained with 45PC3. The presence of ions in solution influences the interaction superplasticizer–powder, thus lowering the adsorption of both PCEs. However, highly anionic 8.5PC3 is much more affected by ions than 45PC3.

4.2.3. ζ-potential

In order to evaluate the possibility of electrostatic forces interacting between particles coated by superplasticizer molecules, ζ-potential measurements were performed. Fig. 9 shows particle charge values at different concentrations of superplasticizers.

Adsorption of 8.5PC3 on MgO enables to change the particle ζ-potential from positive to negative. On the other side, 45PC3, which has a lower charge density, brings the MgO particle to values of ζ-potential around zero.

In this set of measurements, the presence of ions in solution highly affects the conductivity of the suspensions (deionized water = 0.7 mS/cm, pore solution = 35 mS/cm), and consequently it affects particle charges. Indeed, measurements of ζ-potential show that titration of superplasticizers is highly different according to the used solution. When the measurements are performed in synthetic pore solution, the initial value of MgO particles is negative, and it remain almost constant during the PCE titration.

4.2.4. Rheology

It is known that a higher dosage of PCE gives more effective rheological properties to cement pastes. For consistence, apparent yield stresses obtained with MgO suspensions in water and pore solution with different concentrations of 8.5PC3 and 45PC3 are provided in Fig. 10.

Differences in side chain length and in ionic composition of the solution again affect the efficiency of PCE. Indeed, addition of 8.5PC3 to a suspension grants lower apparent yield stress compared to the addition of 45PC3. However, when exceeding a certain PCE dosage (4 mg/g of solid), this difference is not that significant any more: the apparent yield stress values are similar, with the exception of 45PC3 in pore solution.

On the other hand, the measurements obtained in pore solution display poor rheological properties, compared to the suspension mixed with deionized water. This fact reveals that the presence of ions, maybe mainly of sulfates, reduces superplasticizer performance, reasonably disturbing the adsorption of polymer on the particles, and thus the dispersion force as well.

4.2.5. Discussion about dispersion forces

As shown in the previously discussed data, differences in superplasticizer architecture produces different results on adsorption and rheological properties. In addition to these observations, superplasticizer dosage highly influences apparent yield stress data,

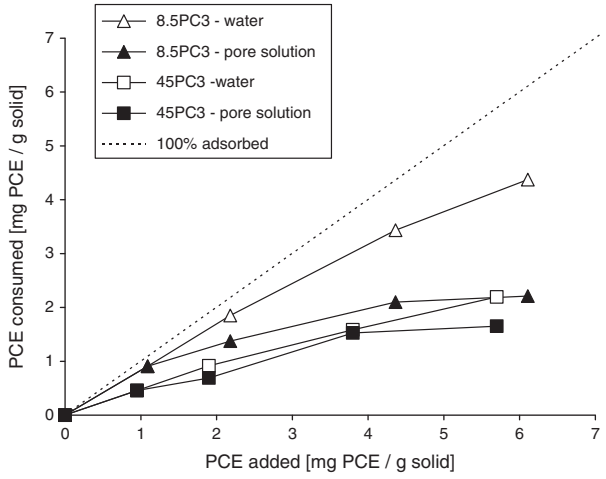

Fig. 8. Adsorption isotherms for different PCEs in MgO suspensions prepared with water or synthetic cement pore solution.

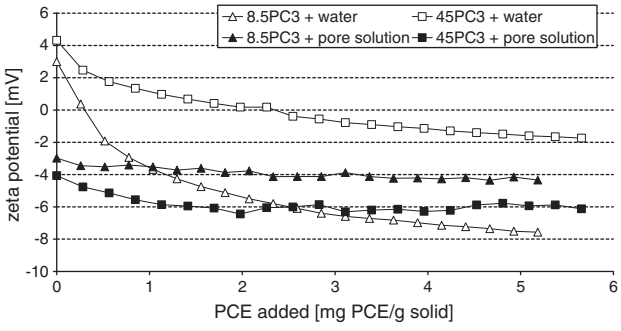

Fig. 9. ζ-potential of MgO at different concentrations of superplasticizer in deionized water or in pore solution.

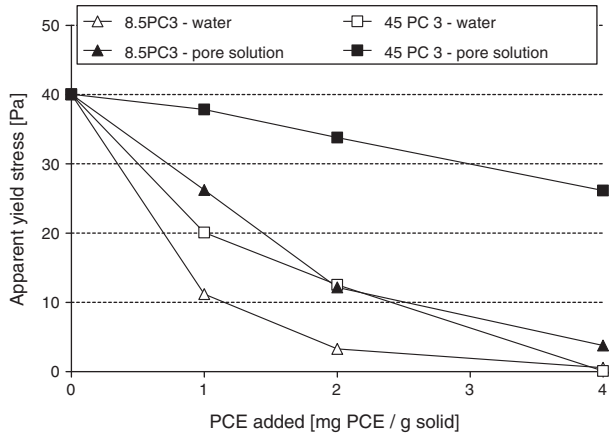

Fig. 10. Apparent yield stress of MgO suspensions at different PCE concentrations.

even in systems where the dispersion forces did not increase with PCE concentration (see data collected with 45PC3). In other words, even when the dispersion forces, steric and electrostatic, do not increase with increase of dosage of superplasticizer, the rheological properties of the suspensions improve. Hence, from microscopic point of view, no differences occur at the surface level of individual particles. However, probably a larger amount of particles is covered by superplasticizers, and this fact reduces the apparent yield stresses of the paste. In any case, it is possible to conclude that shorter side chains afford higher performances in adsorption and rheology. Furthermore, AFM results show that they provide stronger dispersion forces that increase with the concentration of PCE in solution.

On the other side, ionic species in solution disturb superplasticizer behavior in each aspect analyzed here: adsorption on particle, dispersion steric forces, ζ-potential, and consequently rheology. The adsorption of sulfate ions on positive particles influences the ζ-potential, which influences the adsorption process. The ions in solution also affect the steric dispersion forces by reducing force ranges and intensities, thus influencing the rheology. Of course, in an actual cement suspension, there is no possibility of avoiding the interaction superplasticizer–ions, but we find these results to present a good starting point to understand cases of unexpected incompatibility between PCE and cement.

5. Conclusions

This study shows that superplasticizer architecture affects the efficiency of PCE. Generally, the addition of PCE to a particle suspension provides more effective rheological properties, thus reducing the apparent yield stress of the mixture. The results elucidate that high polymer charge affords strong adsorption of the superplasticizer, then high dispersion forces, and thus good rheology. The AFM measurements also show that certain PCE architectures lead to dispersion of local forces which vary with the concentration of superplasticizer in solution.

Tests on two kinds of cement with different amounts of ettringite formed after 10 min of hydration reveal that this hydration product strongly affects the workability of the cement paste, by increasing the surface area of the cement particles and providing high adsorption of superplasticizer.

Tests on inert powders clarify that the presence of different ion species in solution may impede PCE adsorption, and so the apparent yield stress values. The use of an AFM plateau tip coated with platinum reveals that dispersion forces are also affected by high ionic strength.

Another aspect emerging from this multi-method analysis concerns the idea that rheological properties are not only depending on PCE adsorption and PCE dispersion forces. Our analysis starts from macroscopic observations, i.e. rheological measurements, and it zooms in focusing on details of superplasticizer behavior at the solid liquid interface, i.e. adsorption and dispersion forces. However, suspensions of calcite treated with water, where adsorption and the dispersion forces are not optimal, give surprisingly low apparent yield stress values. This observation could potentially be explained by the existence of a third effect, namely the filling of the interstitial spaces between neighbor particles, to avoid their direct contact and lubricating their surfaces, in order to reduce the friction between adjacent particles. Furthermore, it is expected that properties of the liquid also are affected by PCE presence: if the water–solid interface is energetically convenient, it increases the wettability of particle surface and the water will have the tendency to distribute around particles. More research in this direction is hence needed.

Concluding, major reason of incompatibility phenomena has been clarified and additional information was elucidated by this study. However, in order to complete the study on this topic, further investigation is important and indispensable.

Acknowledgments

The authors thank Florian Deschner, Angela Steffen, Emilie L'Hopital, Wolfgang Kunther (Empa) and Carolina Di Paolo (eawag) for their technical support.

References

[1] S.K. Agarwal, I. Masood, S.K. Malhotra, Compatibility of superplasticizers with different cements, Constr. Build. Mater. 14 (5) (2000) 253–259.
[2] W. Prince, M. Espagne, P.-C. Aitcin, Ettringite formation: a crucial step in cement superplasticizer compatibility, Cem. Concr. Res. 33 (5) (2003) 635–641.
[3] P.-C. Nikinamubanzi, P.-C. Aitcin, Cement and superplasticizer combinations: compatibility and robustness, Com. Concr. Agg. 26 (2) (2004) 102–109.
[4] T.G. Mezger, The Rheology Handbook, 2nd Edition, Vincent Network, Hannover, 2006 Coatings Compendia.
[5] G.H. Kirby, J.A. Lewis, Comb polymer architecture effects on the rheological property evolution of concentrated cement suspensions, J. Am. Ceram. Soc. 87 (9) (2004) 1643–1652.
[6] S. Hanehara, K. Yamada, Interaction between cement and chemical admixture from the point of cement hydration, adsorption behaviour of admixture, and paste rheology, Cem. Concr. Res. 29 (8) (1999) 1159–1165.
[7] A. Zingg, F. Winnefeld, L. Holzer, J. Pakusch, S. Becker, R. Figi, L. Gauckler, Interaction of polycarboxylate-based superplasticizers with cements containing different C_3A amounts, Cem. Concr. Compos. 31 (2009) 153–162 [1].
[8] J. Plank, C. Hirsch, Impact of zeta potential of early cement hydration phases on superplasticizer adsorption, Cem. Concr. Res. 37 (2007) 537–542.
[9] Y.F. Houst, P. Bowen, F. Perche, A. Kauppi, P. Borget, L. Galmiche, J.-F. Le Meins, F. Lafuma, R.J. Flatt, I. Schober, P.F.G. Banfill, D.S. Swift, B.O. Myrvold, B.G. Petersen, K. Reknes, Design and function of novel superplasticizers for more durable high performance concrete (superplast project), Cem. Concr. Res. 38 (2008) 1197–1209.
[10] J. Plank, K. Pöllmann, N. Zouaoui, P.R. Andres, C. Schaefer, Synthesis and performance of methacrylic ester based polycarboxylate superplasticizers possessing hydroxy terminated poly(ethylene glycol) side chains, Cem. Concr. Res. 38 (2008) 1210–1216.
[11] J. Plank, Z. Dai, N. Zouaoui, Novel hybrid materials obtained by intercalation of organic comb polymers into Ca-Al-LDH, J. Phys. Chem. Solids 69 (2008) 1048–1051.
[12] J. Plank, Ch. Winter, Competitive adsorption between superplasticizer and retarder molecules on mineral binder surface, Cem. Concr. Res. 38 (2008) 599–605.
[13] A. Zingg, F. Winnefeld, L. Holzer, J. Pakusch, S. Becker, L. Gauckler, Adsorption of polyelectrolytes and its influence on rheology, zeta potential, and microstructure of various cement and hydrate phases, J. Coll. Int. Sci. 323 (2008) 301–312.
[14] H. Uchikawa, S. Hanehara, D. Sawaki, The role of steric repulsive force in the dispersion of cement particles in fresh paste prepared with organic admixtures, Cem. Concr. Res. 27 (1997) 37–50.
[15] A. Kauppi, K.M. Andersson, L. Bergström, Probing the effect of superplasticizer adsorption on the surface forces using the colloidal probe AFM technique, Cem. Concr. Res. 35 (2005) 133–140.
[16] L. Ferrari, J. Kaufmann, F. Winnefeld, J. Plank, Interaction of cement model systems with superplasticizers investigated by atomic force microscopy, zeta potential, and adsorption measurements, J. Coll. Int. Sci. 347 (2010) 15–24.

[17] B. Beyribey, B. Corbacioglu, Z. Altin, Synthesis of platinum particles from H_2PtCl_6 with hydrazine as reducing agent, G.U. J. Sci. 22 (4) (2009) 351–357.
[18] F. Winnefeld, S. Becker, J. Pakusch, T. Götz, Effects of the molecular architecture of comb-shaped superplasticizers on their performance in cementitious systems, Cem. Concr. Compos. 29 (2007) 251–262.
[19] A. Otha, T. Sugiyama, T. Uomoto, Study of dispersion effect of polycarboxylate-based dispersant on fine particles, in: V.M. Mahlotra (Ed.), 6th CANMET/ACI, Nice, France, 2000, pp. 211–227.
[20] R.J. Flatt, Y.F. Houst, P. Bowen, H. Hofmann, J. Widmer, U. Sulser, U. Maeder, T.A. Bürge, Interaction of superplasticizers with model powders in a highly alkaline medium, in: V.M. Malhotra (Ed.), 5th CANMET/ACI, Farmington Hills, MI, 1998, pp. 743–762.
[21] J. Plank, D. Zhimi, H. Keller, F.V. Hössle, W. Seidl, Fundamental mechanisms for polycarboxylate intercalation into C_3A hydrate phases and the role of sulfate present in cement, Cem. Concr. Res. 40 (2010) 45–57.
[22] B. Lothenbach, F. Winnefeld, Thermodynamic modeling of the hydration of Portland cement, Cem. Concr. Res. 36 (2) (2006) 209–226.
[23] K. Yamada, A summary of important characteristics of cement and superplasticizers, Proceedings of the 9th International Conference on Superplasticizers and Other Chemical Admixtures in Concrete, ACI SP-262, , 2009, pp. 85–95.
[24] G. Möschner, B. Lothenbach, F. Winnefeld, A. Ulrich, R. Figi, R. Kretzschmar, Solid solution between Al-ettringite and Fe-ettringite ($Ca_6[Al_{1-x}Fe_x(OH)_6]_2(SO_4)_3\cdot 26H_2O$), Cem. Concr. Res. 39 (6) (2009) 482–489.
[25] K. Yamada, S. Ogawa, S. Hanehara, Controlling of the adsorption and dispersing force of polycarboxylate-type superplasticizer by sulfate ion concentration in aqueous phase, Cem. Concr. Res. 31 (3) (2001) 375–383.
[26] J. Sindel, N. Bell, W. Sigmund, Electrolyte effects on nonionic steric layers: bis-hydrophilic PMAA-PEO Diblock copolymers adsorbed on barium titanate, J. Am. Ceram. Soc. 82 (1999) 2953–2957.
[27] L. Ferrari, M. Ben Haha, J. Kaufmann, F. Winnefeld, Force measurements by AFM on clinker surfaces and model systems in aqueous solutions containing superplasticizer, Proceedings of the Thirty-Second Conference on Cement Microscopy, 2010, New Orleans, LA, USA.
[28] L. Ferrari, J. Kaufmann, F. Winnefeld, J. Plank, Multi-method approach for the characterization of the behavior of superplasticizer in cement suspensions, Proceedings of the XIII ICCC International Congress on the Chemistry of Cement, Madrid, 2011.

Paper 3

Multi-method approach for the characterization of the behavior of superplasticizer in cement suspensions

L. Ferrari, J. Kaufmann, F. Winnefeld, J. Plank

Proceedings of the XIII ICCC International Congress
on the Chemistry of Cement, Madrid 2011

Multi-method approach for the characterization of the behavior of superplasticizer in cement suspensions

[1, 2] Lucia Ferrari[*], [1] Josef Kaufmann, [1] Frank Winnefeld,
[a]*Empa, Swiss Federal Laboratories for Materials Testing and Research,*
Laboratory for Concrete/Construction Chemistry, Ueberlandstr. 129, 8600 Duebendorf, Switzerland.
[2]Johann Plank
[b]*Technische Universität München,* Department of Chemistry, *Lichtenbergstr. 4, 85747 Garching, Germany*

Abstract
Superplasticizers (also known as High-Range Water-Reducing Admixtures) are fundamental chemical admixtures to disperse the colloidal particles in fresh concrete and mortar mixtures. Besides improving the workability properties, many other aspects are positively influenced, allowing the production of high performance concrete or self-consolidating concretes. Despite this wide use of superplasticizers, their fundamental mechanisms of interaction at the solid-liquid interface are not completely understood yet, sometimes leading to unexpected effects, e.g. cement sensitivity, fast slump loss, flash setting or delay setting. The main working principles of these admixtures are related to their adsorption on the colloidal particles and the dispersion nano-forces exerted by their side chains. Furthermore, this adsorption process provokes significant alteration in the surface charge, hence in the ζ-potential of the particles in suspension.

A study including all these aspects (rheology, adsorption isotherms, force characterization by atomic force microscopy -AFM- and ζ-potential) is presented here. A comprehensive understanding of superplasticizers fundamentals principles is emphasized. Besides fresh cement pastes, model inert powders in combination with synthetic solutions are used to monitor the effect of different ions contents. A detailed analysis about polymer architecture and about ionic species in solution is presented in order to illustrate the influence of these parameters on superplasticizer behavior. Moreover, the AFM results clarified the formation of superplasticizer multilayer, and highlighted changes in side chain conformation according to the solution used to monitor it.

Originality
This work presents a wide set of techniques which allows a complete characterization of the action of superplasticizer in suspension. Previous work based on selections of these methods only included the possibility of capturing some of all the involved aspects of the complex mechanisms of these polymers. The comparison and correlation of these results obtained with different facilities permitted to detect separately different sides of the same phenomena and gives a detailed view of the effect of these chemical admixtures on particles suspensions.

Chief contributions
The combination of these different methods offers a high quality characterization of the superplasticizer interaction at the solid-liquid interface. This study is important to understand the main factors relating these chemical admixtures with their effect on the workability and rheology of fresh cement suspensions. A detailed analysis of polymer architecture and of ionic species in solution is presented in order to clarify how these parameters can affect superplasticizer efficiency. Furthermore, the direct detection of multilayer formation is experimentally measured by AFM. These observations may open many possibilities for development of new admixtures and to improve the performances of the fresh concrete.

Keywords: *atomic force microscopy; zeta potential; adsorption; rheology; superplasticizer; cement.*

[*] **Corresponding author: Email lucia.ferrari@empa.ch Tel +41 (0)44 823 43 60, Fax +41 (0)44 823 40 35**

Introduction

Polycarboxylate ether-based superplasticizer (PCE) is a chemical admixture broadly used in cement applications. Its addition to concrete or mortar allows the reduction of the water to cement ratio, not affecting the workability of the mixture. This effect drastically improves the performance of the hardening fresh paste. Despite many studies have been done about these polymers, their working mechanisms lack of a full understanding, revealing in certain cases cement-superplasticizer incompatibilities [1].

PCEs are usually composed by a main chain where side chains of different lengths can be grafted according to different densities [2]. The backbone, which is negatively charged, permits the adsorption on the positively charged colloidal particles [3]. In a suspension, the adsorption of superplasticizers on solid particles is important to avoid the formation of aggregates, which obstruct the paste flow, leading to bad rheological properties [4]. As a consequence of PCE adsorption, the ζ-potential of the suspended particles may change, owing to the adhesion of the negatively charged backbones on the colloid surface [5]. This attachment of the polymer to the particle surface ensures for the side chains the possibility to exert repulsion forces, which disperse the particles of the suspension [6]. In the past, these forces were directly detected by the use of AFM, working with model substances in liquid environment [7]. The application of model materials is necessary since the AFM technique requires very smooth and almost non-reactive substrates. A multi-method approach is thus necessary to investigate all these aspects of superplasticizer behavior.

In this study, different techniques (rheology, adsorption measurements, ζ-potential and AFM) are involved to enable a complete understanding of the working mechanisms of superplasticizers. These methods offer different points of view of PCE effects, from a macroscopic to a microscopic analysis. The comparison of these results puts in relation the polymer architecture with the relative performances observed. Moreover, the use of an inert model powder helped to distinguish superplasticizers efficiency according to different ionic solutions.

Materials

Superplasticizers

The polycarboxylate superplasticizers investigated in this work are composed of methoxy-polyethylene-glycol side chains attached on a poly-methacrylic-acid backbone. Three different polymer architectures (see Table 1) were tested in order to understand how superplasticizers efficiency is influenced by the side chain length, represented by the number of polyethylene oxide (PEO) units p , and by the side chain density, represented by the number of grafted side chains n . Polymer synthesis of 8.5PC3 and 45PC3 is described in [8] and synthesis of 45PC12 is described in [9], while main chain length (MCL) and side chain length (SCL) were estimated according to [10].

Tab. 1: Characteristic properties of superplasticizer samples tested.

p PC n	M_n [1] (g/mol)	M_w [2] (g/mol)	PDI [3]	MCL (nm)	SCL (nm)	CD[4] (mmol/g)	Schematic Illustration
8.5 PC 3	25,800	106,000	4.1	36.3	2.4	4.2	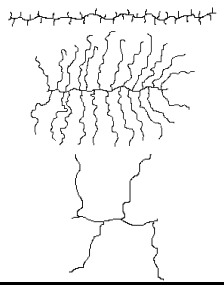
45 PC 3	50,100	156,700	3.1	21.7	12.5	1.4	
45 PC 12	11,800	342,500	2.9	12.5	12.5	3.9	

[1] M_n = number-average molecular weight.

[2] M_w =mass-average molecular weight.

[3] $PDI = M_n / M_w$ = polydispersity index.

[4]CD = anionic charge density.

Cements and model powders

To investigate the action of superplasticizer on different suspensions, two kinds of cement were used (see Table 2). They were selected to test how the different amount of tricalcium-aluminates content may influence the fresh paste, and the relative PCE effect.

Tab. 2: Characteristi properties of cement and MgO tested in this study.

material	name	Blaine (cm^2/g)	BET (m^2/g)	Density (g/cm^3)	% volume diameters (µm)		
					d_{10}	d_{50}	d_{90}
Cement N	CEM I 42.5 N	3150	0.94	3.11	2.8	17.1	52.74
Cement HS	CEM I 42.5 N HS	4050	1.21	3.11	2.9	14.2	45.3
Magnesium Oxide	Magnesia 298 (Magnesia GmbH)	-	5.77	3.51	1.8	7.4	65.3

Chemical composition of cements are reported in Table 3, while the content of main clinker phase (mass%) was calculated by Bogue method (Cement N: C_3S=58, C_2S=14, C_3A=6, C_4AF=11; Cement HS: C_3S=47, C_2S=15, C_3A=1, C_4AF=18). Additional to those materials, an almost inert powder of magnesium oxide (see Table 2) treated with water and artificial pore solution was involved to monitor the influence of ion species in solution, and to allow the measurements of AFM dispersion forces in liquid. The used solution intends to simulate the ion content found in real pore solutions after 1 h of hydration [11]: $[K^+]$=444 mM/L, $[Na^+]$=40 mM/L, $[Ca^{2+}]$=10 mM/L, $[OH^-]$=104 mM/L, $[SO_4^{2-}]$=200 mM/L; pH=12.8.

Tab. 3: Oxide composition of the cement samples studied.

Oxide composition (wt%)	CaO	SiO_2	Al_2O_3	Fe_2O_3	MgO	Na_2O	K_2O	SO_3^-	CO_2
Cement N	62.6	19.0	4.5	3.1	2.2	0.21	0.82	3.3	2.1
Cement HS	59.8	17.9	4.3	5.9	2.4	0.59	0.82	3.1	2.7

Methods

Rheology

Rheology tests were performed to record the PCE impact on the workability of a particle suspension. They were achieved using a Paar Physica MCR 300 rheometer with concentric cylindrical geometry. A rotating bob was lowered to the measuring position, and shear stress was detected recording a flow curve with shear rate from 10 up to 100 s^{-1} and from 100 down to 10 s^{-1}. Apparent yield stress was estimated interpolating the data of the return curve to find the intercept of the linear fit.

The w/c ratio was fixed at 0.36, while the water-to-solid ratio of MgO was adjusted to reach a value of initial apparent yield stress around 35±5 Pa. The solid fractions highly change depending on the kind of powder: the two cements display a w/c ratio of 0.36, while MgO displays a water-to-powder ratio of 1. All the suspensions were mixed by hand for 2 minutes prior to the measurement, and the temperature was kept fix at 20°C by a water bath. PCEs were added in dosage of 1, 2 and 4 mg/g of powder.

Adsorption

The quantification of the amount of polymer consumed by the particles in suspension was detected by adsorption isotherms. The solution depletion method was applied to measure the total organic carbon (TOC) of the liquid part of a suspension containing PCE. The TOC value gives information about the quantity of polymer not adsorbed on the particles, then remaining in the solution. Subtracting it from the initial amount of superplasticizer used for the mixture, the value of the polymer consumed by the suspension can be calculated.

Volume fractions and superplasticizer dosages were the same as used for the rheology measurements. 10 minutes after the mixing, the samples were centrifuged, then the liquid part was filtered by 0.45 Nylon filters. The TOC values of this left solution were determined by a Sievers 5310 Laboratory TOC-Analyzer.

ζ-potential

The ζ-potential values represent the colloid charge measured on a slipping plane at a certain distance from the particle surface. The adsorption of electrolytes and/or polyelectrolytes at the liquid-solid interface highly influences these values.

In this study, titration of PCE (up to 5 mg/g of powder) on diluted suspension (solid fraction=5 wt%) of MgO treated with water and synthetic pore solution were measured by a ZetaProbe (Colloidal Dynamics Inc., North Attleboro, MA), in order to capture the eventual presence of electrostatic forces acting as particle dispersant.

Atomic force microscopy

AFM force measurements in liquid solutions and images of the superplasticizers displacement on flat surfaces were performed by a commercial instrument (Nanoscope IV, Veeco Digital Instruments, Santa Barbara, CA). This atomic force microscope consists of a cantilever with a sharp tip (probe) at its end, which deflects whenever the tip is experiencing some interaction with the substrate. This deflection is used to give information about substrate topography and to translate the deflection signal into a force-distance curve, as explained in [12].

A commercially available plateau tip (width=1.8 µm, NanoAndMore GmbH, Wetzlar, D), coated with a platinum layer of 20 nm of thickness, was applied to probe the dispersion steric forces due to PCE in liquid solutions, avoiding electrostatic interaction and preventing superplasticizer adsorption on the probe. Water or artificial pore solutions with different concentrations of superplasticizers (1, 2 and 4 g/L), corresponding to the ones used for the rheology and adsorption experiments, were flushed into a fluid cell and the forces were then detected.

In a second attempt, images of PCE attachment on mica surface were scanned with tapping mode in air. A drop of solution containing superplasticizer (4 mg/L) was added on a freshly cleaved square of mica (1 cm^2), on which a drop of 0.1 molar solution of $MgNO_3$ was previously deposited. After 10 minutes, the solutions were washed away by about 3 mL of milli-Q water, and the sample was dried with air pressure. The positive Mg^{2+} ions work as binder between the negatively charged surface of mica and the negative main chain of PCE. This technique, commonly used for DNA experiments [13], allows the adhesion of the polymer on mica surface, and gives the possibility to scan images of their attachment to the surface.

Results and discussion

Table 4 reports the data obtained by rheology tests. The two kinds of cement give different apparent yield stresses in suspension without superplasticizer, despite they were mixed with the same w/c ratio. This is probably due to the high C_3A content in cement N, which forms a high amount of early hydration products, mainly ettringite. This corresponds well to the results obtained by Zingg et al. [14].

Tab. 4: Apparent yield stress of suspensions mixed with different PCE dosages.

Apparent yield stress (Pa)	Without PCE	8.5 PC 3 (mg/g)			45 PC 3 (mg/g)			45 PC 12 (mg/g)		
		1	2	4	1	2	4	1	2	4
Cement N	35	13	8	0	28	26	2	7	0	0
Cement HS	26	4	0	0	10	3	0	0	0	0
MgO - water	40	11	3	1	20	13	0	18	6	0
MgO - pore solution	40	26	12	4	38	34	26	39	26	8

The differences of polymer architecture and of charge density provide different apparent yield stress values. Less efficiency is provided by 45PC3, which reported the lowest anionic charge density. On the other hand, 45PC12 shows, compared to 8.5PC3, better effects on cement, and worst performance on MgO. Apparently, there is no specific explanation for this.

Experiments prepared with inert model powder allow the detection of a strong impact of ions on the action of superplasticizers. Indeed, results obtain with MgO in water are rather different from results obtained in pore solution. Probably this is due to presence of sulfate ions, which were shown to be the most probable competitor of PCE to occupy the surface of positively charged particles, thus affecting the adsorption process [3].

Admixture adsorption measurements were carried out on the same kind of suspensions (see Table 5). Cement N shows higher affinity with PCEs compared to cement HS. This effect is reasonably due to the higher C_3A content, which was shown to form ettringite that well adsorb superplasticizers [14].
Once again, the three kinds of superplasticizer give different results. The low charge density of 45PC3 enables poor adsorption of this polymer on the particles in suspension. On the other side, the presence of ions, and especially sulfate, in solution strongly disturbs the adsorption process, which leads to best results from MgO treated with water.

Tab. 5: Adsorption of PCE on powders mixed with different PCE dosages.

PCE consumed (mg/g)	8.5 PCE 3 (mg/g)			45 PC 3 (mg/g)			45 PC 12 (mg/g)		
	1	2	4	1	2	4	1	2	4
Cement N	0.7	1.3	2.0	0.5	0.7	1.0	1.0	2.0	2.8
Cement HS	0.7	1.1	1.2	0.4	0.7	1.1	0.9	1.5	1.9
MgO - water	0.9	1.9	3.4	0.5	0.9	1.6	1.0	2.0	4.0
Mgo - pore solution	0.9	1.4	2.1	0.5	0.7	1.5	0.9	1.7	3.0

In order to look at PCE from a microscopic point of view, additional experiments with ζ-potential and AFM were performed to study the dispersion forces produced by the polymers. The characteristic of the AFM instrument restricts the set of the used substances to MgO only, mixed with water or artificial pore solution.
Figure 1 shows ζ-potential values of suspensions of magnesium oxide with different PCE dosages. Superplasticizer with the same side chain length displays comparable curves, while 8.5PC3 provides a stronger impact on particle charge.

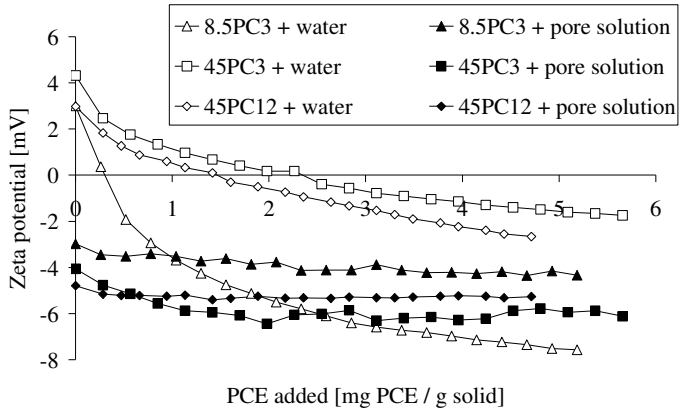

Fig. 1: ζ-potential of suspensions prepared with magnesium oxide at different superplasticizer concentrations.

The conductivity values of the two used solutions (water=0.7 mS/cm, pore solution=35 mS/cm) are rather different, strongly affecting the measurements. Indeed, suspensions treated with pore solution initially report negative charge values, due to the adsorption of the sulfate ions, and titration of superplasticizer does not change them significantly. On the other hand, suspensions mixed with water report initial positive values, and an inversion of charge is occurring at a certain PCE concentration. This concentration is around 0.5 mg/g for 8.5PC3, while it is nearly 1.5 mg/g for 45PC3 and 45PC12, showing that the charge of the COO^- ions of the main chain produces stronger electrostatic impact when surrounded by short side chains.
The investigation of steric dispersion forces was provided by the AFM work. Results obtained with 45PC3 are comparable to 45PC12, so for simplicity they are not reported. Force-distance plots obtained with 8.5PC3 and 45PC12 in water or synthetic pore solution containing different amount of PCE (1, 2 and 4 g/L) are reported in Figure 2. To insure a better visibility, the scales for force and distance were chosen different.

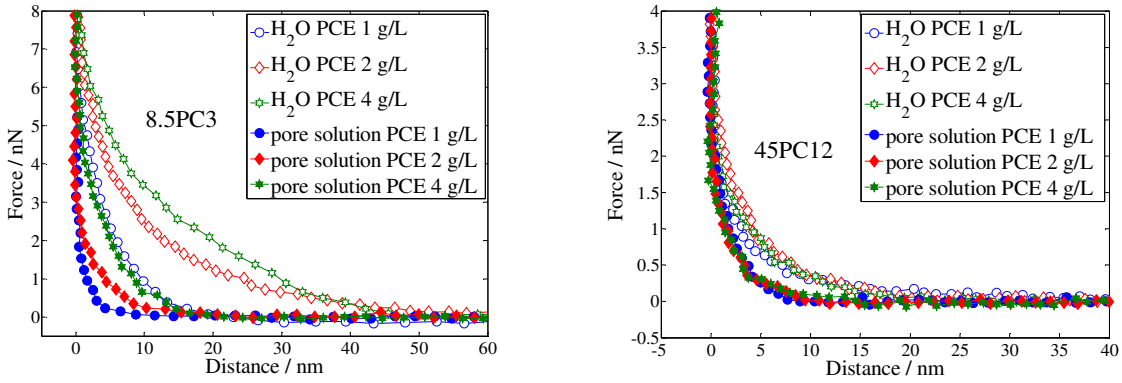

Fig. 2: AFM force measurements on MgO substrate with different PCE concentrations in water or pore solution.

The two plots display a great difference in superplasticizer behavior at the solid-liquid interface: 8.5PC3 gives dispersion forces which are affected by the PCE concentrations, while 45PC12, and 45PC3, give force-curve plots which display the same ranges even with different polymer dosages. Probably, 8.5PC3, *i.e.* short side chain superplasticizer, accumulates on MgO surfaces forming multi-layers, which gives stronger dispersion. These differences in force curves depending on different concentrations were already detected on MgO surface [15].
Furthermore, the presence of ions in solution reduces the ranges of the measured forces. Similar effects of ion species on the PEO unit conformation were reported by Sindel et al. [16]. They speculated about the presence of hydrogen bonds, which allow the stretched polymer conformation in water and their deconstructions owing to high ionic strength.
To investigate the possibility of multi-layer formation, AFM images of PCE displacement on mica surface were scanned as described in the methods section. These images are reported in Figure 3, where the white in-plots represent the height profile of the sections indicated by the straight line.

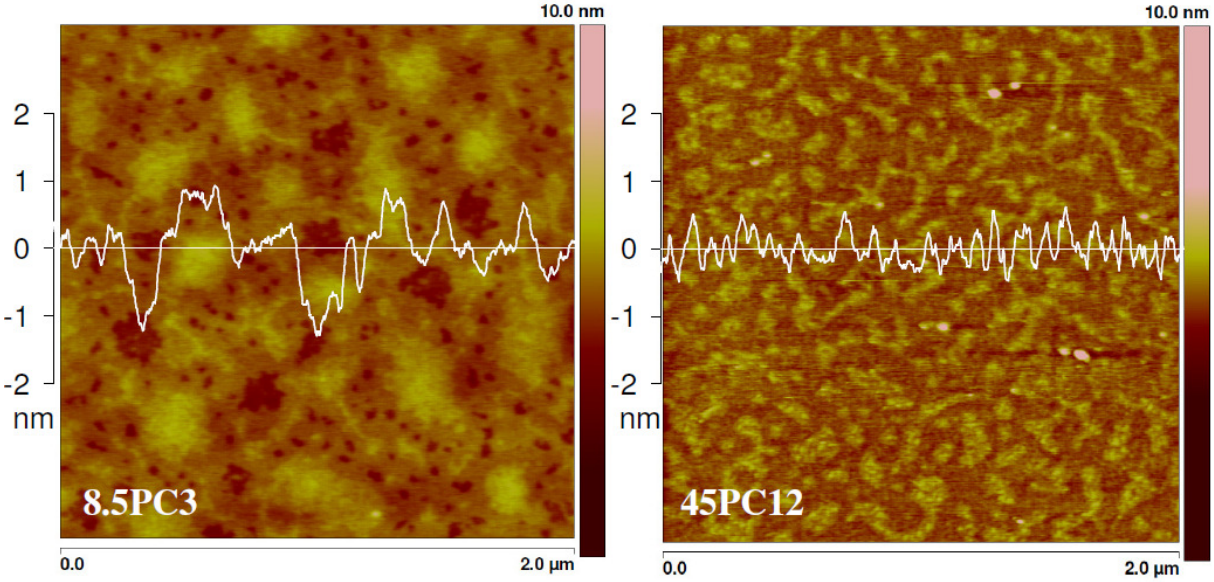

Fig. 3: AFM images of superplasticizers on mica surface.

It is evident, also from the section profiles, that the distribution of the analyzed superplasticizers on mica surface is rather different. 8.5PC3 tends to accumulate to form hills with a range of height around 2 nm, while 45PC12 tends to distribute more uniformly, covering the surface with islands of nearly 1 nm of height. Therefore, even if side chain length is lower for 8.5PC3, it forms greater accumulation of polymer, compared to 45PC3 and 45PC12. This effect provides stronger dispersion forces, hence better rheological properties, and better efficiency.

Conclusions

The variety of techniques involved here allows the understanding of some aspects which are important to characterize superplasticizer behavior at the solid-liquid interface.
As first remark, PCE architecture highly influences the efficiency of the polymer. The results show that short side chain superplasticizer enables high range dispersion forces, supported by good adsorption, and consequently good rheological properties. They have the tendency to accumulate on the particle surface to form multi-layers of polymer, which provide a stronger steric repulsion in comparison to the one provided by longer side chains PCE.
As second remark, the presence of ions, and specifically sulfates, in solution strongly disturbs the action of superplasticizers. Rheology and adsorption measurements display poorer results on inert model powder when it was treated with pore solution, compared to results obtained with deionized water. Indeed, a detailed analysis of the dispersion forces, electrostatic and steric, reveals that in ionic environment the influence of adsorbed polymer on the ζ-potential is relatively low, and that the side chains collapse when immersed in a solution with such a high ionic strength. Of course, in a proper cement paste, there are no possibilities of avoiding these ion effects. However all these results may be important to understand why sometimes the addition of superplasticizer to fresh concrete paste leads to incompatibilities and poor performance.

References

[1] Agarwal SK, Masood I, Malhotra SK. Compatibility of superplasticizers with different cements. Constr Build Mater 2000; 14(5) 253-9.
[2] Winnefeld F, Becker S, Pakusch J, Götz T. Effects of the molecular architecture of comb-shaped superplasticizers on their performance in cementitious systems. Cem Concr Compos 29 (2007) 251-262.
[3] Zingg A, Winnefeld F, Holzer L, Pakusch J, Becker S, Gauckler L. Adsorption of polyelectrolytes and its influence on rheology, zeta potential, and microstructure of various cement and hydrate phases. J Coll Int Sci 323 (2008) 301-312.
[4] Hanehara S, Yamada K. Interaction between cement and chemical admixture from the point of cement hydration, adsorption behavior of admixture, and paste rheology. Cem Concr Res 1999; 29(8) 1159-65.
[5] Plank J, Hirsch C. Impact of zeta potential of early cement hydration phases on superplasticizer adsorption. Cem Concr Res 37 (2007) 537-542.
[6] Uchikawa H, Hanehara S, Sawaki D. The role of steric repulsive force in the dispersion of cement particles in fresh paste prepared with organic admixtures. Cem Concr Res 27 (1997) 37-50.
[7] Kauppi A, Andersson K M, Bergström L. Probing the effect of superplasticizer adsorption on the surface forces using the colloidal probe AFM technique. Cem Concr Res 35 (2005) 133-140.
[8] Plank J, Pöllmann K, Zouaoui N, Andres P R, and Schaefer C. Synthesis and performance of methacrylic ester based polycarboxylate superplasticizers possessing hydroxy terminated poly(ethylene glycol) side chains. Cem Concr Res 38 (2008), 1210-1216.
[9] Plank J, Winter Ch. Competitive adsorption between superplasticizer and retarder molecules on mineral binder surface, Cem. Concr. Res. 38 (2008) 599-605.
[10] Otha A, Sugiyama T, and Uomoto T. Study of dispersion effect of polycarboxylate-based dispersant on fine particles. In: V. M. Malhotra (Ed.), 6th CANMET/ACI, Nice, France (2000), 211-227.
[11] Lothenbach B, Winnefeld F. Thermodynamic modeling of the hydration of Portland cement. Cem Concr Res 36 (2) (2006) 209-226.
[12] Ferrari L, Kaufmann J, Winnefeld F, Plank J. Interaction of cement model systems with superplasticizers investigated by atomic force microscopy, zeta potential, and adsorption measurements. J Coll Int Sci 347 (2010) 15-24.
[13] Witz G, Rechendorff K, Adamcik J, and Dietler G. Conformation of Circular DNA in Two Dimensions. Phys. Rev. Lett. PRL 101, (2008) 148103-1-4.
[14] Zingg A, Winnefeld F, Holzer L, Pakusch J, Becker S, Figi R, Gauckler L. Interaction of polycarboxylate-based superplasticizers with cements containing different C_3A amounts. Cem Conc Comp 31 (2009) 153-162.
[15] Ferrari L, Ben Haha M, Kaufmann J, Winnefeld F. Force measurements by AFM on clinker surfaces and model systems in aqueous solutions containing superplasticizer. XXXII Conference on Cement microscopy, New Orleans, LA, USA (2010).
[16] Sindel J, Bell N, and Sigmund W. Electrolyte Effects on Nonionic Steric Layers: Bis-Hydrophilic PMAA-PEO Diblock Copolymers Adsorbed on Barium Titaneate. J Am Ceram Soc 82 (1999) 2953-2957.

Paper 4

Reaction of clinker surfaces investigated with atomic force microscopy

L. Ferrari, J. Kaufmann, F. Winnefeld, J. Plank

Construction and Building Materials

(in review)

Reaction of clinker surfaces investigated with atomic force microscopy

L. Ferrari[a, b,1], J. Kaufmann[a, 1], F. Winnefeld[a], J. Plank[b].

[a]*Empa, Swiss Federal Laboratories for Material Science and Technology, Laboratory for Concrete/Construction Chemistry, Ueberlandstr. 129, 8600 Duebendorf, Switzerland.*

[b]*Technische Universität München, Department of Chemistry, Lichtenbergstr. 4, 85747 Garching, Germany*

Abstract

The application of microscopy to investigate cement hydration has widely spread in the last decades. For instance, scanning electron microscopy (SEM) is of primary importance to detect the formation of microstructures and quantify their chemical composition. In this work, atomic force microscopy (AFM), which is a relatively less diffused technique, is applied to illustrate and quantify changes of the surface roughness of a clinker surface treated with different electrolytic solutions with and without superplasticizer at different times of hydration. Furthermore, SEM images are collected to characterize the chemical composition of hydration products formed on the clinker surface. It is shown that surface reaction increases drastically with the increase of the pH, and that surface roughness changes occur mainly in the first 10 minutes of hydration. Moreover, the formation of hydration products is reduced when the clinker is treated with solutions containing polycarboxylate superplasticizer. Additionally, AFM images collected in tapping mode revealed the presence of nano-structures on calcium silicate phase after 30 minutes of hydration.

Keywords: AFM, EDX, superplasticizer, cement, clinker.

[1] Corresponding authors

E-mail address: lucia.ferrari@empa.ch tel: +41 (0)58 765 43 60

josef.kaufmann@empa.ch tel: +41 (0)58 765 40 95

1 Introduction

Ground clinker is the main component of Portland cement, and it is produced by sintering an ensemble of limestone with silica, alumina, and iron oxide-containing materials. This process results in a multi-phase solid consisting of round micron-sized calcium silicate particles of two different chemical compositions ($3CaO{\cdot}SiO_2$ and $2CaO{\cdot}SiO_2$), immersed in an interstitial matrix of aluminate and ferrite ($3CaO{\cdot}Al_2O_3$ and $4CaO{\cdot}Al_2O_3{\cdot}Fe_2O_3$). These four components, which represent the main cement phases, can be directly observed by microscopy on a polished clinker surface [1]. When clinker surface is brought in contact with an aqueous solution, amorphous and crystalline hydration products of different types according to the time of hydration are formed [2].

Relatively few studies were performed by atomic force microscopy (AFM) on cement. Indeed, most of the studies conducted with the AFM aim to measure surface forces in liquid containing polycarboxylate-ether based superplasticizer (PCE). These polymers generally adsorb on particles surfaces and provide dispersion forces which, reducing the formation of agglomerates, improve the workability of the cement paste [3]. Due to the high reactivity if cement with water, this AFM methodology applied in aqueous solutions requires the use of model materials [4]. However, images scanned with this kind of microscope were collected to directly observe the hydration process of cement paste at different relative humidities [5]. The results show that the process completes at about RH = 20% and no further change of structure were detected when the humidity was increased. A recent work illustrated that lateral force microscopy (LFM) can distinguish between calcium silicate hydrated particles and crystals of portlandite [6].

The focus of this study is to quantify clinker hydration by measuring changes in surface roughness. Clinker surfaces were scanned by AFM after the immersion in different solutions at various times of hydration. Energy-dispersive X-ray spectroscopic (EDX) analysis was performed by scanning electron microscopy (SEM) to characterize the hydration products formed on the surface. The combination of these two methods allows clear direct observations of the effect of different electrolyte solutions, of pH and PCE on clinker hydration.

2 Materials

2.1 Clinker

The chemical composition of the clinker was investigated by quantitative X-ray diffraction analysis (see table 1) using a PANalytical X'Pert Pro MPD diffractometer in a θ-2θ configuration employing CuK_α radiation (λ=1.54 Å) with a monochromator, a fixed divergence slit size of 1° and a rotating sample stage. The diffractograms were collected over a 2θ range of 5°-70° using X'Celerator detector.

Four different measurements were made for each kind of powder preparation: clinker ground by hand, clinker ground with alcohol using a Mc Crone mill to reduce particle size to d_{50}= 5µm, salicylic acid-methanol extraction to dissolve silicate phases, KOH/sugar treatment to remove aluminate and ferrite phases [7].

Table 1: phase composition of the OPC clinker in weight fraction (%).

Phase	Alite	Belite	Aluminate	Ferrite	Periclase	Quartz
Chemical formula	$3CaO{\cdot}SiO_2$	$2CaO{\cdot}SiO_2$	$3CaO{\cdot}Al_2O_3$ ortho	$4CaO{\cdot}Al_2O_3{\cdot}Fe_2O_3$	MgO	SiO_2
Content	68.5	13.8	4.3	12.2	0.5	0.8
Standard deviation	2.2	1.4	0.7	0.9	-	-

In order to study clinker surface, the clinker grain was impregnated with an epoxy resin, and then polished with oil based diamond suspensions until a grain size of 1/10 µm to obtain a mirror-quality surface.

2.2 Solutions

To study the reaction of clinker surface, water and different synthetic electrolytic solutions were chosen on the basis of ionic species present in cement pore solutions (see table 2). Since it was established that after 1 h of hydration the pore solution of cement is dominated by K^+, SO_4^{2-} and OH^- ions, while other cations and anions exist in lower concentrations [8], the analysis of clinker hydration was performed on potassium sulfate and potassium hydroxide solution in order to understand the influence of different anionic species on cement hydration. A synthetic pore solution was also applied to simulate a real cement solution.

Table 2: Chemical compositions of the tested solutions (mmol/L)

	SO_4^{2-}	Na^+	K^+	Ca^{2+}	OH^-	pH
0.1 M KOH			100		100	13.0
0.1 M K_2SO_4	100		200			8.1
Synthetic pore solution	200	40	444	10	104	12.8

An additional solution of water and polycarboxylate ether-based superplasticizers (3 g/L) was used to treat the clinker surface, in order to observe if any differences in hydration could occur. The architecture of the polymer used in this study, identified with 23PCE6, shows side chains with a length of 23 polyethylene oxide units connected by 6 carboxylic groups [10]. The number average molecular weight (M_n) was 7,600, the average molecular weight (M_w) was 18,900 g/mol, and the corresponding charge density (CD), calculated as the ratio between the moles of anionic charge and the molar mass of each PCE unit, was 3.8. This composition with a relatively low density of side chains affords a highly charged backbone that enables high adsorption on Portland cement and high effect on cement rheology [9].

3 Methods

3.1 AFM: principles and image processing

The AFM system consists of a cantilever with a sharp tip (probe) at its end, which is used to scan the specimen substrate (see figure 1). When the tip is brought into proximity of a sample surface, forces between the tip and the sample lead to a deflection of the cantilever. Typically, the cantilever deflection is measured using a laser beam reflected from the top surface of the cantilever to an array of photodiodes. This deflection of the cantilever hence provides information about substrate topography and allows direct measurements of the force between the tip and the substrate as a function of the distance separating them.

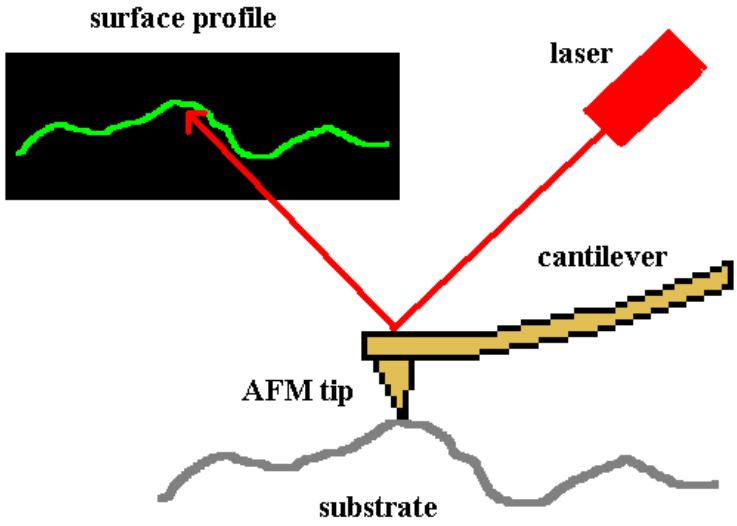

Figure 1: General AFM setup.

All AFM measurements were performed with a commercial instrument (Nanoscope IV by Veeco Digital Instruments, Santa Barbara, CA), using V-shaped tips made of silicon nitride. Clinker surface was examined after different times of immersion in different electrolytic solutions. The solutions were applied externally, then the samples were washed with deionized water and ethanol, and scanned by AFM in contact mode. Each substrate was scanned on 25 different areas of 1×1 μm^2 in dry conditions. In order to allow to scan of the same region after the removal of the sample from the AFM scanner, pictures of the cantilever position on the substrate were captured from an optical microscope positioned on top of the AFM. Figure 2 shows a typical picture illustrating the cantilever over a clinker surface. A pen spot mark was used to be able to find specific area previously scanned.

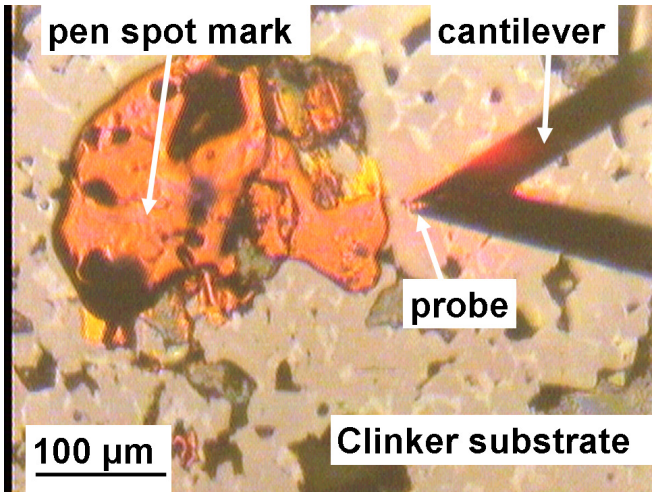

Figure 2: Image of the AFM cantilever scanning a clinker substrate.

The AFM software offers a section analysis module, which allows to calculate the standard deviation, *RMS*, of the vertical movement of the tip, *Z*, on a mean plane, Z_{ave}, while scanning a selected area. Therefore roughness quantification is calculated as

$$RMS = \sqrt{\frac{\sum_{i=1}^{N}(Z_i - Z_{ave})^2}{N}} \qquad (1)$$

where Z_i is the value of *Z* in the point *i*, and *N* is the number of points (pixels) within the given area.

Additionally to roughness information, the relative elasticity of the different clinker phases is detected by scanning the clinker substrate in tapping mode. A tapping AFM image is produced by detecting the force of the intermittent contacts of the tip with the sample surface, by producing oscillations which are close to the resonance frequency. Hence, different images of a calcium silicate grain were collected in tapping mode before and after 30 minutes of hydration in deionized water, in order to observe the differences in the elasticity of different hydration products.

3.2 SEM

Energy dispersive X-ray spectroscopy (EDX) was applied to quantify the elemental composition of the clinker surface and its hydration products, collecting back-scattered electron (BSE) images and energy-dispersive spectra. A scanning electron microscope (Philips SEM FEG XL 30) with a multichannel Princeton Gamma Tech analyzer was used. The accelerating voltage of the beam was adjusted to 15kV, to provide a good compromise between spatial resolution and adequate excitation of the FeKα peak. For the back-scattered electron (BSE) imaging, the spot size was chosen to have a good resolution of image and to generate reasonable X-ray results for the EDX analysis.

Five samples of clinker surfaces after 18 hours of immersion in deionized water, 0.1 M K_2SO_4, 0.1 M KOH, synthetic pore solution or water containing 3 g/L of PCE, were coated with a thin film of carbon (around 5 nm), to avoid charging, and then analyzed by EDX in high vacuum. After the collection of the BSE images of the substrate, nearly twenty points for each image were labeled on different phases in order to measure the corresponding element spectra.

4 Results

4.1 AFM investigations

RMS values of the surfaces scanned after different periods of immersion in several liquid environments are shown in figure 3. In some cases, the large amount of hydration products formed on the substrate impeded to the tip to properly scan the surface, obstructing the collection of well resolved AFM images. This is the reason why some columns are missing on the plot (NA= Not Adjusted).

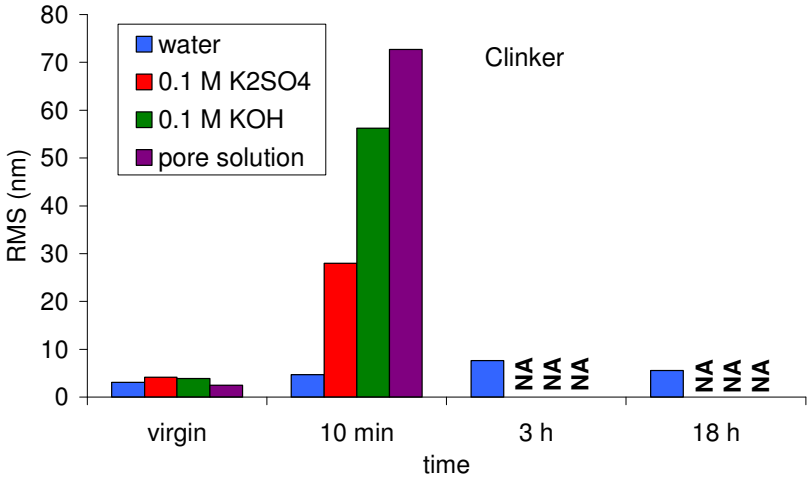

Figure 3: *RMS* values calculated on surfaces scanned after different times of immersion in several solutions. To note that due to high reactivity of clinker surfaces, the adjustment was not possible for all the data (NA columns).

AFM images scanned on OPC clinker surface at different periods of hydration with water are shown in figure 4. Note that with the help of the optical microscope place in the top of the AFM setup it was possible to scan exactly the same surface area. They show a rapid topography change in the first 10 minutes of hydration, while in longer time not significant changes are observed.

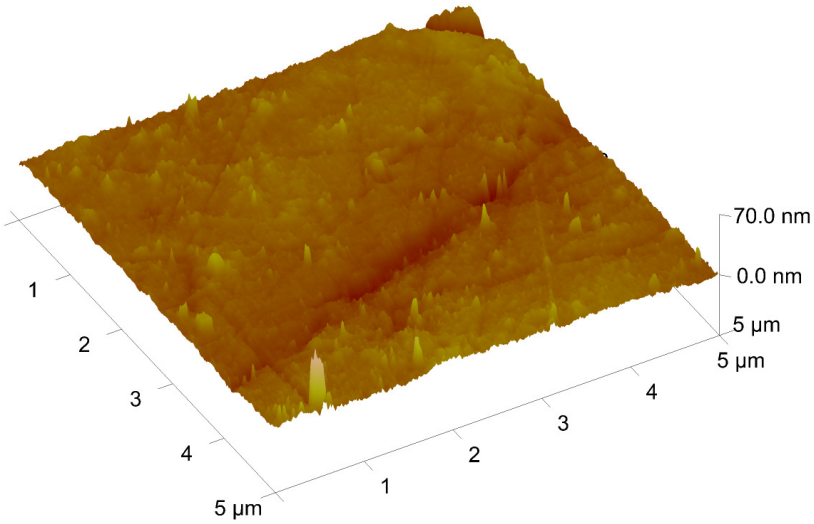

virgin surface

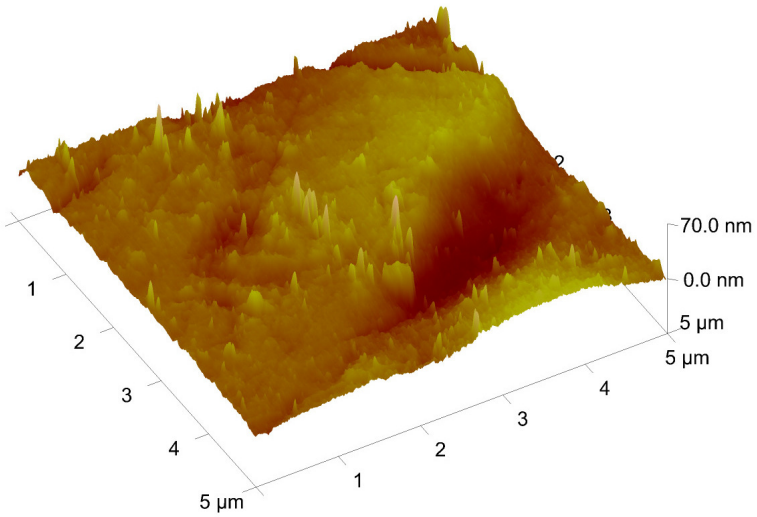

10 minutes

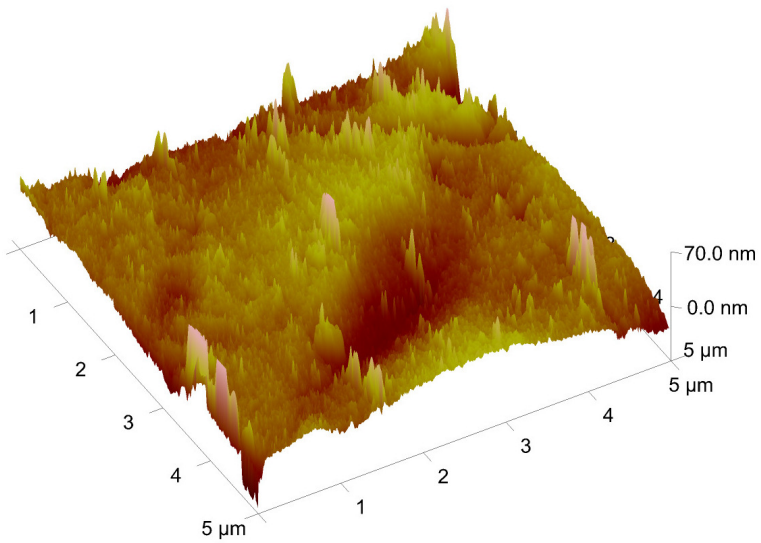

3 hours

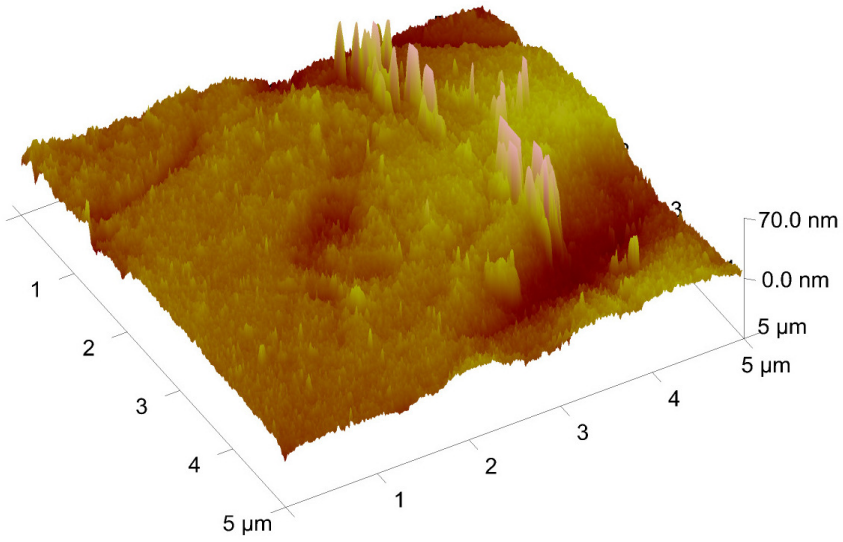

18 hours

Figure 4: AFM images of the topography of a clinker surface site scanned after different times of immersion in deionized water.

Figure 5 displays AFM images captured in tapping mode on a calcium silicate grain before (above) and after (below) 30 minutes of hydration in deionized water. From left to right it shows the height signal in nm (A & C) and the phase signal in degrees (B & D) collected while scanning the surface.

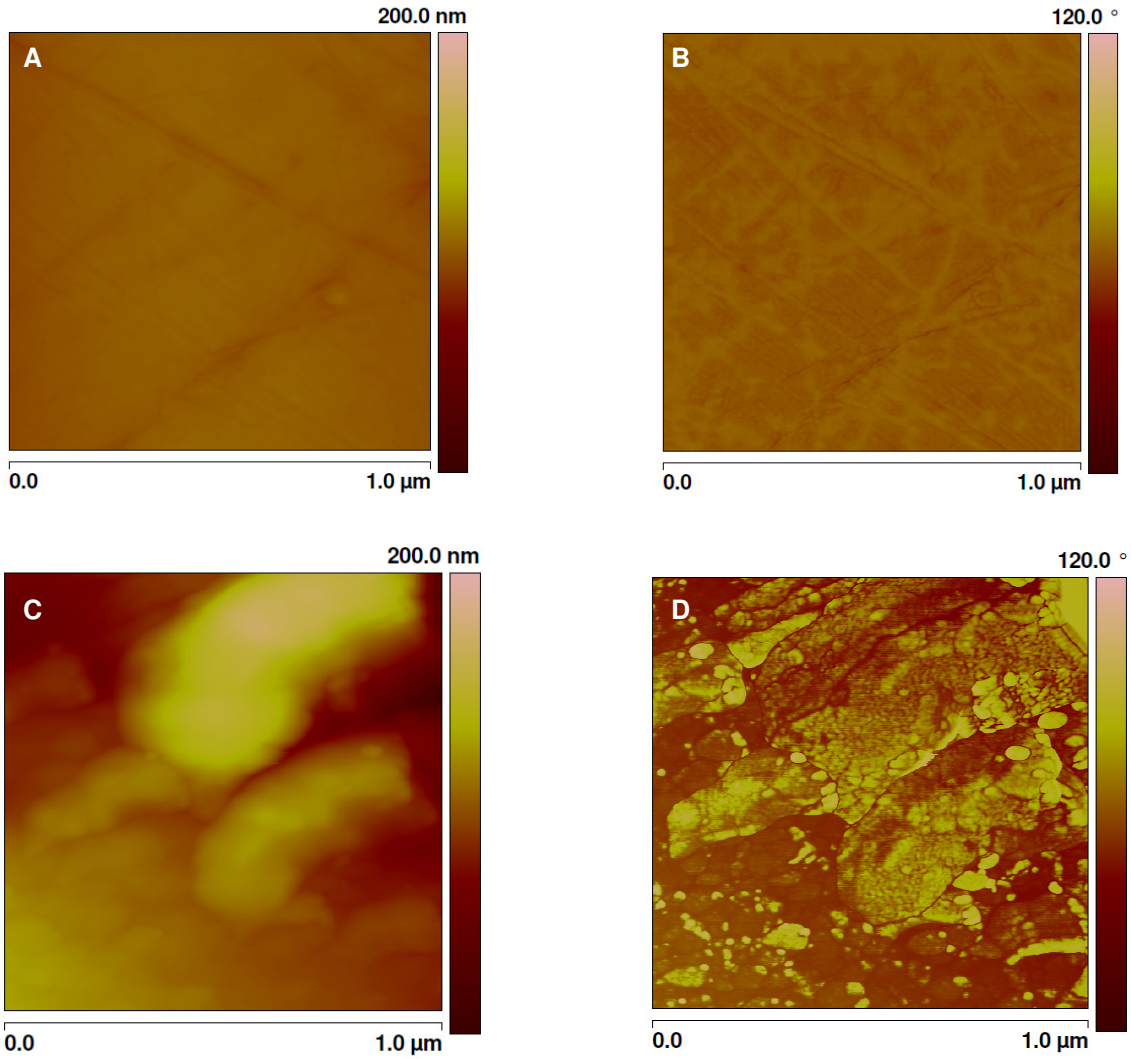

Figure 5: Clinker areas of a calcium silicate phase scanned in tapping mode before (above) and after (below) 30 minutes of hydration in deionized water. From left to right: height signal (A & C), and phase signal (B &D). Note that the phase image of clinker surface after 30 minutes of hydration (D-below) displays nano-structures that are not detectable with the topographic signal.

The height images (A & C) represent surface topography, while the phase images (C & D) distinguishes between different elasticity responses and adhesion forces on the substrate. The two images above (figure 5, A & B) illustrate the un-hydrated clinker surface. The main color contrast is due to the scratches caused by the polishing procedure. The two images below (figure 5, C & D) illustrate the change on the surface appearance after 30 minutes of hydration. The formation of large amorphous precipitates can be observed there. Specifically, the phase image (figure 5, D) reveals the presence of some nano-structures that are not detectable by the height and the amplitude signal. This result highlights the presence of significant non-homogeneities in the inner structure of these early hydration products.

4.2 SEM

The microstructures of hydrated clinker substrates after 18 hours in different liquid environment are shown in figure 6. Clinker surface after 18 h of hydration in: (A) deionized water, (B) solution of K_2SO_4 0.1 molar, (C) solution of KOH 0.1 molar, (D) synthetic pore solution and (E) deionized water containing 3 g/l of superplasticizer are displayed.

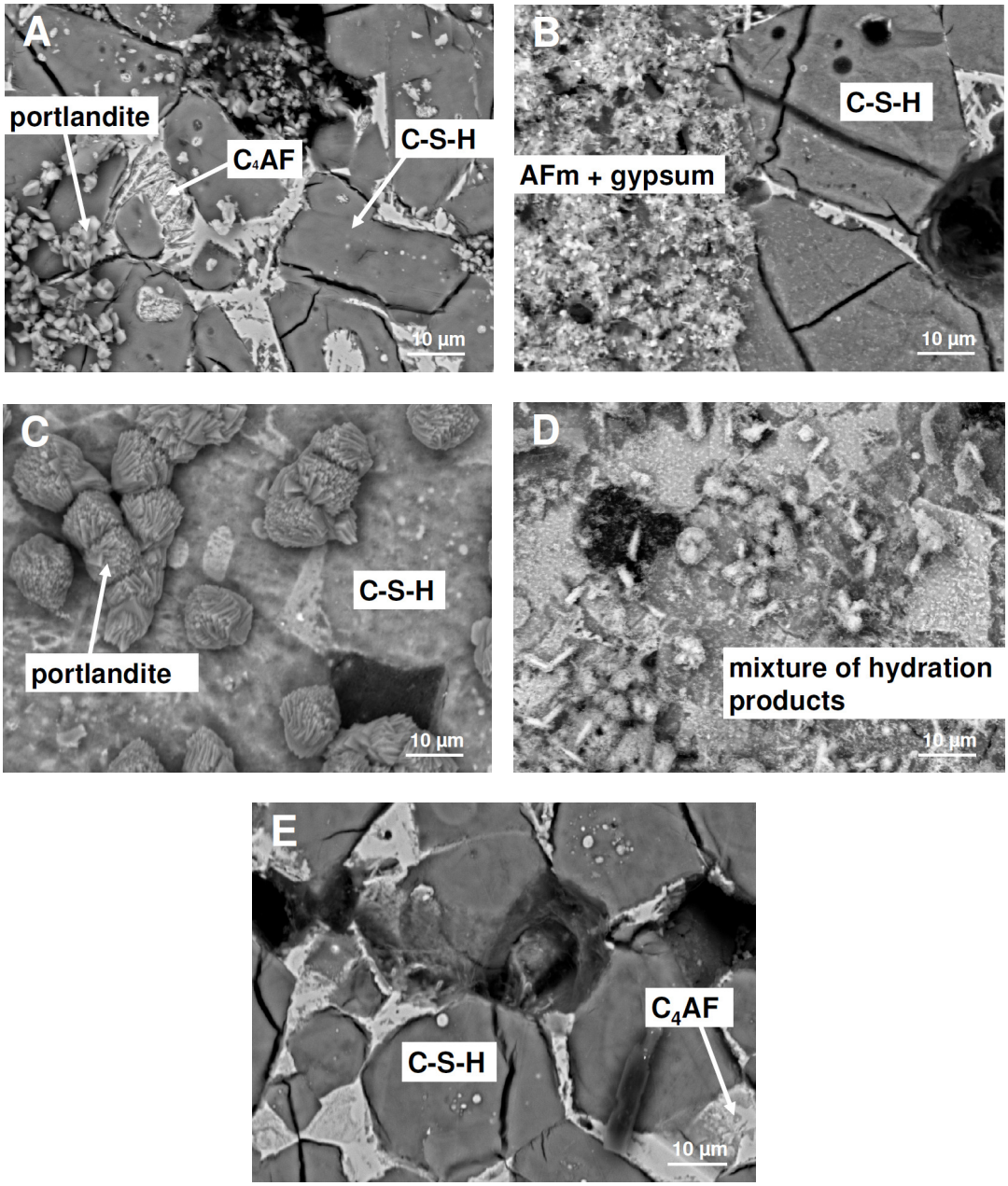

Figure 6: Microstructures of the clinker substrates after 18 hour of hydration in different solutions. A=deionized water, B= 0.1 M K_2SO_4, C= 0.1M KOH, D=synthetic pore solution, E=deionized water with 3 g/l of superplasticizer.

These results report that the reaction is relatively slow when the sample is treated with deionized water (figure 6 A). The image shows small deposits of portlandite as well as calcium silicate hydrate (C-S-H) layers covering some clinker phases. Almost no AFm precipitates are observed. The use of 0.1 M K_2SO_4 solution (figure 6 B) instead of water causes a corresponding increase in the rate of hydration. The surface shows many deposits of long and thick AFm phase are scattered across the matrix, as well as some gypsum particles. The immersion in 0.1 M KOH (figure 6 C) leads then to a high degree of hydration. The C-S-H layer is thicker and a significant amount of portlandite is distributed over the clinker substrate. The images clearly illustrate that these crystals formed in this solution are much larger in size than the crystals formed in pure water. Therefore, alkaline solution accelerates the reaction and favors the formation of portlandite. Working with the synthetic cement pore solution (figure 6 D), the amount of precipitates is much higher. In comparison to the other electrolyte solutions applied and to pure water, where the hydration products are mainly distributed around the anhydrous grains, here the crystals are scattered across the entire surface. All types of hydration products, including C-S-H phase, portlandite phase and some AFm phases, can be observed. Due to the relatively high degree of hydration, the area between individual crystals is well filled and the C-S-H is covered by other hydration products. However they were detected through the EDX analyses performed on the samples. After treatment of the sample with water containing superplasticizers (figure 6 E), the hydration process slows down. No portlandite crystals are observable any more, external C-S-H has precipitated in the matrix to cover the clinker particles, and the ferrite phase (C_4AF) is well distinguishable.

5 Discussion

The results of the surface roughness analysis performed with the AFM show that the *RMS* of clinker surface rapidly increases depending on the ionic strenght and on the pH, while deionized water works as slow activator for the hydration process. Furthermore, the AFM images show that the main change in topography on this substrate occurs in the first 10 minutes of hydration, while after longer time of hydration the surface does not show particular changes anymore. On the other side, to operate in tapping mode allows to detect heterogeneities in the elasticity and adhesion of the hydration products, revealing the presence of some nano-structures on a calcium silicate grain after 30 minutes of hydration.

The SEM images illustrate how the different electrolyte species in solution and the different pH values achieve various hydration products and precipitations on the clinker surface. In deionized water the precipitation of portlandite and the hydration of calcium silicate phases are much lower compared to the precipitation observed in presence of potassium and hydroxide ions, which favor the formation of large crystals of portlandite. The presence of sulfate promotes the precipitation of portlandite and AFm phase on the clinker surface, which strongly disturbs the AFM tip while it scans images. That is the reason why no good resolution images of the scanned area could have been obtained.

On the clinker surface hydrated in presence of superplasticizers, retardation in the formation of precipitates was observed. In agreement with the literature, the addition of PCE in a cement suspension disperses the early age hydration products, which, instead of precipitate on the clinker particles, remain suspended filling the interspaces between bigger particles [11]. In the case of clinker surface, small hydration products remained suspended in the solution and they did not precipitate due to the effect of the superplasticizer. In this way, these suspended particles were removed while washing the sample after the immersion in solution. Hence, PCE, which are known to work as retarders, reduces the precipitations of portlandite particles, reasonably dispersing them in solution. This effect in a cement mixture may avoid the formation of particle agglomerates, which strongly disturb cement rheology. Thus superplasticizer improves the workability of cement pastes by reducing the precipitation of small hydration products on larger clinker grains.

6 Conclusions

Surface reactions occurring on a cement clinker was studied by AFM and EDX to observe the formation of different hydration products after different times of hydration in a variety of solutions. Topography images collected with the AFM in contact mode allowed the quantification of changes in the surface roughness, while EDX analysis showed the chemical composition of the formed hydration products.

Surface reactions in most of the studied cases occur very fast depending on the electrolyte types in solution and on the pH. AFM images in tapping mode revealed the presence of nano-structures with heterogeneous elasticity on a calcium silicate grain after 30 minutes of hydration. On the other side, the presence of superplasticizer reduces the formation of portlandite precipitates, thus preventing the formation agglomerates that disturb cement workability

Acknowledgments

The authors wish to thank Boris Ingold, Mohsen Ben-Haha and Gwen Le Sout (Empa) for their technical contributions.

7 References

[1] Taylor H F W, Cement Chemistry, second ed., Thomas Telford Publishing, London, 1997.

[2] Kreppelt F, Weibel M, Zampini D, Romer M. Influence of solution chemistry on the hydration of polished clinker surfaces – a study of different types of polycarboxylic acid-based admixtures, Cem Concr Res 32 (2002) 187-198.

[3] T. G. Mezger. The rheology handbook. Hannover, Vincent Network (2006), 2nd Edition Coatings Compendia.

[4] Kauppi A, Andersson KM, Bergström L. Probing the effect of superplasticizer adsorption on the surface forces using the colloidal probe AFM technique. Cem Concr Res 35 (2005) 133-140.

[5] Yang T, Keller B, Magyari E. AFM investigation of cement paste in humid air at different relative humidities. J Phys D: Appl Phys 2002; 35 (8), 25-8.

[6] Peled A, Weiss J. Hydrated cement paste constituents observed with Atomic Force and Lateral Force Microscopy. Constr Build Mater (2011).

[7] Le Saout G, Kocaba V, Scrivener K. Application of the Rietveld method to the analysis of anhydrous cement. Cem Concr Res 41 (2011) 133-148.

[8] Lothenbach B, Winnefeld F. Thermodynamic modeling of the hydration of Portland cement. Cem Concr Res 36 (2006) 209-226.

[9] Ferrari L, Kaufmann J, Winnefeld F, Plank J, Multi-method approach to study influence of superplasticizers on cement suspensions. Cem. Concr. Res. (2011) In press.

[10] Ferrari L, Kaufmann J, Winnefeld F, Plank J. Interaction of cement model systems with superplasticizers investigated by atomic force microscopy, zeta potential, and adsorption measurements. J Coll Int Sci 347 (2010) 15-24.

[11] Zingg A, Holzer L, Kaech A, Winnefeld F, Pakusch J,Becker S, GauckIerL. The microstructure of dispersed and non-dispersed fresh cement pastes — New insight by cryo-microscopy. Cem Concr Res 38 (2008) 522–529.

Paper 5

Study of polycarboxylate-ether based superplasticizers on cement clinker surfaces by TOF-SIMS and AFM

L. Ferrari, L. Bernard, F. Deschner, J. Kaufmann, F. Winnefeld, J. Plank

Journal of American Ceramic Society

(in review)

Study of polycarboxylate-ether based superplasticizers on cement clinker surfaces by TOF-SIMS and AFM

L. Ferrari[a, b,1], L. Bernard[c], F. Deschner[a], J. Kaufmann[a, 1], F. Winnefeld[a], J. Plank[b].

[a]*Empa, Swiss Federal Laboratories for Material Science and Technology, Laboratory for Concrete/Construction Chemistry, Ueberlandstr. 129, 8600 Duebendorf, Switzerland.*

[b]*Technische Universität München, Department of Chemistry, Lichtenbergstr. 4, 85747 Garching, Germany*

[c]*Empa, Swiss Federal Laboratories for Material Science and Technology, Laboratory for Nanoscale Materials Science, Ueberlandstr. 129, 8600 Duebendorf, Switzerland.*

Abstract

The application of Ordinary Portland Cement (OPC) based binder is commonly improved by the addition of rheology modifying agents, *i.e.* superplasticizer. In the present work the interaction between polycarboxylate-ether based superplasticizers (PCEs) and the hydration products formed in aqueous solutions after 30 minutes on polished OPC clinker surfaces is studied. Energy-dispersive X-ray spectroscopy (EDX) provides the chemical analysis and the localization of the different phases below the surface hydration products. Time-of-flight secondary ion mass spectrometry (TOF-SIMS) allowed to detect on which cement phases PCE preferentially adsorbed and is used to map the distribution of the chemical elements at the surface of the clinker. Force measurements in liquid, performed by atomic force microscopy (AFM) with sharp tips, test the surface-tip interactions in presence/absence of PCE. The results show that superplasticizers induce precipitation of arcanite. When K_2SO_4 precipitates, the concentration of sulfate ions in the solution is reduced, disturbing ettringite formation. AFM force measurements allow the distinction between positively and negatively charged hydration products, revealing that most of the clinker phases are negatively charged. Through the application of TOF-SIMS, it was possible to observe for the first time preferential adsorption of superplasticizer on cement phases.

***Keywords**:* TOF-SIMS; AFM; clinker; cement; superplasticizer.

---

[1] Corresponding authors

E-mail address:	lucia.ferrari@empa.ch	tel: +41 (0)58 765 43 60
	josef.kaufmann@empa.ch	tel: +41 (0)58 765 40 95

1 Introduction

The main component of Portland cement is ground clinker, which is obtained by sintering an ensemble of limestone with silica, alumina, and iron oxide-containing materials. The result of this process is a multi-phase solid consisting of round micron-sized calcium silicate particles of two different chemical compositions ($3CaO{\cdot}SiO_2$ and $2CaO{\cdot}SiO_2$), immersed in an interstitial matrix of aluminate and ferrite ($3CaO{\cdot}Al_2O_3$ and $4CaO{\cdot}Al_2O_3{\cdot}Fe_2O_3$). These four components represent the main cement phases, and they can be directly observed with microscopy on a polished clinker surface. When clinker surface is brought in contact with an aqueous solution, amorphous and crystalline hydration products are formed according to the time of hydration [1]. Not all the phases react equally. In general $3CaO{\cdot}Al_2O_3$ is the most reactive component, and at very early age (10-15 minutes) it forms ettringite ($3CaO{\cdot}Al_2O_3{\cdot}3CaSO_4{\cdot}32H_2O$) [2] and syngenite ($K_2Ca{\cdot}2SO_4{\cdot}H_2O$) [3]. The formation of these crystals is one of the main parameters affecting the workability of cement suspensions [4-5]. The elongate shape of these crystals increases the surface area of the cement particles, consequently increasing the demand of water.

Polycarboxylate-ether based superplasticizers (PCEs) are used in different industrial sectors to generally increase the workability of granular materials. To improve the rheological properties of cement paste and to reduce the water necessary for its blending, PCE are usually applied to the fresh concrete mixtures [6]. Different studies were carried out on the interaction between these admixtures and pure cement phases, in order to highlight the fundamental mechanisms governing the effect of PCE on cement. Plank (2007) analyzed the influence of zeta potential on the adsorption of superplasticizer, finding that a positive particle charge provides strong affinity between PCE and the surface of hydration products [7]. Zingg (2008) confirmed that polycarboxylate preferentially adsorb on positively charged particle, thus in a cement suspension they are mainly consumed by the ettringite formed in the first minutes of hydration [8].

PCEs present a comb structure, in which side chains of different lengths are grafted with different frequencies on a main chain, called backbone [9]. The main chain, which is negatively charged, allows the electrostatic adsorption on positively charged particles [8]. This adhesion of the polymer on the particle surface ensures the possibility to exert electrostatic and/or steric repulsion forces, in order to avoid the formation of agglomerates which could disturb the flowability of the paste [10]. These forces were directly detected by the use of an atomic force microscope (AFM), working in liquid environment on a calcium silicate hydrated surface, in order to model the molecular structure of superplasticizers

[11]. Due to the high reactivity of cement, magnesium oxide was used as a model system to characterize the dispersion forces by AFM [12], also manufactured in spherical probes [13].

In this study, direct observations of the adsorption and interaction forces between PCE and different clinker phases are presented. An impregnated clinker with polished surface is studied by energy-dispersive X-ray spectroscopy (EDX) to localize the two and three calcium silicate, the aluminate and the ferrite phases. The elemental distribution on clinker surfaces with and without deposition of superplasticizers was mapped with time-of-flight secondary ion mass spectrometry (TOF-SIMS) on the first surface layer (~ 5 nm) [14], providing the possibility to directly localize PCE position. This would not be possible with EDX due to the significantly high excitation volume of X-rays (1-2 μm) [15]. Additionally, AFM force measurements on surface crystals formed in correspondence of the aluminate phase, reasonably ettringite, and on calcium silicate grains were performed to test the interaction forces occurring in presence or absence of superplasticizers. The combination of these experimental techniques reveals useful information about influence of PCE on element precipitation and dissolution in early hydration, competitive adsorption on different phases, and the resulting dispersion forces. Although the kinetic of the reaction occurring on clinker surface may be rather different from the real cement paste, this study on clinker surface allows the direct observation of the localization and the interaction of PCE with cement phases. This is a first important step in understanding how superplasticizers influence hydration of single phases.

2 Materials

2.1 PCE

Polycarboxylate ether-based superplasticizer was synthesized as described in [9]. Its chemical structure is schematically represented in figure 1. The two monomers forming the copolymer have different functions: the carboxylic group n provides the negative charge on the main chain when the carboxylic group COONa dissociates in COO^- and Na^+; the monomer m, polyethylene oxide (PEO) grafted on the main chain, provides the side chain length which varies according to the number of p units. In the present work, side chains with a length of 23 PEO units and grafting density of 6:1 (n:m) was applied. This composition with a relatively high charge density enables good adsorption on OPC and ettringite [8]. Measurements by size exclusion chromatography (SEC) detected that the number-average molecular weight (M_n) is 7600 g/mol, the mass-average molecular weight (M_w) is 18900 g/mol, and the polydispersity index (M_w/M_n) is 2.5 [4].

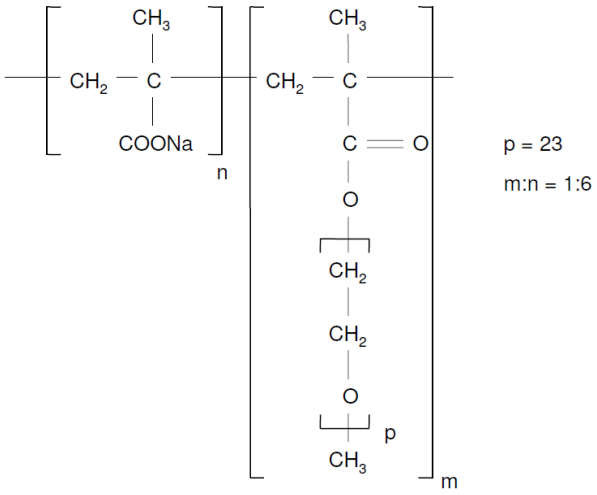

Figure 1: PCE chemical structure: n=anionic carboxylic group, p=PEO unit, m=side chain.

2.2 Clinker surface preparation

To study the chemical composition of the cement clinker (see table 1), quantitative phase analysis was performed by X-Ray-Diffraction (XRD) using a PANalytical X'Pert Pro MPD diffractometer in a θ-2θ configuration employing CuK_α radiation (λ=1.54 Å) with a monochromator, a fixed divergence slit size

of 1° and a rotating sample stage. The diffractograms were collected over a 2θ range of 5°-70° using X'Celerator detector.

Four different measurements were made for each kind of powder preparation: clinker ground by hand, clinker ground with alcohol using a Mc Crone mill to reduce particle size to d_{50}= 5µm, salicylic acid-methanol extraction to dissolve silicate phases, KOH/sugar treatment to remove aluminate and ferrite phases [16].

Table 1: phase composition of the OPC clinker in weight fraction (%).

Phase	Alite	Belite	Aluminate	Ferrite	Periclase	Quartz
Chemical formula	$3CaO{\cdot}SiO_2$	$2CaO{\cdot}SiO_2$	$3CaO{\cdot}Al_2O_3$ ortho	$4CaO{\cdot}Al_2O_3{\cdot}Fe_2O_3$	MgO	SiO_2
Content	68.5	13.8	4.3	12.2	0.5	0.8
Standard deviation	2.2	1.4	0.7	0.9	-	-

In order to study clinker surface, the clinker grain was impregnated with an epoxy resin (Araldit 158 mixed with Aradur 21, Huntsman Advanced Materials GmbH, Basel Switzerland), and finally polished with oil based diamond suspensions until a grain size of 1/10 µm to obtain a smooth surface. The average of the RMS values over 25 scanned areas of 1 μm^2 was nearly 2 nm [17].

Since it was observed that PCE mainly adsorbs on ettringite [8], the clinker surface was treated with the same procedure following Kreppelt (2002), in order to induce formation of this hydration product [1]. Polished clinker surfaces were left in solution of 0.1 M KOH saturated with gypsum at 20°C under nitrogen atmosphere to avoid carbonation. The dissolution of gypsum during clinker hydration provides a large amount of calcium and sulfate ions in order to promote the formation of ettringite. Furthermore, a solution containing dissociated KOH and $CaSO_4{\cdot}2H_2O$ represents well the ionic composition of cement pore solution after 1 hour of hydration [18]. The samples were dipped for few seconds in milli-Q water and twice in ethanol solution to remove the eventual precipitations after 30 minutes of immersion in the previously described solution. Then they were left to dry for 1 hour in nitrogen atmosphere. Note that the kinetic of the reaction might be quite different from a normal cement paste due to the lower amount of surface in contact with water.

The obtained clinker surfaces were then treated in different ways. A part of the samples was left untouched (clinker without PCE), while the other part was placed again in nitrogen atmosphere, and

some drops of solution containing PCE at a concentration of 1 g/L was placed on its surface. Superplasticizer solutions were prepared with milli-Q water or with a synthetic solution, chosen according to the typical ionic composition of the cement pore solution after 1 hour of hydration: $[K^+]$=444 mM/L , $[Na^+]$=40 mM/L , $[Ca^{2+}]$=10 mM/L , $[OH^-]$=104 mM/L , $[SO_4^{2-}]$=200 mM/L, pH=12.8 [18]. It was shown that this solution simulates well the properties of a properly extracted pore solution [8]. The drops of solution containing superplasticizer were left on the clinker surface for 15 minutes. Subsequently, the samples were washed with 2 mL of milli-Q water to remove the not-adsorbed PCE, and left to dry in nitrogen atmosphere. With this method, only the polymer which adsorbs on the clinker phases remains on the surface. These two additional kinds of sample are labelled as clinker - H_2O+PCE and clinker - pore solution+PCE.

3 Methods

3.1 SEM

Energy dispersive X-ray spectroscopy (EDX) was applied to quantify the elemental composition of the clinker surface, collecting back-scattered electron (BSE) images and energy-dispersive spectra. A scanning electron microscope (Philips SEM FEG XL 30) with a multichannel Princeton Gamma Tech analyzer was used. The accelerating voltage of the beam was adjusted to 15kV, to provide a good compromise between spatial resolution and adequate excitation of the FeKα peak. For the back-scattered electron (BSE) imaging, the spot size was chosen to have a good resolution of image and to generate reasonable X-ray results for the EDX analysis.

Three samples (clinker - without PCE, clinker - H_2O+PCE and clinker - pore solution+PCE) were coated with a thin film of platinum (around 10 nm), to avoid charging, and then analyzed by EDX in high vacuum. After the collection of the BSE images of the substrate, nearly twenty points for each image were labeled on different phases.

3.2 TOF-SIMS

Secondary ion mass spectrometry (SIMS) was used to detect the chemical composition of surfaces by scanning the sample with a focused ion beam (primary ions) [19 -20]. In the setup we used (TOF.SIMS 5, ION-TOF, Münster, D), the extracted ions from the surface (secondary ions) are accelerated and analyzed by time-of-flight (TOF) [21]. Note that this technique does not only provide a 2-dimentional (2D) image of a selected specie on the surface, but provides a full mass spectrum at each pixel of the 2D map, allowing the precise determination of the full chemical composition at every point of the area investigated.

In this work, TOF-SIMS mapping of each sample was performed to visualize the distribution of individual chemical species on the surface in the mass range 0-300m/e. Bi_3^{++} beam was used as primary ions in burst-alignment mode with an extractor voltage of 8.5kV. The total ion dose was below the static limit ($<10^{12}$ ions/cm^2), which indicates the limit to study the surface without deep penetration into the sample. Secondary ions of both polarities were collected by scanning areas of 200x200 □m^2 on the prepared surfaces. Charge compensation was obtained by using an electron flood gun.

Different elements and their compounds were selected as signature to distinguish between different phases. Silicon compounds represented the calcium silicate areas, while the sulphur compounds indi-

cated the regions occupied by different oxidation of sulphur. The polymer deposited on the clinker surface was identified by hydro-carbonated fragments analysis (see method in [22-23]). Specifically, fragments between 100 and 217 mass units were considered, and representative peaks are displayed in figure 2.

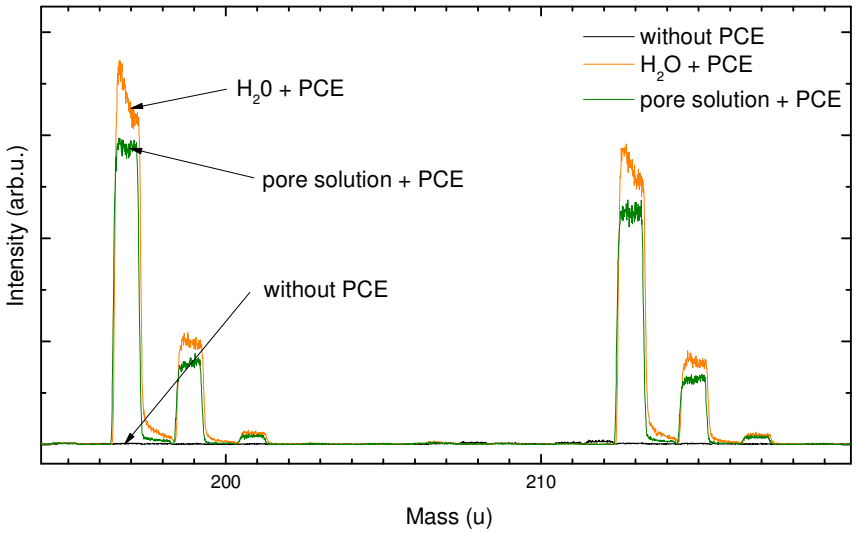

Figure 2: ToF-SIMS signature of PCE fragments on the three sample types: black: clinker - without PCE, green: clinker - H_2O+PCE and orange: clinker - pore solution+PCE. Positive polarity, Note that PCE is present in both immersed samples and is absent from the clinker - without PCE sample, as expected.

Note that the signals of same molecules at different level of oxidation or hydration were added together for each compound to get more contrasted images. For instance, when an element appears in the mass-spectrum with a first peak and at a mass-distance of 16 (atomic mass of oxygen) or multiples of it there is a second peak, then this second peak is reasonably due to an oxidation of the element of the first peak (see figure 2). On the other hand, when the distance between peaks is 18 (atomic mass of a water molecule) or multiples of it, then the second peak represents a certain degree of hydration.

3.3 Atomic force microscopy

The atomic force microscopy (AFM) was used to characterize the interaction forces occurring in aqueous solution at the solid–liquid interface on different clinker phases. The measurements were performed by a commercial instrument (Nanoscope IV, Veeco Digital Instruments, Santa Barbara, CA), that, recording the interaction between the AFM tip and the substrate, allows to perform topography images and force-distance curves. A schematic representation of AFM general setup and the translation of a deflection signal into a force-distance curve, using the cantilever spring constant, are presented elsewhere [12].

Sharp silicon tips (Bruker AFM Probes, Camarillo, CA, USA) were used to probe the interaction forces at the clinker surface. The radius of the used tips was estimated to be around 2 nm. The small area of contact between the tip and the substrate allowed the detection of very local forces, as it is desirable on heterogeneous substrates to distinguish between forces caused by one phase or the other. An increase of radius size causes an increase of the interaction area with the sample, thus a sharp tip is required to probe a narrow region. Furthermore, the choice of a sharp tip allowed to scan images of the substrates in liquid in contact mode, to investigate and select the areas where to perform the force measurements.

Force-distance curves were collected on different parts of the samples, distinguishing between position 1, interstitial aluminate phase, and position 2, two or three calcium silicate grains (see figure 3). No distinction between two and three calcium silicate phases was done due to similar results in the force curves collected on these regions. Milli-Q water and synthetic pore solution, with and without 1 g/L of PCE, were titrated on the samples and ten curves were collected for each solution on both the clinker positions.

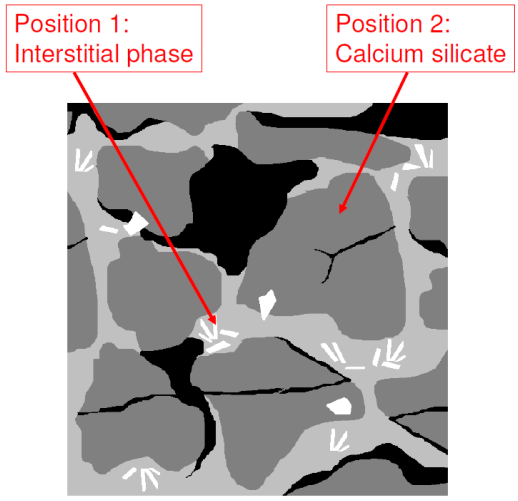

Figure 3: schematic illustration of the positions where force measurements were performed.

4 Results and discussion

4.1 Surface analysis

SEM images of the three sample types are presented in figure 4. Since no reaction was displayed by the two different calcium silicate phases, no distinction between them was done in the discussion of the results. Furthermore, aluminate and ferrite phases are mixed in the interstitial matrix. Thus the debate is mainly leaded commenting the ensemble of the silicate phases versus the ensemble of the interstitial phases.

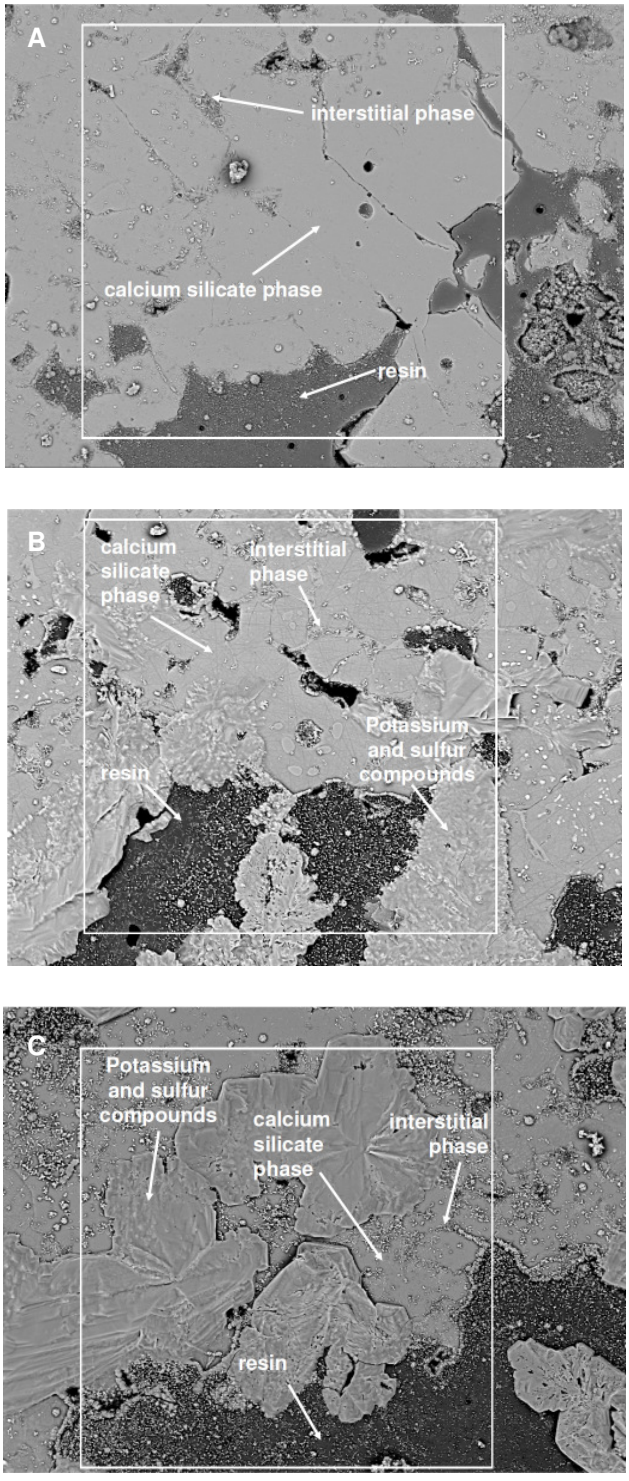

Figure 4: SEM image of the three different samples: A clinker - without PCE, B clinker - H_2O+PCE and C clinker - pore solution+PCE. The size of the white squares is 200x200 µm².

The different components of the sample surfaces, such as calcium silicate, interstitial phase, and resin, were identified by means of EDX analyses. The white arrows indicate representative positions and typical morphology of the phases are located. Despite the samples were coated with Pt to avoid con-

tamination of carbon, EDX analysis could not identify the carbon belonging to PCE, due to the depth penetration of the X-ray (~2 μm) in comparison with the thin layer thickness of superplasticizer in dry condition (~1nm) [24]. Hence the identification of PCE had to be made by TOF-SIMS and discussed later.

Calcium silicate areas maintain smooth surfaces even after 30 minutes of hydration, with the exception of few precipitations. A relatively large amount of small crystals occupies the interstitial spaces between adjacent grains, reasonably due to the high reactivity of the $3CaO \cdot Al_2O_3$ phase. Owing to the X-ray high penetration, the chemical composition of these crystals cannot be carefully investigated. However, from topographic observations one could refer to the elongated crystals as ettringite, typically formed on clinker surface after few minutes of hydration [1].

The EDX spectra showed a strong amount of potassium and sulfur precipitations in the samples treated with superplasticizer, while similar hydration products did not form on clinker without PCE. No differences in the chemical composition of the precipitates were observed between clinker - H_2O+PCE and clinker - pore solution+PCE. Since the concentration of the ions contained in the solution with PCE and milli-Q water is lower than 3 mmol/L, the K^+ and SO_4^{2-} ions most likely come from the dissolution of the clinker, and their precipitation may be induced by the presence of superplasticizer. S/Ca ratio versus K/Ca ratio revealed that in these regions K/S=2.0±0.2 (see figure 5).

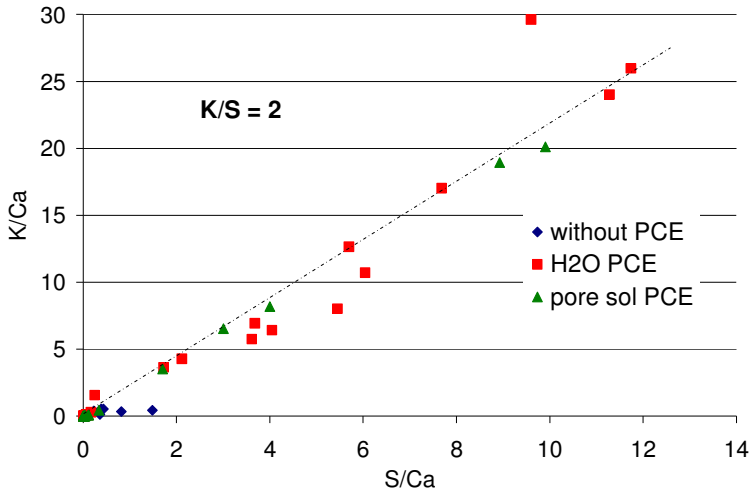

Figure 5: correlation between S/Ca ratio versus K/Ca ratio as resulting from EDX analysis.

This fact excludes the possibility of syngenite formation, while it suggests the presence of arcanite. Other possible minerals with K/S ratio equal to 2 are excluded due to the absence of the other constituents in clinker chemical composition. Precipitation of K_2SO_4 is not expected due to its high solubility, though the presence of superplasticizer in solution apparently influences the dissolution process.

Indeed it was observed that during intercalation processes with superplasticizers, intersalated alkali sulfates are formed [26]. On the other side, it was shown by Möschner (2009) that the addition of citric acid, mainly composed by carboxylic acids, to the cement pastes reduces the concentration of K^+ ions of the pore solution [25]. These findings support the hypothesis of the precipitation of potassium sulfate salts in presence of PCE.

Figure 6 illustrates representative TOF-SIMS maps of the most significant compounds on clinker surface, *i.e.* Si, SO_n, and PCE. As described in the method section, these elements were selected as tracers of the different phases. From left to right the pattern of silicon compounds, the overly of the sulfate pattern at different level of oxidation, and the pattern of the PCE are displayed. The portion of clinker shown in this figure is the same illustrated in figure 4 B. The morphology of the sulfur follows exactly the morphology of the PCE pattern.

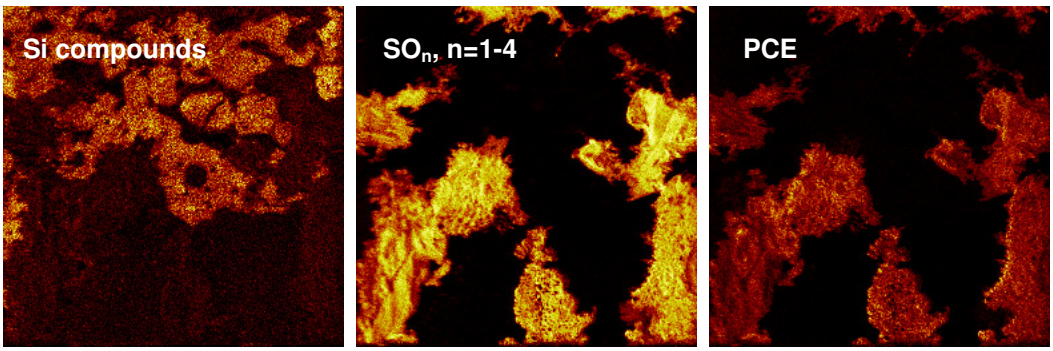

Figure 6: ToF-SIMS representative maps of most significant compounds, *i.e.* Si, SO_n, and PCE, on the clinker with deposition of PCE in water solution. Negative polarity, 200x200µm². Note that this area is the same shown in figure 4 B.

Figure 7 B organizes the maps shown in figures 6 in three types of overlays. Additionally also maps collected for the other samples are displayed (figure 7, A and C). The sum of the silicon species at various level of oxidation and hydration are plotted in green, SO_n (n=1-4) signal is displayed in blue, and the sum of main fragment of PCE is red. The images appear violet where SO_n and PCE compounds are overlaid. The large dark areas indicate the epoxy resin areas. Note that images of calcium species or other constituting elements are not reported as they are evenly distributed on the sample.

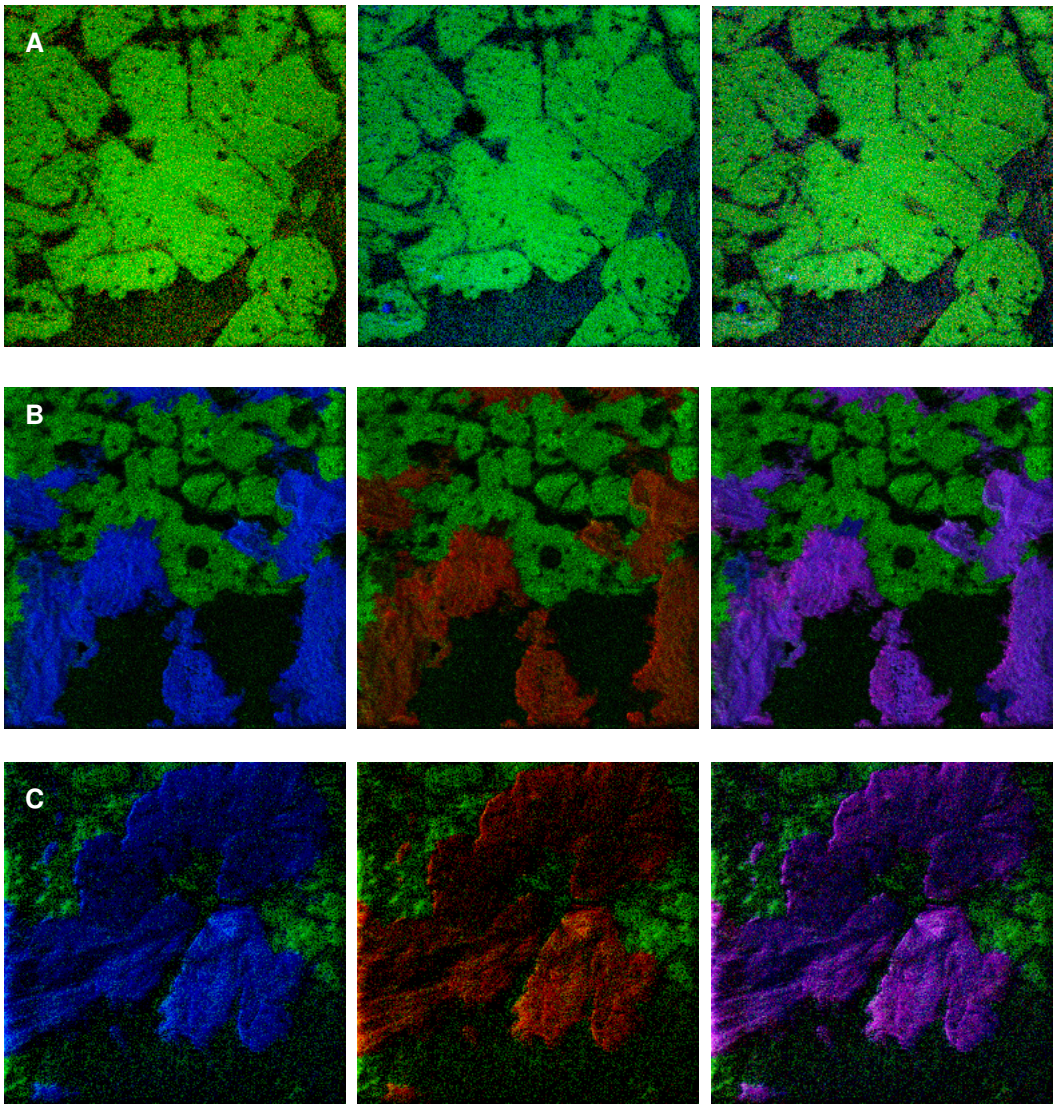

Figure 7: Overlays of the selected compounds: green: Si-compounds, blue: SO_n (n=1-4), red: PCE, violet: overlap of red and blue. A) clinker - without PCE, B) clinker - H_2O+PCE and C) clinker - pore solution+PCE. Negative polarity, 200µmx200µm. Note that SO_n and PCE features overlap remarkably, whereas no overlap is observed between Si-compounds and PCE.

By comparing the 3 overlay images for each sample containing PCE, it appears clear that the super-plasticizer covers the same regions as sulfur compounds, which was revealed to be K_2 SO_4 by EDX analysis. On the other side, the areas of silicon compounds, which indicates the two and three calcium silicate phase, remains almost free of PCE. On clinker surface in absence of PCE (figure 7 A), the sulfate compounds are absent as well, and no precipitation of sulfur compounds are detected. This is a confirmation that arcanite in absence of PCE remains dissolved in solution, thus it was removed by the washing of the sample, while in presence of PCE it precipitates. As in the SEM measurements, no sig-

nificant differences are observed between the sample treated with water (figure 7 A) or the one treated with synthetic pore solution (figure 7, B and C).

The occurrence of PCE in direct proximity to ettringite was originally expected, proving the tendency of superplasticizer to preferably adsorb on this hydration product. Nevertheless neither the TOF-SIMS and nor the EDX chemical analysis, could detect large regions occupied by ettringite. Since this washing procedure was already applied on similar samples without removing ettringite [1], the possibility of having removed this phase by the water and ethanol treatment after the 30 minutes of hydration can be excluded.

In an actual cement paste, the precipitation of arcanite due to superplasticizers may reduce the concentration of potassium and sulfate ions in the pore solution, thus disturbing ettringite and syngenite formation. In fact it was shown that the size of ettringite crystals is reduced in presence of admixtures [1-3]. Modification of crystal shape is important for rheological properties of the paste. Needles have a high surface area which provokes high demand of water. In this way the PCE influences cement hydration conditioning ettringite formation by the precipitation of arcanite.

4.2 AFM force measurements

Further investigation was performed via AFM to probe the interaction forces in liquid at the clinker surface. The different sensitivity of the AFM did not allow to study an area as large as the one studied by EDX and TOF-SIMS. Furthermore, the observed precipitations of arcanite show a relatively rough surface, which is not ideal for the application of AFM. For these reasons, the force measurements were performed on position 1 and position 2, as explained in the method section, not directly probing potassium sulphate areas.

Since the silicon AFM tips were stored in air, it was assumed that at the surface of the tip some oxidation occurred forming SiO_2. Silicon dioxide was shown to be negatively charged and to provide almost no-adsorption of PCE [12]. From this point of view, if some electrostatic attraction between the tip and the substrate is observed in solution without superplasticizer, this means that the substrate is carrying a positive charge. Vice versa, if there is repulsion between the tip and the substrate, the probed clinker phase is negatively charged.

The clinker surfaces were probed in milli-Q water with and without PCE. Some tests were also made with synthetic pore solution, but the high pH induced a strong reaction of the clinker surface, as already observed in [17], resulting in a large scatter of the measurements, thus they are omitted.

As explained in the method section, the force-distance curves were performed in two different positions (on interstitial phase, position 1, and on the calcium silicate phase, position 2) taking care of probing the sample on positively and negatively charge phases (see figure 8). Figure 9 displays a typical AFM topography of the interstitial phase, position 1. The sharpness of the tip allowed to collect curves in position 1 on this elongate surface crystal only 40 nm width.

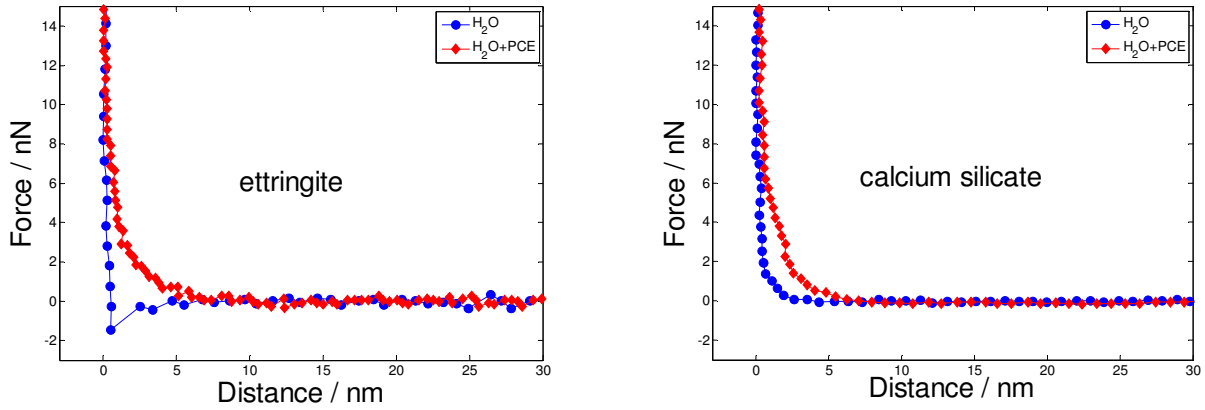

Figure 8: AFM force-distance curves measured on ettringite crystal (position 1) or on calcium silicate (position 2). Note that the force was calculated as explained in [12].

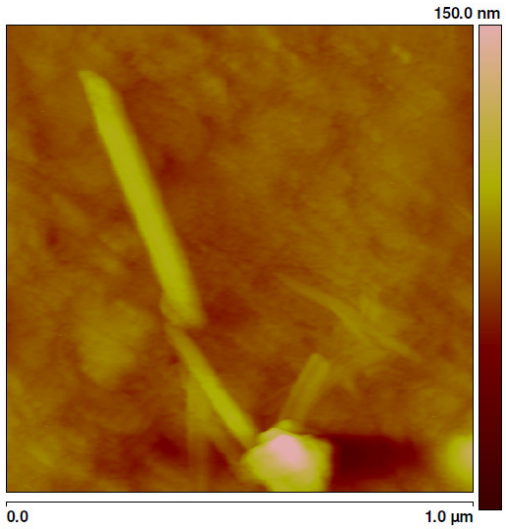

Figure 9: AFM topography image of clinker surface at the interstitial phase with ettringite crystals. Measurements done in water without PCE, in contact mode.

The force-distance curves performed in H_2O display attraction between the tip and the substrate in position 1, interstitial phase (figure 8, left, H_2O curve), and repulsion in position 2, calcium silicate phase (figure 8, right, H_2O curve). According to what discussed about the tip charged, these different interactions reveal the positive charge of the crystal surface in position 1 and the negative charge of

the calcium silicate probed in position2. Actually, on most of the areas of clinker surface scanned, repulsive interaction was observed, with the exception of some surface crystals where attraction was detected. This occurs because the charge of the substrate is mainly negative, as expected for calcium silicate substrates, and the resulting electrostatic repulsion is stronger than the adhesion forces usually experienced by the AFM tip in absence of PCE.

Regarding forces collected in presence of PCE, only repulsion was observed on each phase, regardless the adsorption of superplasticizer on that specific phase. Particularly on the calcium silicate substrate (position 2), the range of the repulsion already existing without PCE is slightly amplified by the presence of superplasticizer, reaching the same ranges observed on the ettringite surface.

Referring to figure 8 and 9, due to their positive charge, to their needle morphology, and to their location on interstitial phase, these elongate thin crystals were recognized to be ettringite formed as early hydration products. Indeed ettringite was measured to have a positive zeta potential in water [8] and to form in proximity of the interstitial phase [1].

Concluding, AFM force measurements show that distinguished phases may provide opposite electrostatic interactions. Nevertheless, when PCE are present in solution, electrostatic and steric dispersion forces tends to homogenize the interactions of different phases, in order to avoid attraction between differently charged particles.

5 Conclusions

Portland cement clinker surfaces after 30 minutes of hydration with and without deposition of superplasticizer were investigated. Results obtained with TOF-SIMS, in combination with EDX analysis, illustrate the morphology and the chemical distribution of elements on the substrate. The comparison between spectra obtained on samples with and without superplasticizer gives the opportunity to directly detect PCE fragments, and to directly observe its position on clinker surfaces.

The regions where superplasticizers are deposited are mainly composed by potassium and sulfur in ratio of 2. Then, PCE induces precipitations of K_2SO_4 thus reducing the amount of sulfate ions available in the pore solution. This could explain why in presence of superplasticizer ettringite formation is affected, resulting in a better workability of the cement paste.

Force measurements by AFM reveal the different charge of cement phases, which is negative in most of the investigated cases. Curves detected on needle-shaped ettringite crystals were possible owing to the application of a sharp tip. The collected plots support the idea that in a multiphase suspension superplasticizer leads to a homogeneity in charge and interaction between phases. Better characterization of the ettringite phase is then required to allow further information about the role of this phase in cement workability.

Acknowledgments

The authors are grateful to Boris Ingold, Angela Steffen, Gween Le Saout (Empa), and Stefan Kaufmann (ETH Zürich) for their technical support and interesting scientific discussions.

References

[1] F. Kreppelt, M. Weibel, D. Zampini, M. Romer, Influence of solution chemistry on the hydration of polished clinker surfaces – a study of different types of polycarboxylic acid-based admixtures, Cem. Concr. Res. 32 (2002) 187-198.

[2] H.F.W. Taylor, Cement Chemistry, second ed., Thomas Telford Publishing, London, 1997.

[3] C. Rössler, A. Eberhardt, H. Kucerova, B. Möser., Influence of hydration on the fluidity of normal Portland cement pastes, Cem. Concr. Res. 38 (2008) 897-906.

[4] A. Zingg, F. Winnefeld, L. Holzer, J. Pakusch, S. Becker, R. Figi, and L. Gauckler, Interaction of polycarboxylate-based superplasticizers with cements containing different C_3A amounts, Cem. Concr. Compos. 31 (2009) 153-162.

[5] L. Ferrari, J. Kaufmann, F. Winnefeld, J. Plank, Multi-method approach to study influence of superplasticizers on cement suspensions, Submitted in December 2010 for Cem. Concr. Res.

[6] S. Hanehara, K. Yamada, Yamada, Interaction between cement and chemical admixture from the points of cement hydration, admixture adsorption and paste rheology, Cem. Concr. Res. 29 (8), (1999) 1159-65.

[7] J. Plank, C. Hirsch, Impact of zeta potential of early cement hydration phases on superplasticizer adsorption, Cem. Concr. Res. 37 (2007) 537-542.

[8] A. Zingg, F. Winnefeld, L. Holzer, J. Pakusch, S. Becker, L. Gauckler, Adsorption of polyelectrolytes and its influence on the rheology, zeta potential and microstructure of various cement and hydrate phases, J. Coll. Int. Sci. 323 (2008) 301-312.

[9] F. Winnefeld, S. Becker, J. Pakusch, T. Götz, Effects of the molecular architecture of comb-shaped superplasticizers on their performance in cementitious systems, Cem. Concr. Compos. 29 (2007) 251-62.

[10] H. Uchikawa, S. Hanehara, D. Sawaki. The role of steric repulsive force in the dispersion of cement particles in fresh paste prepared with organic admixture Cem. Concr. Res. 27 (1997) 37-50.

[11] R.J. Flatt, I. Schober, E. Raphael, C. Plassard, and E. Lesniewska, Conformation of adsorbed comb copolymer dispersants, Langmuir 25 (2009) 845-55.

[12] L. Ferrari, J. Kaufmann, F. Winnefeld, J. Plank, Interaction of cement model systems with superplasticizers investigated by atomic force microscopy, zeta potential, and adsorption measurements, J. Coll. Int. Sci. 347 (2010) 15-24.

[13] A. Kauppi, K. M. Andersson, L. Bergström, Probing the effect of superplasticizer adsorption on the surface forces using the colloidal probe AFM technique, Cem. Concr. Res. 35 (2005) 133-140.

[14] A. Benninghoven, F. Rüdenauer and W.Werner, Secondary Ion Mass Spectrometry. John Wiley & Sons Ltd, Chichester, UK (1987).

[15] K. L. Scrivener, Backscattered electron imaging of cementitious microstructures: understanding and quantification, Cem. Concr. Compos. 26 (2004) 935-945.

[16] G. Le Saout, V. Kocaba, K. Scrivener, Application of the Rietveld method to the analysis of anhydrous cement, Cem. Concr. Res. 41 (2011) 133-148.

[17] L. Ferrari, M. Ben Haha, J. Kaufmann, F. Winnefeld. Proceedings of the 32nd conference on Cement microscopy, New Orelans, LA, USA, March 2010.

[18] B. Lothenbach, F. Winnefeld. Thermodynamic modeling of the hydration of Portland cement, Cem. Concr. Res. 36 (2) (2006) 209-226.

[19] J.C. Vickerman, A. Brown and N.M. Reed (Eds), Secondary Ion Mass Spectrometry, Principles and Applications. Oxford University Press (1989).

[20] J.C. Vickerman and D. Briggs, ToF-SIMS, Surface Analysis by Mass Spectrometry. IM Publications and SurfaceSpectra (2001).

[21] A. Benninghoven (Ed.), Ion Formation from Organic Solids in Springer Series in Chemical Physics. Springer-Verlag, Berlin (1983).

[22] G.J. Leggett and J.C. Vickerman, Int. J. Mass Spectrom. Ion Phys. 122, 281 (1992).

[23] G. Leggett, in The Static SIMS Library, Ed by J.C. Vickerman, D. Briggs and A. Henderson, SurfaceSpectra Ltd, Manchester, UK (1999).

[24] L. Ferrari, J. Kaufmann, F. Winnefeld, J. Plank, Proceedings of the XIII International Congress on Chemistry of Cement, Madrid, Spain, July 2011.

[25] G. Möschner, B. Lothenbach, R. Figi, R. Kretschmar, Influence of citric acid on the hydration of Portland cement, Cem. Concr. Res. 39 (2009) 275-282.

[26] J. Plank, D. Zhimin, H. Keller, F. v. Hössle, W. Seidl, Fundamental mechanisms for polycarboxylate intercalation into C_3A hydrate phases and the role of sulfate present in cement, Cem Concr. Res. 40 (2010) 45-57.

[27] C. Rössler, B. Möser., J. Stark. Proceedings of the 12th International Congress on the Chemistry of Cement, Montreal, Canada, July 2007.

Supplementary results

Interaction forces between spherical AFM probes and ettringite crystals in polyelectrolyte solutions

L. Ferrari, J. Kaufmann, F. Winnefeld, J. Plank

Interaction forces between spherical AFM probes and ettringite crystals in polyelectrolyte solutions

Lucia Ferrari [a, b, *], Josef Kaufmann [a, 1], Frank Winnefeld [a], Johann Plank [b]

[a] *Empa, Swiss Federal Laboratories for Materials Testing and Research, Laboratory for Concrete/Construction Chemistry, Ueberlandstr. 129, 8600 Duebendorf, Switzerland.*

[b] *Technische Universität München, Department of Chemistry, Lichtenbergstr. 4, 85747 Garching, Germany*

Abstract

Dispersion forces due to polycarboxylate-ether-based superplasticizer (PCE) in different electrolyte solutions at the surface of ettringite crystals were studied by atomic force microscope (AFM) applying a spherical glass probe. The goal was to reproduce in the AFM setup the attraction, usually occurring in cement mixtures, between positively charged ettringite particles and negatively charged cement grains. The combination of AFM with zeta potential measurements allows the distinction between steric and electrostatic dispersive effects.

Results show that in deionized water the attraction between the two minerals is strong because of the electrostatic opposite charge. However, in high pH and high ionic strength the ettringite substrate and the silicon dioxide tip spontaneously repulse each other, most likely due to electrostatic effects.

Keywords: superplasticizer, ettringite, zeta-potential, AFM, colloidal probe.

---

[*] Corresponding authors: lucia.ferrari@empa.ch and josef.kaufmann@empa.ch

The goal of this study

This work aims to reproduce in the AFM setup the attractive forces usually occurring in cements between silica particles and ettringite crystals immersed in aqueous solution. Since the zeta potential of these two materials is opposite, they have the tendency to attract each other forming agglomerates, which disturb cement workability. With this purpose, ettringite crystals were sued as substrates and colloidal SiO_2 AFM tips were used to probe the ettringite (see figure 1).

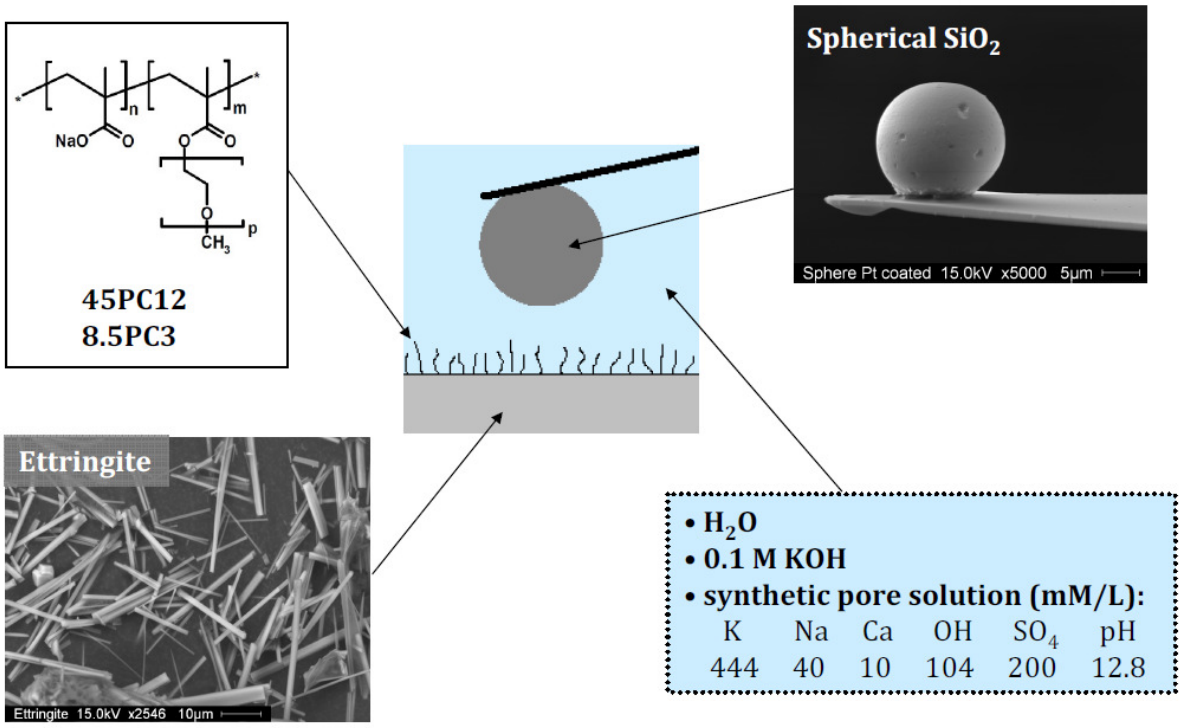

Figure 1: AFM setup

The tests were performed in different solutions (Table 1), with different superplasticizers (Table 2).

Table 1 – Electrolytes chemical composition.

	SO_4^{2-}	Na^+	K^+	Ca^{2+}	OH^-	pH
0.1 M KOH	0	0	100	0	100	13.0
Synthetic pore solution	200	40	444	10	104	12.8

Table 2 – Characteristic properties of tested PCE.

p PC n	M_n [1] (g/mol)	M_w [2] (g/mol)	PDI [3]	MCL[4] (nm)	SCL[5] (nm)	CD[6] (mmol/g)
8.5 PC 3	25,800	106,000	4.1	36.3	2.4	4.2
45 PC 12	11,800	342,500	2.9	12.5	12.5	3.9

[1] M_n = number-average molecular weight. [2] M_w =mass-average molecular weight.

[3] $PDI = M_n / M_w$ = polydispersity index. [4]MCL=main chain length.

[5]SCL=side chain length. [6]CD = charge density.

Theoretical background

In colloid science, the stability of the particles in suspension and the rheology of the mixture are affected by forces among colloidal particles. The dominating forces at the solid-liquid interface are: Van der Waals, steric, and electrostatic. The combination of all these effects provides the DLVO theory, which includes the effect of the Van der Waals attraction and the double-layer repulsion as function of the distance between the particles.

In this study, the experimental investigations of these forces playing a role at the solid liquid interface were analyzed in details. Solution containing different concentrations of electrolytes and polyelectrolytes were studied to allow a comprehensive understanding of the behavior of polycarboxylate superplasticizer in cement mixtures.

Results

Results of zeta potential measurements collected during PCE titration in suspensions of silicon dioxide and ettringite powders are reported in figure 2.

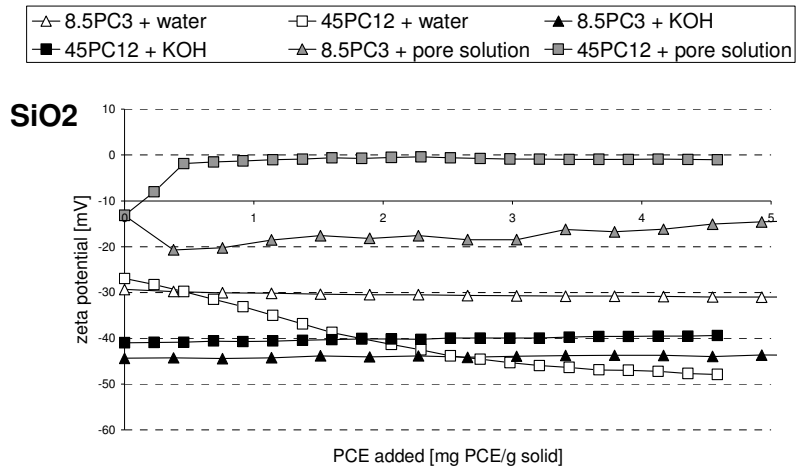

(A)

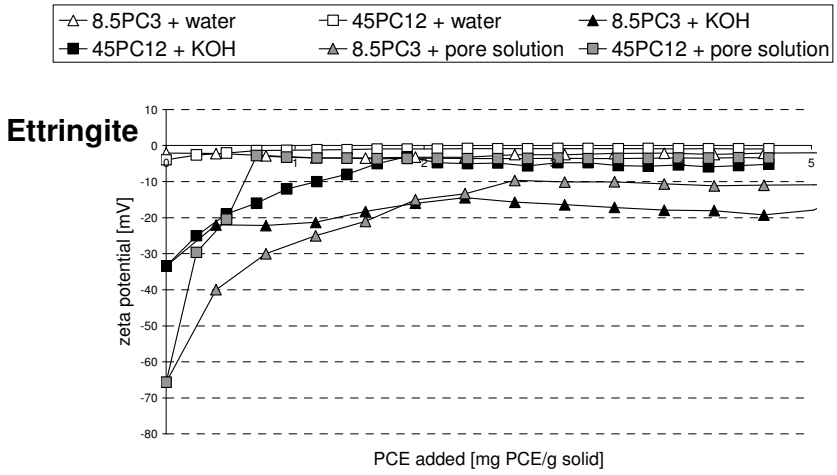

(B)

Figure 2: zeta potential measured during PCE titration on SiO_2 powder (A), and on ettringite powder (B).

Results of AFM dispersion forces collected on ettringite substrates applying a colloidal glass probe are reported in figure 3.

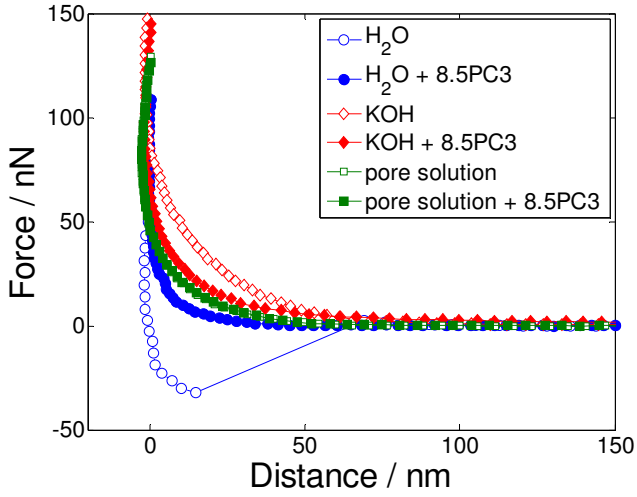

(A)

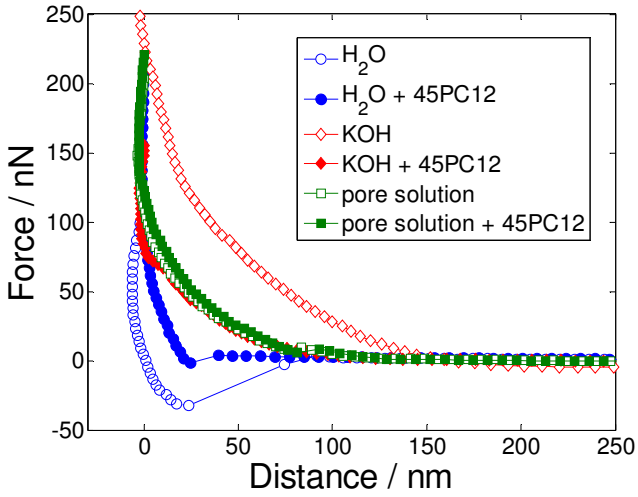

(B)

Figure 3: AFM force measurements with 1g/L of 8.5PC3 (A) and 45PC3 (B) in different electrolyte solutions.

It has to be noticed that forces collected in water without PCE present a strong attraction between the silicon dioxide tip and the ettringite crystal. However, when the pH and the ionic strength increase, the ettringite substrate becomes negatively charged (see Figure 3 (B)), and the tip and the substrate experience repulsion forces even in absence of PCE.

Curriculum Vitae

LUCIA FERRARI

Date of birth: 11th April 1983

Nationality: Italian

Academic education

2008-2011	Ph.D. student at Empa, Lab for Concrete / Construction Chemistry, Dübendorf, Switzerland, in collaboration with Technische Universität München (TUM), Bauchemie, Germany. Summa cum laude. Thesis: *Interaction of PCE polyelectrolytes with cement mineral surfaces: a study from the macro to the nano scale.*
2006-2008	MSc in Material Physics, University of Milan, Italy. 110/110 cum laude.
2007-2008	Erasmus student at Danmarks Tekniske Universitet (DTU), Lyngby, Denmark. Thesis: *Probabilistic model of protein structure*.
2002-2006	Bachelor in Physics, University of Milan, Italy. 106/110. Thesis: *Physical-Mathematical aspects of soap films*.

Publications

L. Ferrari, J. Kaufmann., F. Winnefeld, J. Plank. Reaction of clinker surfaces investigated with atomic force microscope. *Construction and Building Materials,* in review.

L. Ferrari, L. Bernhard, F. Deschner, J. Kaufmann, F. Winnefeld, J. Plank. Study of polycarboxylate-ether based superplasticizer on cement clinker surface by TOF-SIMS and AFM. *Journal of American Ceramic Society*, in review.

L. Ferrari, J. Kaufmann, F. Winnefeld, J. Plank. Parametric analysis of superplasticizer behavior at cementitious interfaces. *Proceedings of the Tenth International Conference on Superplasticizers and Other Chemical Admixtures in Concrete*, Prague 2012, in review.

L. Ferrari, J. Kaufmann, F. Winnefeld, J. Plank. Multi-method approach to study influence of superplasticizers on cement suspensions. *Cement and Concrete Research* 41 (2011) 1058-1066.

L. Ferrari, J. Kaufmann, F. Winnefeld, J. Plank. Multi-method approach for the characterization of the behavior of superplasticizer in cement suspensions. *Proceedings of the XIII ICCC International Congress on the Chemistry of Cement*, Madrid 2011.

L. Ferrari, J. Kaufmann, F. Winnefeld, J. Plank. Interaction of cement model systems with superplasticizers investigated by atomic force microscopy, zeta potential, and adsorption measurements. *Journal of Colloid and Interface Science* 347 (1) 2010, 15–24.

L. Ferrari, M. Ben Haha, Kaufmann J., Winnefeld F. Force measurements by AFM on clinker surfaces and model systems in aqueous solutions containing superplasticizer. *Proceedings of the 32nd conference on Cement Microscopy*. New Orleans, LA, USA, March 2010.

Languages	Italian	Mother language
	English	Fluent
	German	Good
	French	Basic
	Spanish	Basic